DISSERTATION

SUBMITTED TO THE

COMBINED FACULTY OF NATURAL SCIENCES AND MATHEMATICS

OF THE RUPERTO CAROLA UNIVERSITY HEIDELBERG, GERMANY

FOR THE DEGREE OF

DOCTOR OF NATURAL SCIENCES

PRESENTED BY

M. SC. CHRISTOPHER ARMIN DÄCHERT

BORN IN BURGLENGENFELD, GERMANY

ORAL EXAMINATION: 19.06.2020

MATHEMATICAL MODELING OF

HOST CELL DETERMINANTS

AND PHARMACOLOGICAL INTERVENTION

IN HEPATITIS C VIRUS REPLICATION

Referees:

Prof. Dr. Ralf Bartenschlager

Dr. Marco Binder

Declaration

The applicant, Christopher Armin Dächert, declares that he is the sole author of the submitted dissertation and no other sources or help from those specifically referred to have been used. Additionally, the applicant declares that he has not applied for permission to enter an examination procedure at any other institution and that this dissertation has not been presented to any other faculty and has not been used in its current or in any other form in another examination.

_____   _____

MEINER FAMILIE.

IV

"Nothing in this World That's Worth having Comes Easy."

Bob Kelso

"Der Sinn des Leben's ist Leben. Das War's."

Casper

ACKNOWLEDGEMENTS

Summary

Hepatitis C virus (HCV) is a blood-borne, enveloped, single-stranded, (+)-oriented RNA virus that mainly infects hepatocytes. Most infections progress into chronicity and eventually lead to severe liver disease. Although effective treatments have been developed, access to diagnosis and treatment is low, particularly in non-developed countries. Thus, eradication of the disease is unlikely without a prophylactic vaccine. Research, therefore, has to continue despite the high cure rates of today's HCV regimens.

We use mathematical modeling to study HCV replication and its intricate connection with the infected host cell. A model that is able to simulate intracellular HCV RNA replication suggested a host factor species (HF), representing a protein (complex) or a host process, to be critically involved in HCV replication. Gene expression profiling revealed several candidates potentially representing this HF. We validated those candidates in two variants of the human hepatoma cell line Huh7 and could confirm that five of them indeed played a role for HCV replication, namely CRAMP1, LBHD1, CRYM, THAP7, and NR0B2. The latter three are nuclear receptors or transcriptional (co-)repressors, suggesting they could influence HCV replication indirectly, *e.g.* through glucose, lipid, or cholesterol metabolism. Follow-up studies will help to understand the implication of those factors in HCV replication and reveal important insights into the metabolic pathways regulating HCV replication.

Model analyses also revealed the most sensitive steps in HCV RNA replication that could potentially be targeted by specific intervention. The standard of care for chronic HCV infection has been interferon alpha (IFN-α) therapy that elicited a very broad but rather unspecific antiviral response of the host cell and came along with severe side effects. IFN-α activates signaling cascades that lead to the expression of hundreds of interferon stimulated genes that exert antiviral action. Despite its decades-long use, the exact mechanism of the suppression of HCV replication by IFN-α treatment remains elusive. We thus combined experimental data with an intracellular model for HCV replication and revealed the steps in the viral replication cycle that are most probably affected by IFN-α treatment. The obtained findings were well in line with *in vitro* data and confirmed the validity of our intracellular model to make such analyses.

Recently, direct-acting antivirals (DAAs) have replaced IFN-α-containing regimens as the standard of care for chronic HCV infection. Those DAAs possess much less side effects, can be taken orally, and give extraordinarily high cure rates. Mainly three classes exist: inhibitors of the viral protease, the viral polymerase, and a viral multifunctional phosphoprotein. The latter class constitutes highly potent inhibitors of the HCV NS5A protein, exerting effects in the low picomolar range. However, due to the many roles of NS5A in the HCV life cycle, the exact mechanism of action of those DAAs remains unclear. For the other two classes, the mode of action is distinct and well defined. We, thus, used one representative member of each of these classes to validate the capacity of our model to implement drug effects and predict HCV replication correctly. Model predictions upon *a priori* fixing of the affected parameters in the model qualitatively resembled HCV replication dynamics under the respective drug treatment. This allowed us to apply our model to HCV replication data under treatment with an NS5A inhibitor in order to gain insights into its mode of action. The model revealed that the translation rate of HCV RNA as well as RNA synthesis steps in the HCV replication compartment are most probably affected by the drug. These findings were reasonable and supported by known roles of NS5A in the HCV life cycle. However, our model was limited to intracellular HCV replication and did not account for steps like particle assembly or infection of target cells. Therefore, we extended our intracellular model to cover the full viral life cycle. Our new full life cycle model could simulate viral (+)- and (-)-strand RNA, viral titers as well as spread of the infection, and was able to correctly predict HCV replication under drug treatment.

Our new model will be helpful in further elucidating the mode of action of NS5A inhibitors and IFN-α and in deciphering the role of host factors that determine permissiveness for HCV.

Hence, this study provides a novel, extended mathematical model of the full HCV life cycle with the proven capacity of simulating and analyzing HCV replication even under pharmacological intervention. It can serve as an invaluable tool to study further molecular details of HCV replication and to devise and test novel therapeutic approaches.

X

ZUSAMMENFASSUNG

Das Hepatitis C-Virus (HCV) ist ein durch Blut übertragenes, umhülltes, einzelsträngiges, (+)-orientiertes RNA-Virus, das hauptsächlich Hepatozyten infiziert. Die meisten Infektionen verlaufen chronisch und führen schließlich zu schweren Lebererkrankungen. Obwohl wirksame Therapien entwickelt wurden, sind die Diagnose- und Behandlungsraten niedrig, speziell in Entwicklungsländern. Daher ist eine Ausrottung der Krankheit ohne einen prophylaktischen Impfstoff unwahrscheinlich. Die Forschung muss daher, trotz der hohen Heilungsraten bei Therapie, fortgesetzt werden.

Wir verwenden mathematische Modelle um die Replikation von HCV und seine komplexe Verbindung mit der infizierten Wirtszelle zu untersuchen. Ein solches Modell, das die intrazelluläre HCV-Replikation beschreibt, legte nahe, dass eine Wirtsfaktor-Spezies (WS), welche ein Protein, ein Proteinkomplex oder ein Wirtsprozess sein kann, entscheidend an der HCV-Replikation beteiligt ist. Die Erstellung von Genexpressionsprofilen ergab mehrere mögliche Kandidaten, die diese WS repräsentieren könnten. Wir validierten diese Kandidaten in zwei verschiedenen Varianten der menschlichen Hepatomzelllinie Huh7 und konnten bestätigen, dass fünf von ihnen tatsächlich eine Rolle für die HCV-Replikation spielten, nämlich CRAMP1, LBHD1, CRYM, THAP7 und NR0B2. Die letzteren drei sind nukleäre Rezeptoren oder transkriptionelle (Co-)Repressoren, was vermuten lässt, dass sie die HCV-Replikation indirekt beeinflussen, zum Beispiel durch den Glukose-, Lipid- oder den Cholesterinstoffwechsel. Folgestudien werden helfen, die Auswirkungen dieser Faktoren auf die HCV-Replikation zu verstehen und wichtige Einblicke in die Stoffwechselwege zu gewinnen, die die HCV-Replikation regulieren.

Eine Modellanalyse zeigte auch die empfindlichsten Schritte in der intrazellulären HCV-Replikation auf, auf die eine spezifische Behandlung möglicherweise abzielen könnte. Die Standardbehandlung der chronischen HCV-Infektion war für lange Zeit die Interferon-alpha-(IFN-α)Therapie, die eine sehr breite, aber eher unspezifische antivirale Reaktion der Wirtszelle auslöste und mit schweren Nebenwirkungen einherging. IFN-α aktiviert Signalkaskaden, die zur Expression von Hunderten von Interferon-stimulierten Genen führen, welche wiederum eine antivirale Wirkung entfalten. Trotz des jahrzehntelangen Einsatzes ist der genaue Wirkmechanismus von IFN-α auf die HCV-Replikation nicht genau bekannt. Wir kombinierten daher experimentelle Daten mit einem intrazellulären, mathematischen Modell der HCV-Replikation und zeigten die Schritte im viralen Replikationszyklus auf, die höchstwahrscheinlich durch eine IFN-α-Behandlung beeinflusst werden. Die erhaltenen Ergebnisse stimmen gut mit experimentellen Daten überein und bestätigen somit die Tauglichkeit unseres intrazellulären Modells für eine solche Art von Analysen.

In den letzten Jahren haben spezifische, auf HCV gerichtete, antivirale Medikamente (DAAs) die IFN-α-basierte Standardtherapie für chronische HCV-Infektionen ersetzt. Diese DAAs zeigen weitaus weniger Nebenwirkungen, können in Tablettenform eingenommen werden und führen zu außerordentlich hohen Heilungsraten. Es gibt hauptsächlich drei Klassen dieser DAAs: Inhibitoren der viralen Protease, der viralen Polymerase und eines viralen multifunktionellen Phosphoproteins. Die letztere Klasse sind hochwirksame Inhibitoren des HCV NS5A-Proteins, die im niedrigen pikomolaren Bereich wirken. Aufgrund der vielen Rollen von NS5A im HCV-Replikationszyklus ist der genaue Wirkmechanismus dieser DAAs jedoch unklar. Für die beiden anderen Klassen ist der Wirkmechanismus allerdings eindeutig und gut definiert. Wir haben daher jeweils ein repräsentatives Mitglied dieser beiden Klassen verwendet, um die Fähigkeit unseres Modells zur Implementierung von Inhibitoreffekten und zur korrekten Vorhersage der HCV-Replikation während der Therapie zu validieren. Modellvorhersagen nach der *a priori*-Festlegung der betroffenen Parameter im Modell ähnelten qualitativ der HCV-Replikationsdynamik unter der jeweiligen Therapie. Dies ermöglichte uns die Anwendung unseres Modells auf HCV-Replikationsdaten unter der Behandlung mit einem NS5A-Inhibitor, um Einblicke in dessen Wirkmechanismus zu gewinnen. Das Modell zeigte, dass sowohl die Translationsrate der HCV RNA als auch die HCV RNA-Syntheseschritte im HCV-Replikationskompartiment höchstwahrscheinlich durch das Medikament beeinflusst werden. Diese Ergebnisse waren sinnvoll und wurden durch die bekannte Rolle von NS5A im HCV-Replikationszyklus unterstützt. Unser Modell beschränkte sich jedoch auf die intrazelluläre HCV-Replikation und berücksichtigte keine extrazellulären Schritte wie die HCV-Partikelproduktion oder die Infektion von Zielzellen. Daher erweiterten wir unser intrazelluläres Modell, um den gesamten viralen Replikationszyklus abzudecken. Unser neues Modell für den gesamten Replikationszyklus konnte virale (+)- und (-)-Strang-RNA, produzierte virale Partikel, sowie die Ausbreitung der Infektion simulieren und war zudem in der Lage, die HCV-Replikation unter medikamentöser Behandlung korrekt vorherzusagen.

Unser neues Modell wird bei der weiteren Aufklärung der Wirkungsweise von NS5A-Inhibitoren und IFN-α sowie bei der Entschlüsselung der Rolle der WS, die die Permissivität für HCV bestimmt, hilfreich sein.

Somit stellt diese Arbeit ein neuartiges, erweitertes mathematisches Modell des gesamten HCV-Replikationszyklus mit der geprüften Fähigkeit, die HCV-Replikation auch unter pharmakologischer Intervention zu simulieren und zu analysieren, bereit. Das Modell kann als sehr wertvolles Werkzeug dienen, um weitere molekulare Details der HCV-Replikation zu untersuchen und neue therapeutische Ansätze zu entwickeln und zu testen.

ABBREVIATIONS

°C	degree celsius
µM	micromolar
µCi	micro curie (radioactivity)
32P	Phosphorus-32 (radioactive isotope)
bp	base pairs
DAA	direct-acting antiviral
DAPI	4',6-diamidino-2-phenylindole
DCV	daclatasvir
DEPC	diethyl pyrocarbonate
DNA	deoxyribonucleic acid
ds	double-stranded
DTT	dithiothreitol
EI	EMCV IRES
ER	endoplasmic reticulum
EV	extracellular vesicle
FCS	fetal calf serum
GITC	guanidinium isothiocyanate
gt	genotype
h	hour/hours
HCV	hepatitis C virus
HIV	human immunodeficiency virus
hpe	hours post electroporation
hpi	hours post infection
HRP	horse radish peroxidase
IC$_{50}$	half maximal inhibitory concentration
IEG	interferon-effector gene
IFN	interferon
IRES	internal ribosome entry site
ISG	interferon-stimulated gene
IU	international units
IVT	*in vitro*-transcribed
kb	kilo base pairs
LCS	low complexity sequence
Luc	firefly luciferase
MOI	multiplicity of infection
nM	nanomolar
ORF	open reading frame
PEG	polyethylene glycol
PI	polio virus IRES
pM	picomolar
nt	nucleotide
RBV	ribavirin
RC	replication complex(es)
RLR	RIG-I-like receptor
RLU	relative light units
RNA	ribonucleic acid
RNase	ribonuclease
rNTP	ribonucleoside tri-phosphate
RVFV	rift valley fever virus
sg	subgenomic
SOF	sofosbuvir
ss	single-stranded
SVR	sustained virologic response
TEL	telaprevir
TMD	transmembrane domain
UTR	untranslated region

TABLE OF CONTENTS

XVIII

1. INTRODUCTION

1.1. Global disease burden by chronic viral infections

Ever since, viral epidemics and pandemics have cost millions of human lives [1]. The first human pathogenic virus isolated in 1901 was yellow fever virus [2], but today we know at least 249 viruses that infect humans [3]. Virological research led to the development and widespread use of vaccinations and treatments for different viral diseases, culminating in the global eradication of smallpox and elimination of polio in most countries [4, 5]. Whereas most of them are very rare or cause only acute but still deadly disease, few of them progress into chronic infections and possess huge burdens for global health, *e.g.* human immunodeficiency virus (HIV), human papillomaviruses (HPV), or hepatitis viruses B and C (HBV, HCV) [6]. Since many of them cause cancers, their attribution to deaths is often underestimated due to limited diagnosis. However, the awareness of infectious diseases contributing to cancer and cancer-related deaths is increasing. As of 2012, at least 15% of all cancers worldwide, even more in low- to middle-income countries, were attributed to infectious agents [7]. In 2017, almost 10 million people worldwide died of cancer [8]. HBV and HCV are the causative agents of around 80% of hepatocellular carcinomas (HCC), the most common type of liver cancer [9]. Liver cancer rose to being the seventh most common and the third most death-causing cancer worldwide in 2014 [10], having killed almost 820.000 people in 2017 [8]. The global disease burden of chronic hepatitis and associated liver cancer is expected to further increase as annual deaths rose from 0.89 in 1990 to 1.45 million in 2013 [11], whereas HIV-associated deaths declined from 2 million in 2005 to 1.1 million in 2015 [6]. In addition, less than 20% of the estimated 71 million people worldwide [12, 13] living with chronic HCV infection were aware of their infection as of 2017, and only roughly 15% received treatment in that same year [14]. It is this low rate of awareness of their infection of patients, among others, which fuels further spread [15]. Most infections are transmitted by sharing needles among people who inject drugs, use of non-sterile medical equipment, transfusion of unscreened blood products, and sexual practices among men who have sex with men [16-18]. For many years now, direct-acting antivirals (DAAs) have replaced interferon (IFN)-α-based regimens and revolutionized HCV treatment, especially regarding cure rates and side effects [19]. Cure is defined as the absence of detectable HCV RNA in patient serum after a certain time of treatment (*e.g.* 8, 12 or 24 weeks) and called sustained virologic response (SVR). Whereas in the IFN era, SVR rates were around 50%, markedly varying depending on the genotype or comorbidities, DAA treatment achieves SVR rates of usually above 90%, independent of genotype, liver disease, or HIV co-infection [20-22]. Still, due to limitations in diagnosis, access to treatment, and the risk of re-infection in high-risk populations, the demand for further research and a prophylactic vaccine is highly warranted [23-25]. The World Health Organization (WHO) defined the goal of eliminating HCV as a global health threat by 2030, meaning a reduction in incidence by 90% and by 65% in mortality [26].

1.2. HCV classification & epidemiology

HCV is the typical member of the *Hepacivirus* genus in the *Flaviviridae* family [28]. Members of the *Flaviviridae* family are enveloped (+)-stranded RNA viruses with genome length roughly between 9–13 kilobases (kb) [29]. Other genera in this family are *Flavivirus*, *Pestivirus*, and *Pegivirus*. Members of the *Flavivirus* genus are usually arthropod-borne, and cause severe disease in humans, *e.g.* yellow fever virus, West Nile virus, dengue virus, or Japanese and tick-borne encephalitis virus [29]. Economically important are members of the *Pestivirus* genus, which can cause severe harm to livestock, like bovine viral diarrhoea virus or classical swine fever virus. One *Pegivirus* representative is human pegivirus (HPgV, formerly GBV-C/HGV) that causes persistent infections in 1–4% of the world's population without apparent disease formation, but rather with an immune-stimulatory effect [29, 30]. Serological studies suggest that the prevalence is even higher as 5–13% of healthy blood donors were shown to be anti-HPgV E2 positive [31]. Interestingly, HPgV seems to improve disease outcomes in HIV- and Ebola virus-infected people [32, 33]. However, a recent case study described two women that succumbed to leukoencephalitis due to an HPgV infection [34]. GB virus B (GBV-B) was for a long time the only other member of the *Hepacivirus* genus [30]. Since deep sequencing methods have become broadly available though, many non-human homologs of HCV have been found, *e.g.* in horses, rodents, and bats [30]. This development also led to the identification of many more (sub)types of HCV, which comprises now eight different genotypes compiling 90 subtypes [28, 35-37]. The geographical distribution as well as incidence of the eight different genotypes varies vastly around the globe with genotypes (gt) 1 (up to 50%) and 3 (17.9–30.1%) being the most common [27, 38, 39] (Figure 1). Gt 1 dominates Europe, America, and most parts of Asia, although gt 3 is common, too. The hotspot for gt 4 is Africa, and gt 6 is mainly found in East and Southeast Asia. There have been only few patients with gt 7 and 8, originating from the Democratic Republic of Congo and India, respectively [40, 41]. Gt 5 spreads almost exclusively in Africa, and gt 2 is most common in West Africa, but also widely found in East Asia and Japan. In European countries along the
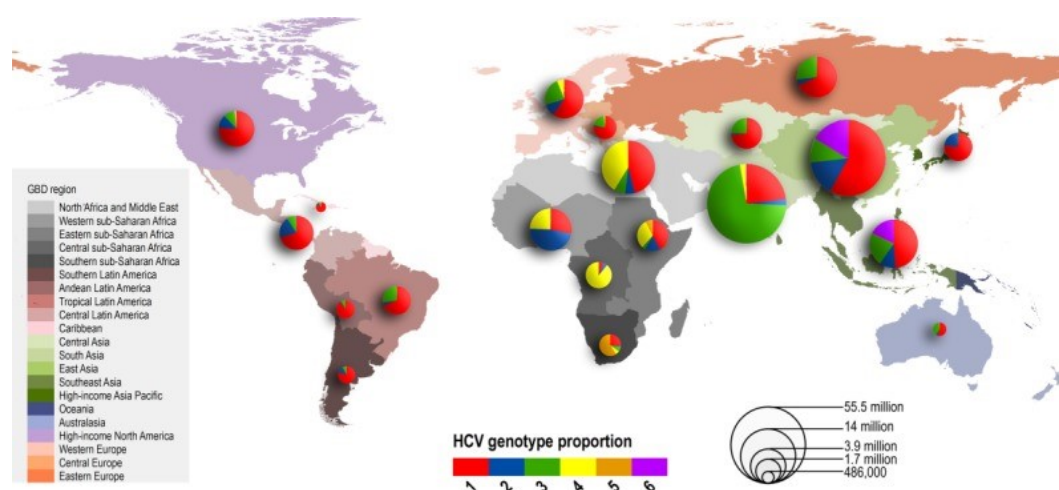
Figure 1 Worldwide prevalence of HCV and distribution of genotypes as of 2015. Genotype (gt) 1 is the most prevalent and dominating gt in most countries, *e.g.* America, Europe, most parts of Asia, Oceania, and North Africa and Middle East. Gt 3 dominates in South Asia and gt 4 is mostly prevalent in Africa. Note that as of 2015 HCV classification compiled only six different gt. Figure from [27].

Mediterranean Sea, gt 2 is highly prevalent in Italy (27%) [42]. The three most common gts in Germany are gt 1 (71.6%), 3 (20.4%), and 2 (5.6%) [27].

1.3. HCV genome organization, polyprotein processing, and protein function

Despite the high diversity of HCV genotypes, there are highly conserved structures and features that hold true for every genotype and subtype. HCV harbors a (+)-oriented, single-stranded RNA genome of about 9.6 kb in length [44]. The 5'- and 3'-ends contain untranslated but highly structured regions essential for RNA translation and replication (UTRs) (Figure 2) [43]. The 5'-UTR contains several stem loops (SL) of which SLII–IV form an internal ribosome entry site (IRES) structure [45-47]. Translation initiates with a very limited set of eukaryotic initiation factors (eIF) and by direct recruitment and binding of the small ribosome subunit 40S and eIF3 to the HCV IRES structure [46, 48, 49]. Upon recruitment of the ternary complex eIF2-GTP-Met-tRNA$_i^{Met}$ and the GTPase-activator protein eIF5, the 80S ribosome is assembled and translation starts from the AUG at position 342 [50, 51]. HCV has also evolved alternative ways of translation initiation in case eIF2 is inhibited by phosphorylation of its α subunit as means of an antiviral response of the cell [52]. In such a case, translation of HCV RNA can be initiated with eIF5B, eIF2B, or eIF2A as replacements for eIF2 [51]. Besides many *trans*-acting host proteins involved in HCV IRES-mediated translation (reviewed in [51]), one micro-RNA (miR) plays an equally unusual as important role, miR-122. The HCV 5'-UTR harbors two conserved miR-122 binding sites around SL1, and four more can be found in the NS5B coding region as well as in the 3'-UTR [53, 54]. MiR-122 is essential for efficient HCV replication, as originally shown by sequestration of miR-122 using complementary 2'-O-methylated RNA oligonucleotides [55]. The miR-122 effects on HCV RNA are multifaceted and include increased translation [56-58], stability [58-61], and replication of the HCV genome [62]. The liver-specific expression of miR-122 likely contributes to the hepatotropism of HCV [63]. The 3'-UTR of the HCV genome contains highly conserved sequences, and especially structures, like a
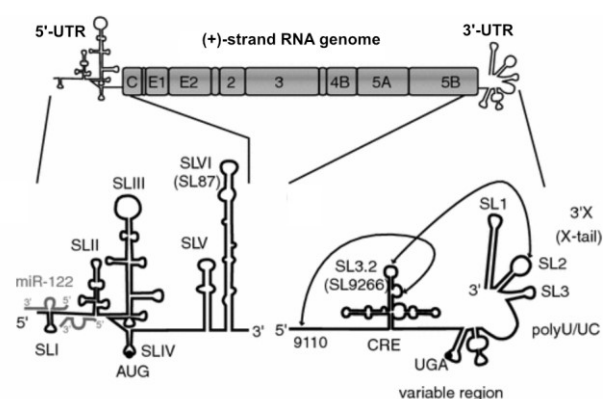
Figure 2 HCV genome organization and features of the highly structured 5'- and 3'-UTRs. The (+)-oriented single-stranded HCV RNA genome is roughly 9.6 kb in length and flanked by untranslated but highly structured regions (5'- and 3'-UTR). The single ORF encodes 10 mature viral proteins, from 5' to 3': Core, E1, E2, p7, NS2, NS3, NS4A, NS4B, NS5A, and NS5B. The 5'-UTR forms an IRES structure and harbors two miR-122 binding sites and several stem loops. The highly structured and partly conserved 3'-end starts already in the NS5B coding region and harbors a *cis*-acting replication element (CRE), a highly conserved polyU/UC tract and the so called X-tail, compiling stem loops 1 to 3 (SL1–3). Arrows indicate long-range RNA-RNA interactions. Adapted from [43].

pseudoknot (CRE) or stem loops SL1–3, that are essential for replication, probably due to their role in (-)-strand synthesis initiation (Figure 2) [43, 64]. Besides the pseudoknot CRE structure that is located in the NS5B coding region, important 3'-components are the variable region, a poly U/UC stretch, and the X-tail, which is composed of SL1–3 [43].

HCV has a single open reading frame (ORF) encoding a large polyprotein that is co- and post-translationally cleaved by host and viral proteases into ten mature proteins (Figure 3) [65]. Core (C) and the two glycoproteins E1 and E2 belong to the structural class of HCV proteins as they form the virus particle [44]. The viroporin p7 and the cysteine protease NS2 are dispensable for replication but essential for assembly [66]. The remaining non-structural proteins are all required for replication: the protease and helicase NS3 with its co-factor 4A, the transmembrane protein NS4B, the phosphoprotein NS5A, and the RNA-dependent RNA polymerase (RdRp) NS5B [67]. The signal sequence between Core and E1 targets the nascent polyprotein to the endoplasmic reticulum (ER), where signal peptidase (SP) cleaves off the immature Core protein from the polypeptide chain [68]. The signal sequence is subsequently cleaved off by the membrane-located signal peptide peptidase (SPP) from the Core C-terminus to yield the mature Core protein (Figure 3) [69]. The mature Core protein forms dimers [70], binds and folds the HCV genome [71], and localizes to lipid droplets [72]. It is required for particle formation as it builds the nucleocapsid. The transmembrane glycoproteins E1 and E2 form heterodimers in the ER membrane and are the major components of the HCV envelope [73]. Their ectodomains, reaching inside the ER lumen, are highly glycosylated (six and eleven glycosylation sites at E1 and E2, respectively) and contain several conserved cysteine residues for potential disulfide bond formation [67]. Indeed, E1 and E2 form oligomers, connected via disulfide bonds upon particle assembly [74].
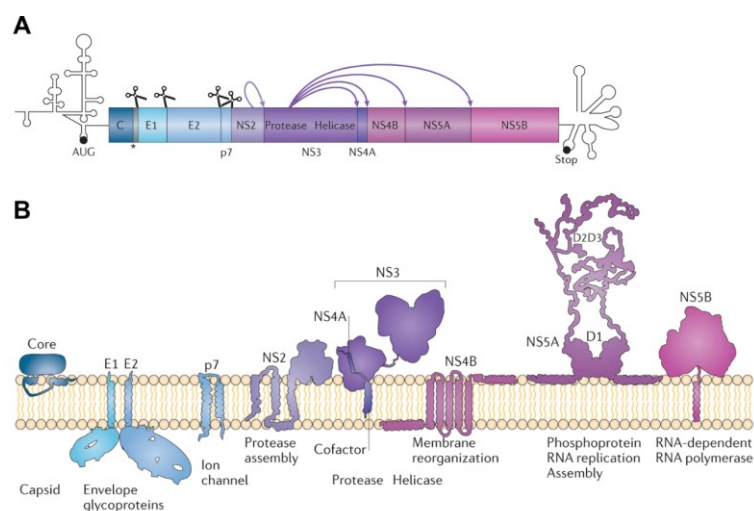
Figure 3 HCV genome organization with indicated cleavage sites of host and viral proteases (A) and mature protein structure and localization (B). (A) The HCV genome harbors highly structured but untranslated regions in its 5'- and 3'-ends. The Core protein (C) is cleaved off from E1 by signal peptidase (indicated by scissors) and further processed by signal peptide peptidase (indicated by *) to the mature version. Further signal peptidase cleavage occurs between E1 and E2, E2 and p7, and p7 and NS2. NS2 cleaves itself off from the polyprotein at its NS3 junction (indicated by light purple arrow) and the NS3 protease processes the remaining polypeptide at the indicated sites (dark purple arrows). AUG = start codon; Stop = stop codon. **(B)** All HCV proteins are membrane-associated, either by one or more amphipathic helices and/or by one or more transmembrane domains. Details are provided in the main text. Adapted from [44].

The viroporin protein p7 forms hexa- and heptameric proton channels to avoid acidification of organelles involved in HCV particle maturation and is required for assembly and release of infectious virions [75, 76]. However, p7 probably exerts other functions in HCV assembly apart from its function as an ion channel [67, 77]. The NS2 cysteine protease liberates itself from the emerging polypeptide by cleaving at the NS3 junction [67]. Apart from this cleavage event, no other targets of NS2 are known [75]. NS2 plays a major role in particle assembly by interacting with various other structural and non-structural HCV proteins [78]; however, NS2 exerts this role independent of its proteolytic activity [79, 80]. NS3 has protease as well as NTPase/helicase function [81]. Its serine protease function is located in the N-terminal part of NS3 with the catalytic triad His-Asp-Ser and is stabilized by a coordinated Zn^{2+} ion between three cysteines and one histidine [81]. The NS3 protease processes the HCV polypeptide at four sites between NS3 and NS5B in a specific, non-sequential order [82]. The NS3 helicase function, which resides in the C-terminal part, is as well required for efficient replication [83] and assembly of infectious particles [84]. It is able to unwind DNA as well as single- and double-stranded RNA (as present in the form of secondary structures in the HCV genome) upon hydrolysis of ATP [81, 85]. The NS3 protease not only processes the HCV polypeptide but also blunts the antiviral response raised by the host cell by cleaving the signaling proteins MAVS [86] and TRIF [87] (details below). NS3's co-factor NS4A helps in proper folding and membrane anchoring of NS3 via its N-terminal transmembrane domain [81, 88] but without affecting RNA unwinding rate or processivity of the NS3 helicase [85]. The highly hydrophobic transmembrane protein NS4B seems to be the major player in inducing the membrane alterations that lead to the formation of the HCV replication compartment (RC), often designated the "membranous web" [89, 90]. NS4B consists of two N-terminal amphipathic helices, four transmembrane domains, and two C-terminal α-helices with two palmitoylation sites [89, 91]. The C-terminal domain is highly conserved and responsible for NS4B oligomerization and membranous web formation [92, 93]. The phosphoprotein NS5A has an N-terminal amphipathic membrane anchor and three domains (D1–3), separated by the two low complexity sequences (LCS) LCS1 and LCS2 [67]. NS5A exists in at least two distinct forms, the hypophosphorylated p56 and the hyperphosphorylated p58 form [94]. The phosphor-sites are serines mainly located in LCS1 and LCS2 [67]. NS5A domains D1 and D2 are indispensable for replication, whereas D3 is required for assembly but dispensable for replication [95-98]. D1 is the only domain for which the structure could be resolved [99] as D2 and D3 are highly unstructured. Accordingly, D1 forms at least dimers in its active form i) in which each monomer coordinates one Zn^{2+} ion and ii) which builds a groove for RNA binding [99]. This theoretical proof for the RNA binding ability of NS5A is supported by biochemical evidence of NS5A binding to HCV RNA [100]. The intrinsically unfolded nature of D2 and D3 is thought to support the various interactions of NS5A with host and viral proteins [67]. Two of these host factors, caseine kinases Iα and II, phosphorylate NS5A and give rise to the hypo- and hyperphosphorylated forms [96, 101]. Another one, phosphatidylinositol-4 kinase III α (PI4KIIIα), is the most robustly reported HCV host factor and recruited as well as activated by NS5A. PI4KIIIα is essential for the formation of the membranous web and thus for HCV replication [102-104]. The last encoded protein on the HCV genome is the viral RdRp NS5B [105]. The polymerase synthesizes the (-)-strand replication intermediate as well as progeny (+)-
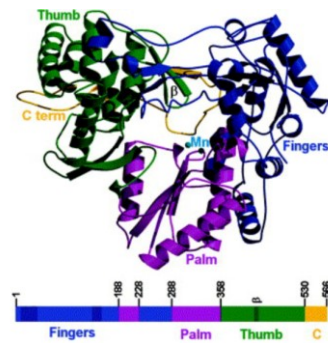
Figure 4 Ribbon diagram of a genotype 1b (J4) RdRp with a C-terminal truncation (NS5BΔC21) representing the so-called right-hand structure with fingers, thumb, and palm. The finger domain is in blue, palm in purple, thumb in green, and the C-terminus in yellow. The position of the inhibitory ß-flap and the complexed Mn^{2+} ions are indicated. Adapted from [112].

strands for translation or particle assembly in the RC. NS5B is a typical RdRp forming a so-called right-hand shape with palm, thumb, and finger domains (Figure 4) [43]. Its active domain is located in the N-terminus, separated by a linker domain from the C-terminal membrane anchor [106]. The C-terminus is dispensable for its RdRp activity but required for HCV replication [107]. Most crystallization studies have used the C-terminally truncated version (ΔC21) due to its largely increased solubility [43, 108]. The active site of the polymerase is the highly conserved GDD motif [109] and has complexed two divalent metal ions for NTP polarization, either Mn^{2+} or Mg^{2+} [110, 111].

1.4. On the history of hepatitis C virus (HCV)

The discovery of hepatitis C, back then non-A non-B hepatitis (NANBH), was already in 1975, when HBV and HAV could be excluded as causative agents of the observed transfusion-mediated hepatitis [113, 114]. It then took almost 15 years until the tremendous efforts undertaken by many groups culminated in the first successfully identified cDNA clones of HCV [115, 116]. This finally allowed the screening of blood products for the presence of HCV antibodies and eventually led to the disruption of this major route of transmission [117, 118]. Having HCV RNA at hand allowed a first characterization of the viral RNA sequence as well as its encoded proteins in expression studies [113, 119, 120]. Ten years later, in 1999, many aspects of HCV biology, like genome orientation, length, polyprotein processing, and the functions of at least the enzymatic HCV proteins had been illuminated [121-123]. However, just then, the first successful, robust and continuous replication of HCV in cell culture was reported [124]. Key to this success was the development of self-replicating subgenomes, dubbed "replicons", where the structural gene information was replaced by a neomycin phosphotransferase gene (neo) conferring resistance to neomycin (G418) (Figure 5) [124]. This allowed the selection of cell clones stably replicating HCV RNA and expressing the antibiotic resistance gene to sufficient amounts. Among many tested cell lines, only one yielded clones with robust replicon levels after selection, the human hepatoma cell line Huh7 [125] (reviewed in [126]). Those stable replicon cells paved the way for studies on replication, pathogenesis, and high-throughput antiviral screening [124]. The replicon in this initial study was based on a genotype 1b isolate and derived from a consensus sequence that was cloned from two genome fragments (Con1). Later, it was found that adaptive mutations that occurred
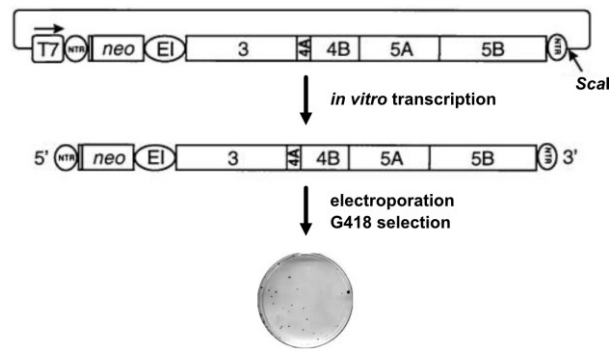
Figure 5 Depiction of the strategy that allowed HCV replication in cell culture for the first time. The consensus sequence, cloned from a patient isolate, was modified as follows. A neomycin phosphotransferase (*neo*) gene, allowing antibiotic selection with G418, replaced the genetic information for the structural genes. For robust expression of the non-structural genes NS3–NS5B (3–5B), an EMCV IRES (EI) was inserted after the *neo* gene. A T7 promoter drove the *in vitro* transcription to gain a high quantity of (+)-strands. These (+)-strands were electroporated into cells, and after few weeks of culture under G418 selection, clones, carrying the replicating HCV subgenome, came apparent. *Sca*I, restriction enzyme cleavage site for terminating transcription; NTR = non-translated region; EI = EMCV IRES; T7 = T7 polymerase promoter. Adapted from [128].

during the selection process were responsible for the efficient replication of that replicon [127, 128]. Stable replicon cell lines were established and named after their encoded genes, for example Huh7-LucUbiNeo (luciferase, ubiquitin, neomycin phosphotransferase) [129, 130]. Similar efforts as for the Con1 replicon yielded the subgenomic Japanese fulminant hepatitis (JFH-1) replicon, which belongs to genotype 2a, and became the gold standard in HCV research due to its unprecedented replication efficiency [131]. Intriguingly, JFH-1 replicated efficiently without conferring any adaptive mutations [131]. It became the first full-length HCV genome that could be propagated in cell culture and produced progeny virus [132, 133]. Still today, it is the only isolate that efficiently replicates in cell culture without requiring adaptive mutations [134]. Based on the JFH-1 replicase, infectious chimeric full-length versions of all seven HCV genotypes have been developed, allowing the study of their differences in infectivity, neutralization, and particle formation [135]. Also the JFH-1 replicon was used to generate a stable replicon cell line, named Huh7-LucUbiNeo-JFH [136], that allowed the development of drugs or testing the impact of different interferons on HCV replication. Curing such cell lines from their replicon by using IFN in combination with nucleotide analogs or drugs directly affecting HCV proteins, yielded cell lines with high HCV replication efficiency that could be used for transient replication or infection assays [126]. Those cell lines support HCV replication to much higher levels than their mother cell lines, although the underlying mechanisms mostly remain elusive [126]. Examples for such cell lines are Huh7-Lunet [137] or Huh7.5 cells [138]. We have learned a lot in the last two decades about the molecular biology of HCV, its host factors as well as viral determinants, and achieved effective treatments [65]. However, there are still many open questions, regarding the role of host factors for viral replication, the molecular processes involved in liver disease formation, and the molecular action of inhibitors of viral proteins [23].

1.5. The HCV life cycle

HCV infection is transmitted parenterally where HCV particles reach hepatocytes, the main HCV target cells, via the bloodstream [139, 140]. HCV particles are tightly associated with lipids, lipoproteins, and cholesteryl esters, forming so-called lipoviroparticles (LVPs), and localize to the low- to very low-density lipoprotein (LDL/VLDL) fraction upon purification from patient serum [141, 142]. The buoyant densities span from 1.25–1.06 in patient serum and are around 1.1 g/mL in cell culture-produced HCV particles (HCV$_{cc}$) due to heterogeneity of the lipid coat [66]. The infection process starts with attachment of the LVPs to the hepatocyte basolateral surface (Figure 6A). This process is mediated by interaction of heparin sulfate proteoglycans (HSPG), LDL receptor (LDLR), and scavenger receptor class B member I (SCARB1 or SR-BI) with mostly the LVP lipoprotein components but also the HCV glycoprotein E2 [143, 144]. Conformational changes in E1 and E2 allow further interactions with cluster of differentiation 81 (CD81) [145] which in turn leads to a re-localization of the LVP to tight junctions and the recruitment of claudin-1 (CLDN) [146] and occludin (OCLN) [147] [143, 148]. The receptor-LVP complex is internalized in a clathrin-dependent manner and the viral envelope fuses with the endosomal membrane in a pH-dependent fashion [149-151]. This fusion liberates the viral RNA genome into the cytoplasm where the host translation machinery directly starts translation via the IRES structure in the 5'-UTR of the genome. After polyprotein processing, replication of the viral genome takes place in specialized, ER-derived replication organelles that form the membranous web (Figure 6A) [90, 152, 153]. Those specialized compartments highly protect the viral genome and its (-)-strand
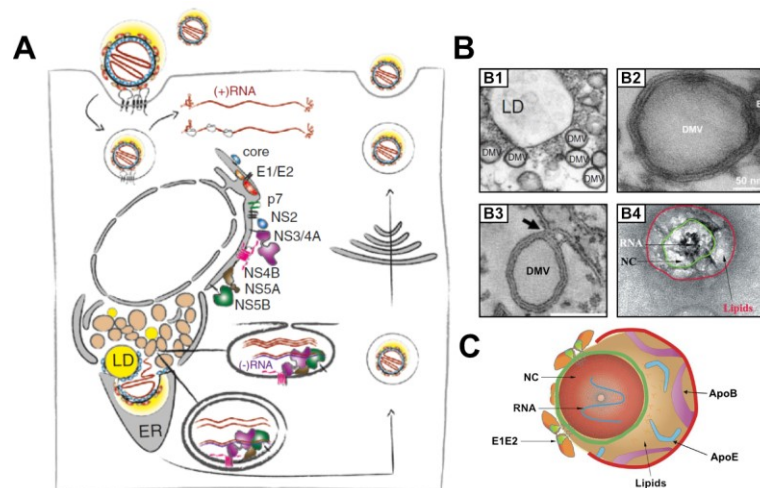
Figure 6 Schematic of the HCV life cycle (A), electron micrographs of the membranous web, DMVs, and HCV particle (B), and cartoon image of a mature HCV LVP (C). (A) The HCV life starts with the infection of a host cell, internalization of the LVP, and release of the viral (+)-RNA (top left corner). Translation yields mature viral proteins at the rough ER, which induce the formation of the membranous web where viral RNA replication takes place in exvaginations from the ER and DMVs, and assembly of viral particles occurs in close proximity to LDs (middle to lower left corner). Assembled particles are secreted via the secretory pathway (right part). **(B)** Electron micrographs showing key features of HCV replication. **B1** shows DMVs in close proximity to LDs. **B2** shows a single DMV in high resolution. **B3** shows a single DMV after putative exvagination from and still connected to the ER. **B4** shows an authentic HCV LVP isolated from patient serum. **(C)** Cartoon image based on findings from electron micrographs, showing the viral genome (RNA) encapsidated by Core (NC), and surrounded by the envelope proteins E1 and E2 (E1E2). The viral envelope is further enwrapped in a lipid layer, containing apoE (ApoE) and apoB (ApoB) apolipoproteins. (A) and B1 are adapted from [43]. B2 and B3 are adapted from [152] and B4 and (C) are adapted from [154].

replication intermediate as well as the viral proteins needed for replication as shown by nuclease and protease treatment [43]. The membranous web is a polymorphic structure that contains single-, double-, and multi-membrane vesicles, originated from various cellular structures, mainly the ER, but also endosomes, mitochondria, and lipid droplets (LDs) (Figure 6A, -B) [152]. The formation of those vesicles is a concerted action of the viral non-structural proteins since expression of neither of the singular ones yields sufficient amounts of especially double-membrane vesicles (DMV) in which replication is thought to happen (Figure 6B1–3) [152, 155]. In contrast to invaginations from the ER membrane as during dengue virus replication [156], DMV structures might rather form from exvaginations from the ER during HCV infection (Figure 6B3) [152]. Besides the non-structural HCV proteins, also host proteins seem to be involved in DMV formation, as suggested for the autophagy protein Atg5 [157] and the vesicle-associated membrane protein-associated proteins A (VAP-A) and B (VAP-B) [155], and convincingly shown for the integral membrane protein Surfeit-4 [158]. The close proximity to LDs and the nature of the LVPs prompted investigators to speculate that LDs are the site of assembly for infectious HCV particles for a long time, although convincing studies were missing [66]. A recent study though provided evidence for putative assembly sites at LDs tightly wrapped by ER membranes and co-localized with the envelope protein E2, the nucleocapsid protein Core, and NS5A as a representative of the replicase machinery [159]. Key roles in this assembly and recruitment processes are not only inherent to Core and NS5A, which are able to localize to LDs via their amphipathic helices [160, 161], but especially to NS2, which presumably via p7 and NS3 recruits the replicase complex to LDs [78, 162, 163]. Due to the pleomorphic structure and lipid composition of HCV particles, visualization of budding particles could still not be achieved in this study [164]. However, another recent study was successful in specifically purifying HCV particles from patient serum and cell culture supernatants to give us high-resolution insights into the face of mature HCV particles (Figure 6B4) [154]. Assembled particles are secreted via the VLDL pathway to enter the bloodstream and accordingly contain apolipoproteins E, B, and others [142, 154, 165, 166].

1.6. Host factors involved in HCV replication

Since HCV brings along only the required machinery to replicate its genome and assemble its particles, it heavily relies on host components in almost every step of its entire life cycle. Before entering the cell, HCV already requires the presence of surface proteoglycans and receptors to be able to attach to and enter the cell, namely SCARB1, CD81, CLDN1, OCCL, and others (see also above) [167]. Interaction with those surface markers is only partly attributable to the HCV envelope but also necessarily to its lipid coat, including apolipoproteins E (apoE), apoB, and many others [168]. After entry, HCV RNA is directly translated via its IRES structure. During translation initiation, miR-122 plays a central role in stabilizing HCV RNA and favoring a translation-competent secondary and tertiary structure [58] (see above). For efficient replication, HCV usurps cellular enzymes and lipids to build its membranous web. One of the key enzymes in this process is PI4KIIIα that is recruited by NS5A and catalyzes the formation of phosphatidylinositol 4-phosphate (PI4P) [104]. PI4P is enriched in HCV replication compartments and recruits further host proteins, like oxysterol-binding protein (OSBP), Niemann-Pick-type C1 (NPC1), and others that contribute to the

optimal lipid and protein composition of the membranous web [167, 169, 170]. NS5A also interacts with a peptidylprolyl isomerase (PPIA, also known as CypA), that is essential for HCV replication [171, 172]. The mechanism of action is still elusive, but certainly affects membranous web formation [173]. However, if the physical interaction between PPIA and NS5A or the prolyl isomerase activity of PPIA is crucial, is hard to determine since both functions reside in the very same site of the protein and cannot be separated from each other ([174] and references therein). The last step of the HCV life cycle, particle assembly and release, heavily depends on the host supply of lipid coat components as well as its secretory pathway. Diacylglycerol O-acyltransferase 1 (DGAT1) is a critical enzyme involved in LD biogenesis and recruits HCV Core to LDs during the assembly process [175]. Upon knockdown of DGAT1 or by using an inhibitor, HCV particle assembly and release are severely impaired [175]. The importance of lipids and lipoproteins during HCV infection can thus not be underestimated and shows its intricate and sophisticated adaption to its human host.

1.7. Treatment of chronic HCV infection

Most HCV infections present with very mild to no symptoms and progress into chronicity in 75–85% of patients [176]. Rare acute hepatitis C shows among other symptoms: jaundice, fatigue, vomiting, and abdominal pain [177]. Worldwide, an estimated 71 million people are chronically HCV-infected [12] and despite effective treatment options, awareness of infection and access to diagnosis are low; hence, numbers of new infections are on the rise [11, 178]. Although NANBH was well-described [114], it was even before HCV was identified as its causative agent in 1989 [115] that the first ten patients were treated in a pilot study using recombinant IFN-α [179]. Remarkably, 50% of those patients achieved long-time SVR and were free of detectable viral load even 15–25 years later [22, 179]. Unfortunately, this clearance rate could not hold up in large trials, and SVR rates turned out be as low as 6–19% [22] (Figure 7). In the following years, SVR rates steadily increased by combining IFN-α with the guanosine analog Ribavirin (RBV) that proved broad antiviral activity [180], and later by covalently attaching chains of polyethylene glycol (PEG) to IFN-α [22] (Figure 7). PEG-IFN-α showed extended serum half-life, which allowed reducing
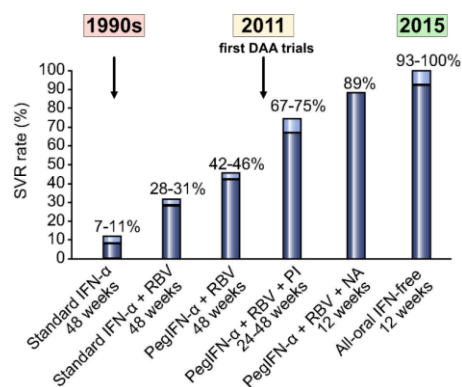
Figure 7 Cure rates (% SVR) of chronic HCV infection in patients from the 1990s to 2015. Treatment of chronic HCV infection started with recombinant IFN-α, was then combined with Ribavirin (RBV) and IFN-α was later replaced by polyethylene glycol (PEG)-IFN-α. The first direct-acting antivirals (DAAs) against HCV used in combination with PEG-IFN-α and RBV were protease inhibitors (PI) targeting HCV NS3/4A. The first nucleotide analog (NA) used in such a combination therapy (instead of PIs) was Sofosbuvir. From 2015 on, IFN-free regimens became widely available. RBV = ribavirin. Adapted from [22].

administration by injection from daily or three times a week to once per week, probably increasing patient compliance [181]. Combination therapies of PEG-IFN-α + RBV led to SVR rates of overall 50% with vast differences between genotypes [22]. The dawn of direct-acting antivirals (DAAs) against HCV improved SVR rates further. The first DAAs used in combination therapies with PEG-IFN-α + RBV were inhibitors against the HCV protease/helicase NS3/4A (PI), Boceprevir [182, 183] and Telaprevir [184, 185] in 2011. These first-wave first-generation PIs increased SVR rates to around 70% but were less well-tolerated, genotype-restricted, and had low barriers to the emergence of resistance mutations [186] (Figure 7). These downsides of first-generation PIs vanished rapidly with the development of second- and third-generation PIs and with the combination of DAAs against other viral proteins [187]. Shortly after, in 2013, the first approved drug against the HCV RdRp NS5B hit the market and raised clearance rates further to 90% on average, the nucleotide analog Sofosbuvir (SOF) [188, 189]. SOF was the first DAA to be administered in an IFN-free regimen, either with [190-192] or without RBV [193-196]. In 2014, the first all-oral single-tablet regimens were available, providing a huge release of administration and side effect burden for the patients [189]. With those, also inhibitors of the HCV phosphoprotein NS5A joined the team of clinically administered DAA, amongst the first ones Ledipasvir and Daclatasvir [193, 196]. As of today, the majority of patients ca be treated with pan-genotypic, all-oral single-tablet regimens once daily [20, 197] and achieve SVR rates of 95–100% in the course of an eight- or 12-week treatment [198-200]. Besides the overwhelming advantages of no to only mild side effects, easy one-pill-per-day-treatments, and short treatment times, hurdles and problems in the DAA era still exist. Treatment costs are often high, especially in the developed world, drug-to-drug interactions do exist and need to be carefully considered, and resistance-associated mutations (RAS) arise during therapy [23, 201, 202].

1.8. The innate immune response to HCV infection

The innate immune response poses the first line of defense against invading pathogens. Upon sensing of infection, many signaling pathways are triggered and specialized immune cells of the innate and adaptive system are recruited [203]. Despite the importance of natural killer (NK) cells, dendritic cells (DCs), neutralizing antibodies, the complement system, as well as CD4+ and CD8+ T cells in HCV clearance [204, 205], the following section focuses on the cell-intrinsic antiviral immune response.

1.8.1. HCV RNA detection and signal cascade activation

The first act of an antiviral response of the host cell is detection of the viral invader. Cells evolved many ways to sense so-called pathogen-associated molecular patterns (PAMPs) that can be nucleic acids or other components of the pathogen body [206]. The main sensors of nucleic acids constitute three classes of pattern recognition receptors (PRRs): toll-like receptors (TLRs), retinoic acid inducible gene I (RIG-I)-like receptors (RLRs), and cytosolic DNA sensors [207]. Since the cytosolic DNA sensors as well as some members of the TLR family mainly recognize bacterial and viral DNA [206-208], this chapter will mainly focus on those receptors sensing single- (ss) and double-stranded (ds) RNA. Those comprise TLR3, -7, and -8 as well as the RLRs RIG-I, melanoma differentiation antigen (MDA5), and DExH-box helicase 58 (DHX58, also called LGP2). The TLRs

sense foreign nucleic acids either on cell surfaces or in endosomal compartments, whereas RIG-I, MDA5, and LGP2 are cytoplasmic RNA sensors [206]. TLR3, -7, and -8 are widely expressed on specialized immune but also on epithelial and other non-immune cells [209]. TLR3, RIG-I, MDA5, and LGP2 are strongly activated upon binding of dsRNA, a side product of HCV replication [210-213]. Consequently, all of them are able to sense HCV infection [214-218], however the main sensor for HCV RNA seems to be RIG-I [219] and LGP2 lacks CARD domains that are essential for signal transduction, thus its role in antiviral signaling is controversial [213]. Also TLR7 has been implicated in HCV RNA sensing in macrophages and plasmacytoid DCs [220, 221], although TLR7 and -8 mostly recognize ssRNA, for example during HIV-I, influenza A virus or vesicular stomatitis virus infections [222, 223]. Although differently located, sensing of such dsRNA by TLR3 or RIG-I and MDA5 culminates in the activation of the same signaling cascades. Activation leads to phosphorylation of the transcription factors interferon regulatory factor 3 (IRF3) and IRF7 by inhibitor of NF-κB kinase (IKK) epsilon (IKKε) and TANK binding kinase 1 (TBK1) [224, 225]. The TLR3-TRIF pathway also activates the transcription factor NF-κB via a different route [211, 223]. Those executive kinases are recruited by the adaptor proteins Toll-interleukin (IL)-1 receptor domain-containing adaptor inducing IFN-β (TRIF) (in case of TLR3) or mitochondrial antiviral signaling protein (MAVS) (in case of RIG-I and MDA5) [206]. The phosphorylated IRFs dimerize and shuttle to the nucleus where they lead to the expression of type I (IFN-β) and III (IFN-λ) IFNs and several ISGs [226-228]. This first wave of IFNs triggers the expression of hundreds of more ISGs via JAK-STAT signaling in auto- and paracrine manner [229]. Type I IFNs, which also include IFN-α and others, signal through a heterodimer of IFN alpha and beta receptor subunit 1 (IFNAR1) and IFNAR2, whereas type III IFNs bind a heterodimer of IFNLR1 and IL10 receptor beta (IL10RB) [230, 231]. This heterodimerization recruits the Janus kinases JAK1 and TYK2, which phosphorylate the intracellular receptor domains, which in turn recruits signal transducer and activator of transcription 1 (STAT1) and STAT2 [229]. Phosphorylated STAT1 forms either homodimers or heterodimers with STAT2, which further recruit IRF9 to form ISGF3. Those complexes translocate to the nucleus and drive transcription of more ISGs [230]. To prevent overshooting of the system, negative regulators are also upregulated that prevent further stimulation of the system (see below). One highly interesting just recently discovered IFN-λ exerts both, anti- as well as pro-viral activities during HCV infection, equally baffling and exciting researchers, IFN-λ4. A single nucleotide deletion leads to a frameshift and creates an ORF, which allows the production of IFN-λ4 and results in reduced rates of spontaneous clearance and achieved SVR in IFN-based treatment outcomes [232]. IFN-λ4 activates JAK-STAT signaling as do the other type I and III IFNs and thus inhibits HCV replication *in vitro*; however, it also leaves the cells refractory to further type I or type III IFN stimulation [232]. HCV infection specifically triggers IFN-λ4 expression and thereby effectively blocks IFN-α signaling via negative feedback by ISG15, ubiquitin-specific peptidase USP18, and suppressor of cytokine signaling 1 (SOCS1) [233, 234]. ISG15 is a ubiquitin-like, IFN-stimulated gene (ISG) that is up-regulated not only upon IFN stimulation but many other stimuli like dsRNA, viral infection, or lipopolysaccharide (LPS) [235, 236]. It can exert its function either unconjugated as a cytokine or by conjugation to other proteins and thus modifying their function, a process known as ISGylation, similar to ubiquitination [235]. One

example is ISGylation of IRF3, which prevents its polyubiquitination and subsequent degradation, thereby preserving the antiviral state of the cell [237]. However, ISGylation can also lead to aggregation and lysosomal degradation of proteins, blockage of interaction with other proteins, or changes in the autophagic flux in the cell, the latter posing a possible explanation for the often chronic course of HCV infection due to increased IFN-λ4 expression [236]. Additionally, it was shown that overexpression of ISG15 or knockdown of a protein involved in ISGylation increases and inhibits HCV replication, respectively [238]. The mechanism though still needs to be determined. USP18, a negative regulator of the IFN pathway cleaves off ISG15 from other proteins and thereby markedly contributes to the suppression of JAK/STAT signaling [239, 240]. USP18 also blocks the interaction between IFNAR2 and JAK independent of its ISG15 protease activity and thus blunts further signal transduction upon IFNAR receptor activation [241]. Collectively, it seems that HCV has subverted the antiviral activities of IFN-λ4 and turned them into its own advantage.

1.8.2. ISGs with anti-HCV activity

Many of the IFN-triggered ISGs exert antiviral activity against HCV as revealed by large overexpression and knockdown studies [242-247]. Most of them have been confirmed in *in vitro* studies, often using the replicon system or transient replication of subgenomic reporter RNAs [226]. However, several examples show that an authentic HCV infection is less sensitive to certain ISGs and IFN treatment, pointing towards effective interfering strategies by especially structural HCV proteins [52, 226, 230]. Still, few examples have robustly proven their anti-HCV action in diverse studies. Among them are the RNA sensors that initiate the antiviral response upon infection or sensing of dsRNA, like RIG-I, dsRNA-activated protein kinase PKR (also known as EIF2AK2), MDA5, or effector and positive feedback loop proteins like many IRFs, IFN-α inducible proteins (IFIs), IFN-induced proteins with tetratricopeptide repeats (IFITs), and IFN-induced transmembrane proteins (IFITMs) [226, 242]. IFIT proteins for example have been shown to inhibit HCV RNA translation by binding and functionally sequestering viral RNA or the translation initiation factor eIF3 [247-250]. IFITM proteins rather affect viral entry by interacting with important receptors or RNA replication by interfering with membranous web formation or homeostasis [247, 251]. The latter mechanism of action might also hold true for viperin (also known as RSAD2), which localizes to the ER-LD interface, a hot spot for viral RNA replication and assembly [247]. Supporting this notion, IFITM1 as well as viperin bind VAP-A, a major component of HCV replication complexes [155, 159, 247]. The role of PKR in controlling HCV replication is ambiguous, as reports for pro- and anti-viral effects exist [52, 244, 250]. However, HCV might induce and activate PKR at first to stop translation of ISGs (PKR phosphorylates and thereby suppresses eIF2 activity, which is required for translation) but later block PKR to assure the supply of host products HCV needs for its replication and particle assembly. Further, the 2'-5'-oligoadenylate synthetase/ribonuclease L (OAS/RNase L) system restricts HCV replication by endonucleolytic cleavage of the HCV genome, liberating dsRNA that in turn again can stimulate the antiviral response [252]. Despite the robust expression of all those ISGs counteracting HCV replication, HCV still persists in a natural infection and high base-level ISGs are even predictive markers for non-responsiveness to IFN treatment [253]. Why this is the case, is not entirely clear, yet, but countermeasures by HCV proteins probably contribute to this phenomenon.

1.8.3. Countermeasures by HCV

The best established counteraction of an HCV protein is cleavage of the adapter protein MAVS by HCV NS3/4A to prevent signaling and activation of IRF3 and similar transcription factors, which could be shown in cell culture [86, 254, 255] as well as *in vivo* [256]. TRIF, the TLR3 signal mediator, was reported to be a target of NS3/4A cleavage *in vitro* and in cell culture systems [87]; however, another group found that NS3/4A is not able to cleave TRIF in such settings [257]. The role of PKR in HCV immune evasion is controversial due to reasons described above, but NS5A and E2 have been reported to suppress PKR activity and thus halt ISG induction [258]. Autophagy, a cellular recycling and homeostasis process, is induced upon HCV infection and helps, especially in the early phase, to establish HCV replication by suppressing the antiviral response of the host cell [259-261]. This induction occurs either indirectly via ER or oxidative stress or directly via physical interaction of HCV and autophagic proteins [259]. In case those countermeasures are not sufficient, HCV has evolved ways to suppress IFN signaling upon activation of the JAK-STAT pathway. NS5A [262] and Core [263] have been shown to reduce phosphorylated (p)STAT1 levels and expression of several HCV proteins leads to lower total STAT1 as well as pSTAT1 levels, although only Core was found to directly bind to STAT1 [264]. Only pSTAT1 forms functional transcription factor complexes that shuttle to the nucleus to activate transcription of ISGs. Further, the HCV viroporin protein p7 was recently reported to induce SOCS3 expression, a negative regulator of the JAK-STAT pathway [265]. In summary, HCV evolved sophisticated and multifaceted ways to avoid a strong antiviral response upon infection, allowing it to build its replication compartment and establish a persistent infection.

1.9. Mathematical modeling of HCV infection

Finding answers to questions regarding the virus-host interplay are difficult considering such intricate biological systems. Thus, researchers developed mathematical models describing biological systems in the most simplified way to gain such insights. The first patient-relevant mathematical models described HIV-1 serum decline upon ritonavir (a protease inhibitor) treatment and gave insights into virion half-life, duration of its replication cycle, and provided first treatment guidelines [266-268]. Mathematical models of HCV infection derived from those and appeared during the IFN-α treatment era [269-271]. Authors explained the dose dependence of viral decline during the first 48 hours of IFN-α treatment by a halt in virion production rate and estimated the same to be around 10^{12} virions per day (untreated), whereas virion half-life should be around 2.7 hours [269, 270]. Modeling HCV RNA serum kinetics after liver transplantation suggested an extrahepatic HCV reservoir that accounts for 3–4% of HCV serum RNA [272, 273] and yielded an estimate of infected hepatocytes in the liver of 19% [273]. Such insights were hard to achieve at a time where no cell culture models for HCV existed and recommendations for improved treatment schedules were highly warranted. The first more detailed model of intracellular HCV replication to learn about the molecular virology was developed by Dahari and colleagues [274] and is based on the first of its kind detailed models of viral replication for the bacteriophage Qβ [275]. Dahari *et al.* showed the necessity of the replication compartment as a restricted space for HCV RNA synthesis to explain intracellular HCV RNA replication dynamics, and

especially steady-state levels of HCV RNA [274]. Further, they gave a rationale for the observed 10:1 ratio of (+)- to (-)-strand RNA in such intracellular settings [274] that could be supported by *in vitro* findings [276]. An extension and refinement of the Dahari model was developed by Binder and colleagues to account for the highly initial phase after transfection of a host cell that could not be explained by the Dahari model [277]. The Binder and the Dahari model are both based on ordinary differential equations (ODEs) that describe every necessary step of intracellular HCV replication to accurately simulate replication dynamics (Figure 8). The Binder model underpinned the importance of the replication compartment to prevent excessive viral RNA replication and translation and allowed to simulate HCV replication in both, lowly and highly permissive cells [277]. The latter was remarkable, and was achieved by the introduction of a host factor species, which might be a protein, a protein complex, or a host process, involved in the establishment of the replication compartment and (-)-strand RNA synthesis [277]. Since the nature of the huge differences in permissiveness between different Huh7 derivatives was and still remains elusive, those modeling-derived insights were highly valuable and allowed further investigations of the key players in this phenomenon [277, 278]. Further, the Binder model was able to simulate the

$$\frac{dR_p^{unp}}{dt} = -k_0 R_p^{unp} - \mu_p^{unp} R_p^{unp} \quad (1)$$
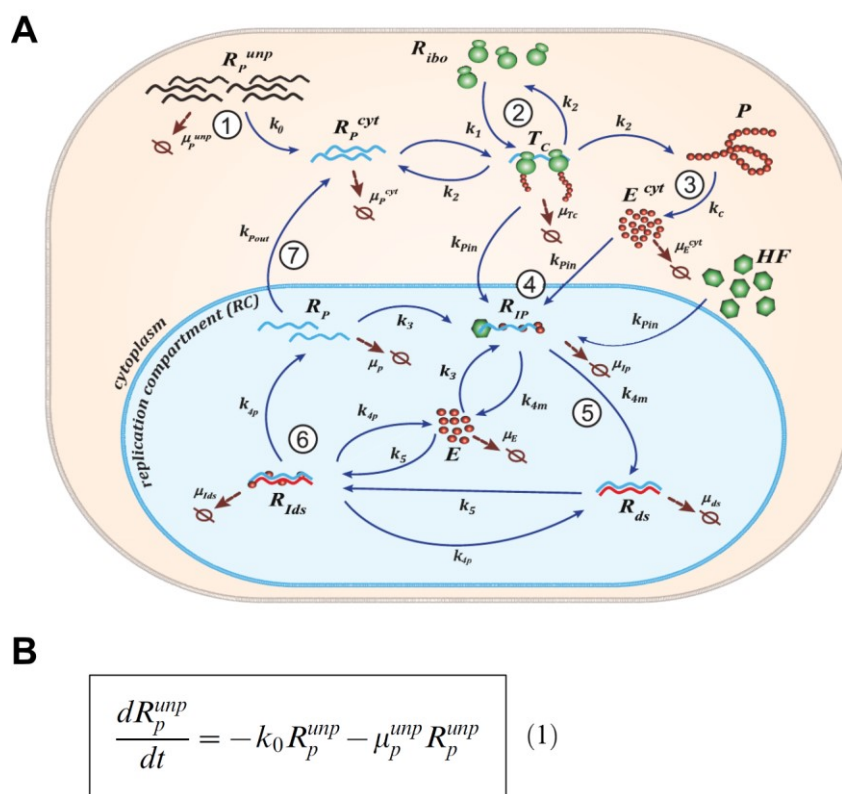
Figure 8 The Binder model for intracellular HCV replication (A) is based on ODEs (B). (A) The model scheme shows one cell with transfected viral RNA ($R_P{}^{unp}$) that is processed to a translation-competent form (step 1), $R_P{}^{cyt}$. $R_P{}^{unp}$ degrades with rate $\mu_P{}^{unp}$ and is processed to $R_P{}^{cyt}$ with rate k_0. These processes are represented in equation (*1*) (B). $R_P{}^{cyt}$ is then able to be translated by the host translation machinery (*2*) and the polyprotein *P* forms. The polyprotein is then processed with rate k_c into the mature viral proteins E_{cyt}. Translated RNA, together with E_{cyt} and a host factor (*HF*) can then initiate (-)-strand synthesis in the replication compartment (RC) (4). The (-)-strand initiation complex R_{IP} forms a double-stranded RNA intermediate R_{ds} (5) which can again associate with the viral polymerase (*E*) (R_{Ids}) to form progeny (+)-strands (6). Those (+)-strands are then exported to the cytoplasm where they re-enter the cycle (7). *k* are rate constants, and *μ* are degradation rates. (B) shows one ODE as an example: equation (1) describing the amount of unprocessed, transfected RNA over time. Adapted from [277].

replication of attenuated versions of the subgenomic HCV RNA that it was calibrated on [277]. A sensitivity analysis revealed that the most influential parameters through therapeutical intervention in the initial phase of replication are the RNA synthesis steps k_{4m} and k_{4p} governed by the viral polymerase NS5B in the RC [277]. Interestingly, a fundamental part of today's HCV regimens is the NS5B inhibitor SOF, targeting exactly those steps. In addition, the model correctly predicted the rather low sensitivity towards targeting the polyprotein processing step k_c, exerted by the NS3/4A protease, and the consequent low barrier of developing resistance mutations at only minor fitness costs that proved correct in the real world [277]. As such, the model gave valuable insights into different aspects of HCV replication that were hard to gain by sole experimental approaches. Still a major limitation of the model was the restriction to only intracellular HCV replication, which did not represent an authentic infection including cell entry, particle production, and spread [277]. In such a model, the impact of pharmacological intervention on virus production or spread of the infection could be assessed, gaining useful information about the real world efficacy of drugs. Thus, it is highly warranted to expedite mathematical models for HCV replication to gain deeper insights into HCV pathogenesis and improve our understanding and treatment of the disease.

2. MATERIAL

2.1. Cell lines

name [reference]	used for	comment
Lunet-CGM [this study]	Jc1 infection dynamics	described in detail in Methods section; based on Huh7-Lunet [137]/Huh7-Lunet-CD81high cells [279]
LucUbiNeo-JFH [136]	validation of putative HCV host factors	Huh7 cells carrying a stably replicating subgenomic reporter version of HCV; under G418 selection (1 µg/mL)
Huh7-LP [277]	validation of putative HCV host factors	low passage and lowly permissive Huh7 cells
Huh7-HP [280]	validation of putative HCV host factors	high passage and highly permissive Huh7 cells
Huh7.5 [138]	Jc1 and JcR2a virus production	highly permissive Huh7 cell clone; created by "curing" a cell line stably replicating a subgenomic version of HCV

2.2. Constructs

name	purpose	reference
pFK-i389-NS3-3'-JFH (sgJFH)	transient HCV replication assay	[281]
pFK-i341-PI-Luc-EI-sgCon1-ET	transient HCV replication assay	[282]
pFK-Jc1	infection dynamics Lunet-CGM cells	[283]
pFK-JcR2a	validation of putative HCV host factors	[104]
pWPI-EF1α::N-HA-THAP7-Puro	validation of putative HCV host factors	[278]
pWPI-EF1α::N-HA-CRYM-Puro	validation of putative HCV host factors	[278]
pWPI-EF1α::N-HA-LBHD1-Puro	validation of putative HCV host factors	[278]
pWPI-EF1α::N-HA-CRAMP1-Puro	validation of putative HCV host factors	[278]
pWPI-EF1α::N-HA-NR0B2-Puro	validation of putative HCV host factors	[278]
pWPI-EF1α::THAP7-FLAG-Bla	validation of putative HCV host factors	[278]
pWPI-EF1α::CRYM-FLAG-Bla	validation of putative HCV host factors	[278]
pWPI-EF1α::LBHD1-FLAG-Bla	validation of putative HCV host factors	[278]
pWPI-EF1α::CRAMP1-FLAG-Bla	validation of putative HCV host factors	[278]
pWPI-EF1α::NR0B2-FLAG-Bla	validation of putative HCV host factors	[278]
pWPI-ROSA26::N-HA-NR0B2-Puro	validation of putative HCV host factors	[278]

2.3. Chemicals and reagents

If not stated otherwise, chemicals and reagents were supplied by Carl Roth, Sigma-Aldrich, Thermo Fisher Scientific, or VWR International in at least molecular biology grade.

name	supplier
ssRNA ladder	Thermo Fisher Scientific
agarose (for RNA gels)	Sigma-Aldrich
agarose (for DNA gels)	Carl Roth
APS	Carl Roth
β-mercaptoethanol	Sigma-Aldrich
Blasticidin	AppliChem
Clarity (Max) ECL Western Blotting Substrate	Bio-Rad
CloneAmp™ HiFi PCR Premix	Takara BioTech
Coelenterazine	PJK Biotech
DAPI	MoBiTec
DEPC	VWR International
D-Luciferin	PJK Biotech
DMEM, high glucose	Thermo Fisher Scientific
DMSO	Carl Roth
DNA loading dye (6x)	Thermo Fisher Scientific
DTT	Sigmal-Aldrich
EasyTides® CTP, [alpha-32P]-, 250µCi	PerkinElmer
Ethanol absolute	VWR International
Exonuclease I	Thermo Fisher Scientific
FCS	Capricorn Scientific
fluoromount G	SouthernBiotech
Gateway™ BP clonase™ II	Life Technologies
Gateway™ LR Clonase™ II	Life Technologies
Geneticin (G418) Sulfate	Santa Cruz Biotechnology
Gentamicin	Thermo Fisher Scientific
Glycerol	Sigma-Aldrich
IFN-α	PBL Assay Science
Isopropanol	VWR International
iTaq™ Universal SYBR® Green Supermix	Bio-Rad
Kanamycin	SERVA Electrophoresis GmbH

Lipofectamine™ RNAiMax	Thermo Fisher Scientific
Maxima H Minus RT	Thermo Fisher Scientific
MEM Non-Essential Amino Acids Solution (100X)	Thermo Fisher Scientific
Methanol	VWR International
Midori Green	Nippon Genetics
MluI-HF restriction enzyme	New England Biolabs
NTP Set, Tris buffered	Thermo Fisher Scientific
Opti-MEM	Thermo Fisher Scientific
Penicillin-Streptomycin	Thermo Fisher Scientific
Powdered milk	Carl Roth
Precision Plus Protein™ Dual Color Standards	Bio-Rad
Puromycin	Sigma-Aldrich
Q5® High-Fidelity DNA Polymerase	New England Biolabs
qScript XLT 1-step RT-qPCR ToughMix	VWR International
Recombinant RNasin® Ribonuclease Inhibitor	Promega
ROTI®Aqua-Phenol	Carl Roth
RQ1 RNase-Free DNase	Promega
Sodium citrate dihydrate tribasic	Th. Geyer
Spectinomycin	Merck KGaA
T3 RNA Polymerase	Thermo Fisher Scientific
TEMED	AppliChem
Trition-X-100	AppliChem
Trypsin-EDTA	Thermo Fisher Scientific
TURBO™ DNase	Thermo Fisher Scientific

2.4. Primary antibodies

target	source	dilution	purpose	supplier/reference
ß-actin	mouse	1:5000	immunoblotting	Sigma-Aldrich (A5441)
calnexin	rabbit	1:2000	immunoblotting	Enzo Life Sciences (ADI-SPA-865-F)
FLAG tag	mouse	1:1000	immunoblotting	Sigma-Aldrich (F1804)
HA tag	mouse	1:2000	immunoblotting	Sigma-Aldrich (H3663)
NR0B2	mouse	1:1000	immunoblotting	Santa Cruz (sc-271511)
NR0B2	mouse	1:50–1:500	immunofluorescence	Santa Cruz (sc-271511)
NS5A	mouse	1:200	$TCID_{50}$	9E10, Charles Rice, Rockefeller, NY, USA
THAP7	mouse	1:1000	immunoblotting	Abonva (H00080764-B01)
THAP7	mouse	1:50	immunofluorescence	Abonva (H00080764-B01)

2.5. Secondary antibodies

target	source	dilution	purpose	conjugation	supplier/reference
mouse IgG	goat	1:10000	immunoblotting	HRP	Sigma-Aldrich
rabbit IgG	goat	1:20000	immunoblotting	HRP	Sigma-Aldrich
mouse IgG	goat	1:1000	immunofluorescence	Alexa Fluor 647	Thermo Fisher Scientific

2.6. Buffers and solutions

name	content
Acetatos	sodium acetate 0.5 M, acetic acid 0.5 M (mix 28.75 ml of glacial acetic acid in 1 L H_2O), keep @ 4°C
Coelenterazine	1.05 mM in methanol
D-Luciferin	1 mM D-Luciferin in 25 mM glycylglycine
GITC buffer	4 M guanidinium thiocyanate, 25 mM sodium citrate, 0.5% sodium lauroyl sarcosinate, freshly added 0.1 M β-mercaptoethanol)
glyoxal loading buffer	0.25 mg/mL bromo phenolblue, 0.25 mg/mL xylene cyanol, 10 mM $NaPO_4$ pH 7.0, 50% (v/v) glycerol
LB agar	30 g peptone, 15 g yeast extract, 15 g NaCl, 15 g agar in 3 L H_2O
Luc Assay Buffer	25 mM glycylglycine pH 7.8, 15 mM KPO_4 buffer pH 7.8, 15 mM $MgSO_4$, 4 mM EGTA pH 7.8, in H_2O
LB medium	50 g peptone, 25 g yeast extract, 25 g NaCl in 5 L H_2O
Luc Lysis Buffer	25 mM glycylglycine pH 7.8, 15 mM $MgSO_4$, 4 mM EGTA pH 7.8, 1% Triton X-100, 10% glycerol, in H_2O add freshly 1 mM final DTT

2.7. Viruses

name	reference	comment
DenR2a	[284]	renilla luciferase reporter version of Dengue virus (DENV)
Jc1	[283]	chimeric virus from a gt2a J6CF (5'-NS2-TMDI) and gt2a JFH-1 (TMDII-3') isolate
JcR2a	[104]	renilla luciferase reporter version based on Jc1
RVFV	[285]	ΔNSs renilla luciferase reporter version of RVFV

2.8. Consumables

All general lab consumables were supplied by the DKFZ store and manufactured by BD, Bio-Rad, Corning, GE Healthcare, Greiner, Merck Millipore, STARLAB, or Thermo Fisher Scientific.

2.9. Instruments

name	manufacturer
C1000 Touch™ Thermal Cycler	Bio-Rad
CFX Connect™ Real-Time PCR Detection System	Bio-Rad
ChemoCam Imager 3.2	INTAS
Gene Pulser Xcell™ Electroporation Systems	Bio-Rad
Mithras² LB 943 multimode reader	Berthold Technologies
NanoDrop 1000 Spectrophotometer	Thermo Fisher Scientific
Nikon Eclipse Ti-E	Nikon
Qubit 1.0 fluorometer	Invitrogen
Storm 860 Molecular Imager	GE Healthcare
Trans-Blot® Turbo™ Transfer System	Bio-Rad
UV transilluminator	Vilber Lourmat

2.10. Software

name	supplier
Affinity Designer	Serif
Bio-Rad CFX Manager	Bio-Rad
EndNote X9	Clarivate Analytics, Thomson Reuters
Fiji - ImageJ	NIH [286]
GraphPad Prism 8	GraphPad
IC Capture	The Imaging Source
Intas Chemostar	INTAS
LabImage 1D	INTAS
Microsoft Office 2016	Microsoft
SnapGene	GSL Biotech LLC
DeepL	DeepL GmbH

3. METHODS

3.1. Bacterial culture

Escherichia coli DH5α cells were used for almost all bacterial culture. Culture conditions were 37°C in LB medium or on LB agar with the respective antibiotics. Empty Gateway™ plasmids were amplified in ccdB Survival™ 2 bacteria (Thermo Fisher Scientific).

3.2. Plasmid purification from bacterial cultures

Plasmid DNA from bacterial cultures was purified using the NucleoSpin® Plasmid (2 mL culture) or the NucleoBond® PC 500 (300 mL culture) kit (Macherey-Nagel) according to the manufacturer protocol.

3.3. Gel or PCR mix purification of DNA

Plasmid or insert DNA was extracted from PCR reactions or agarose gels using the NucleoSpin® Gel and PCR clean-up kit (Macherey-Nagel) according the manufacturer protocol.

3.4. Classical cloning

All classical cloning procedures were performed with restriction enzymes and buffer system from New England Biolabs.

3.5. DNA amplification

Inserts for cloning procedures were amplified from plasmid bank plasmids or cDNA using the Q5® High-Fidelity DNA Polymerase (New England Biolabs) according to the manufacturer instructions or the CloneAmp™ HiFi PCR Premix (Takara BioTech) according to the manufacturer protocol.

3.6. Gateway™ cloning

Gateway™ cloning [287] was used to shuttle cDNAs clones into different expression vectors. Original inserts were created by amplifying the desired region from a plasmid bank plasmid or cDNA with *attB* sites-flanked primers: *attB*-forward 5'-GGGGACAAGTTTGTACAAAAAAGCAGGCTTC-3' and *attB*-reverse 5'-GGGGACCACTTTGTACAAGAAAGCTGGGTC-3'. Inserts were gel-purified and mixed with a *pENTR* vector in a so-called BP reaction using the *BP clonase II* according to the manufacturer protocol to generate a *pDONR* vector. The resulting vector was mixed with a *pDEST* vector in a so-called LR reaction and *LR clonase II* according to the manufacturer protocol to retrieve the expression plasmid.

3.7. Cells and cell culture

All cell lines used in this study for HCV replication experiments were derivatives of the human hepatocellular carcinoma cell line Huh7 [125]. HEK293T [288] cells were used for lentiviral particle production and transduction of Huh7 cells to establish stably overexpressing cell lines as described in [289]. Cells were cultivated in monolayers that were passaged two to three times a week in complete medium (DMEM supplemented with 10% FBS, 100 U/mL penicillin and 100 ng/mL streptomycin, and 1x non-essential amino acids). Cells were kept in a humidified incubator at 37°C with 5% CO_2.

3.8. Lunet-CGM cells

In this study, we make use of a highly permissive Huh7 cell clone (Huh7-Lunet [137]) overexpressing the HCV entry factor CD81 [279] and two more reporters. First, an mCherry-tagged

histone protein H2B to visualize nuclei and allow for automated cell counting, and second, an eGFP$_{NLS}$-MAVS, where the MAVS mitochondrial transmembrane domain and the SV40 nuclear localization sequence (NLS) are fused to the eGFP C-terminus [290]. Thus, the cells give a diffuse to speckle-like cytoplasmic stain. Upon HCV infection, the viral NS3/4A protease cleaves off the MAVS membrane anchor and the eGFP$_{NLS}$ shuttles into the nucleus, giving a sharp nuclear and no cytoplasmic signal, anymore. The cells can thus be quantified in an automated manner using image quantification software. In the course of this study we call these cells Lunet-CGM (Lunet-CD81$_{high}$-eGFP$_{NLS-MAVS}$-H2B-mCherry).

3.9. *In vitro*-transcription of RNA

Production of *in vitro*-transcribed (IVT) RNA, purification and was done as described previously [169]. In brief, plasmid DNA was linearized and *in vitro*-transcribed using a homemade T7 polymerase for (+)-RNA or T3 polymerase for (-)-strand RNA. Plasmid DNA was removed by adding RQ1 DNase. RNA was then purified by phenol-chloroform extraction, concentration was measured at a NanoDrop device (Thermo Fisher Scientific) and integrity was assessed by native agarose gel electrophoresis.

3.10. Preparation of standards for absolute quantification

In vitro transcripts were prepared as described above and additionally treated with TURBO™ DNase to remove residual plasmid DNA. RNA was again purified using the NucleoSpin® RNA Plus (Macherey-Nagel) kit. RNA concentration was assessed on a NanoDrop device as well as on a Qubit fluorometer and diluted to the desired concentration.

3.11. Electroporation of Huh7 cells

In vitro-transcribed RNA (2–10 µg) was used to electroporate $4x10^6$ (Huh7-Lunet, Lunet-CGM) or $6x10^6$ (Huh7-LP, -HP, or Huh7.5) cells in Cytomix [291] using the Gene Pulser system (Bio-Rad). Settings were 975 µF, 270 V for 0.4 cm cuvettes and 500 µF, 166 V for 0.2 cm cuvettes [292]. Electroporated cells were gently resuspended in pre-warmed medium and seeded immediately.

3.12. Virus stocks preparation

Huh7.5 cells [138] were electroporated with Jc1 [283] or JcR2a [104] RNA as described above. 24, 48, and 72 hours later cell culture supernatants were collected, pooled and stored until further use at 4°C. Viral particles were precipitated using sterile-filtered 8% PEG-8000 overnight at 4°C and spun down at 4000 g for 30 min at 4°C. Pellets were resuspended in complete medium, aliquoted and stored at -80°C for further use.

3.13. Titer determination of viral stocks and supernatants

Huh7.5 ($1·10^4$) or Lunet-CGM ($7.5·10^3$) cells were seeded in 96-well plates 16 hours prior to addition of supernatants or stock dilutions. Supernatants were pre-diluted at least 1:3 and stock solutions at least 1:500. All eight wells of one row were used for one dilution. Further dilution series were usually 1:3 to minimize standard deviation. Tips of the 8-channel pipette were changed after each dilution step. Row 12 of the 96-well plate was mock-infected and well A12 served as a positive control by adding undiluted virus stock. After 72 hours, cells were fixed with ice-cold methanol (-20°C), kept at least 15 min at -20°C, and were then transferred to the BSL-2 area. Methanol was removed, plates were quickly air-dried, and washed twice with 1x PBS. We used the mouse monoclonal NS5A antibody 9E10 (a kind gift from Dr. Charles Rice, NY Rockefeller University) in a 1:15.000 dilution in 1x PBS for 1 hour at room temperature or better at 4°C

overnight to detect HCV antigen. Primary antibody was detected with a secondary HRP-conjugated anti-mouse antibody (1:200) for 1 hour at room temperature. Positive cells were then visualized using a homemade substrate (5 ml Acetatos, 1.5 ml Carbazol, 20 µl H_2O_2, per plate, sterile-filtered 0.2 µm) was added for roughly 30 min, depending on the intensity of the appearing stain. Substrate was removed and plates were washed twice with demineralized water. For storage, plates were dried. An Excel spreadsheet for calculating the infectious titer is available at [293].

3.14. "Cold" infection of Lunet-CGM cells

$2x10^5$ cells per 6-well were seeded in 2 mL 16 hours prior to "cold" infection. During "cold" infection, cells were kept at 4°C for 30 min before medium aspiration and inoculation with pre-cooled PEG-precipitated HCV_{cc} (Jc1) at an MOI of 1 (stock A) or 2.42 (stock B) at 4°C for one hour (1 mL per 6-well). The inoculum was removed and cells were covered with 1 ml per well pre-warmed (37°C) medium and incubated for one hour at 37°C (+/- inhibitor). Medium was aspirated and cells were treated with an acid wash protocol to remove extracellular vesicles and unbound virus particles: cells were washed with an acidic solution (0.14 M NaCl, 50 mM Glycine/HCl, pH 3.0, 670 µL per 6-well) for three minutes at 37°C before neutralization with neutralization buffer (0.14 M NaCl, 0.5 M HEPES, pH 7.5, 320 µL per 6-well) and one wash with pre-warmed medium. After that, fresh medium (+/- inhibitor) was added. All experiments of which the results are shown in the Results section were performed with Jc1 stock B. Experiments with Jc1 stock A are only shown in the Appendix and data is accordingly annotated.

3.15. Total RNA extraction (phenol)

Total cellular RNA during Jc1 infections from infected or control cells was extracted by phenol-chloroform. Infected cells were washed prior to lysis according to the acid wash protocol described above. After three washing steps with cold 1x PBS, cells were lysed in GITC buffer (700 µL per 6-well) and RNA was extracted as described [294].

3.16. RNA extraction (supernatant)

RNA from supernatants or virus stock dilutions was extracted by lysing 100 µL in 600 µL GITC buffer and addition of 1–10 µg of total RNA from uninfected Huh7-Lunet cells.

3.17. Strand-specific HCV RT-qPCR

In order to quantify intracellular (+)- and (-)-strand HCV RNA, we performed strand-specific RT-qPCR as described recently [295]. Briefly, 1–2 µg purified RNA from cell extracts, supernatants or virus inoculum or IVT standards spiked with 1 µg total RNA of uninfected Huh7-Lunet cells were reverse-transcribed with a thermostable reverse transcriptase at 55°C in a strand-specific manner using tagged, strand-specific primers. (+)- and (-)-strand reactions were performed in separate reaction tubes. RT reaction was performed on the thermocycler to assure no lower than 55°C reaction temperature. After Exonuclease I digest, qPCR was performed using primers against the strand-specific tags and the respective strand itself. *In vitro*-transcribed (+)- and (-)-strand RNAs were used to generate standard curves for absolute quantification.

3.18. Strand-unspecific HCV RT-qPCR (Taqman)

Strand-unspecific RT-qPCR was performed to determine the $IC_{50}s$ of specific HCV inhibitors as described in [296].

3.19. Luciferase assay

Luciferase activity of subgenomic or full-length reporter constructs after electroporation (sgJFH, sgCon1-ET), infection (JcR2a, DenR2a, RVFV), or from stable replicon cell lines (Huh7-LucUbiNeo-JFH) was assessed as described in [278]. Briefly, homemade Luc Lysis Buffer was used for firefly measurements and commercial Passive Lysis Buffer for renilla measurements. Firefly activity was measured in Luc Assay Buffer with 10 µM D-Luciferin, 2 mM ATP, 1 mM DTT, whereas renilla activity was measured in Luc Assay Buffer with 3.36 µM Coelenterazine.

3.20. Immunoblotting

Immunoblotting to assess expression levels of proteins was performed as described in [278]. PAA gels were blotted using the Trans-Blot® Turbo™ Transfer System (Bio-Rad) or by wet transfer (in case of FLAG tag detection).

3.21. Northern blotting

To assess (+)- and (-)-strand levels, cell lysates after electroporation of Huh7-Lunet cells with sgCon1-ET were analyzed by Northern blotting as described in essence in [277] and [58] with the following minor modifications (a detailed protocol is deposited on the *F170-Projekte/F170/F170 Protocols* drive at the DKFZ, Heidelberg). 10 µL of purified RNA (1 µg/µL) or IVT standards (spiked with 10 µg of cellular RNA from Huh7-Lunet cells) were mixed with 4.1 µL 100 mM $NaPO_4$ pH 7.0, 6 µL glyoxal, and 20.5 µL DMSO and incubated at 50°C for 1 hour. Samples were quickly cooled on ice or -20°C and 10.9 µL of glyoxal loading buffer was added. Transfer of RNA from the native 1% agarose gel (10 mM $NaPO_4$) to the positively charged membrane (highbond N^+-membrane, Amersham) was performed by upward capillary transfer in 20x SSC overnight at room temperature. After disassembling, the membrane was air-dried, UV crosslinked (125 mJ, Bio-Link 254 (nm), Vilber Lourmat), methylene blue stained, cut, and hybridized (upper part against HCV RNA, lower part against ß-actin). Signals were detected in a .

3.22. Fluorescence microscopy of fixed cells

Cells seeded on glass cover slips were washed once with 1x PBS, fixed with 4% paraformaldehyde in PBS for 15 min at room temperature and washed again thrice with 1x PBS. Cell membranes were permeabilized with 0.5% Triton X-100 in PBS for 5 min. Unspecific binding was prevented by blocking with 3% BSA for 30 min to one hour. Primary antibody was applied for 1 hour at room temperature or overnight at 4°C. Secondary antibodies were applied for 1 hour at room temperature. DAPI was added (final dilution 1:5000) during the last five minutes of the secondary antibody stain. Cover slips were washed again three times with 1x PBS and once with demineralized H_2O and mounted with fluoromount G (SouthernBiotech, Birmingham, AL). Images were captured with a Nikon Eclipse Ti-E microscope and processed using Fiji.

3.23. Fluorescence microscopy of live cells & image quantification

During Jc1 infection dynamics, Lunet-CGM cells were directly imaged in the cell culture plate containing complete medium with a 10x phase-contrast objective (Nikon) on a Nikon microscope using the IC Capture software. The GFP signal was captured in the 470 nm channel; the mCherry signal in the 590 nm channel. Images were processed with Fiji [286] and R [297] with the help of Christoph Harmel. At least four images per 6-well were captured for image analysis.

3.24. siRNA reverse transfection

Reverse transfection of siRNA for gene knockdown was performed as described in [278].

3.25. Cloning of host factor candidate cDNAs

cDNA clones were ordered from the *ORFeome Collaboration (OC) cDNA Clones* [298, 299] or cloned by standard molecular biology methods as described in [278].

3.26. Establishment of overexpressing cell lines

To establish stably overexpressing cell lines, Huh7 cells were transduced using lentiviral particles produced in HEK293T cells as described in [278] and [289].

3.27. Total RNA extraction (column) and qPCR

Expression levels of mRNAs in overexpressing of control cell lines was assessed after RNA purification and reverse transcription of cDNA via qPCR as described in [278].

3.28. Live cell imaging (IncuCyte)

Live cell imaging for quantification of cell proliferation was performed as described in [278].

3.29. Cell viability assay

To assess cell viability upon siRNA transfection, intracellular ATP levels were measured using the CellTiter-Glo® Luminescent Cell Viability Assay (Promega) as described in [278].

3.30. Mathematical modeling

To complement our experimental approach, we use mathematical modeling to address questions that are difficult to impossible to test in an experimental setting. For this, we closely collaborate with the Kaderali lab at the University Hospital Greifswald, Germany. The PhD candidate Darius Schweinoch exerted all the mathematical modeling, including model predictions, model fits, and the model extension. For details, I am referring to his PhD thesis or our shared first author publication that will be submitted soon.

Drug effects implementation

We used our intracellular HCV replication model to predict replication dynamics under Telaprevir (NS3/4A protease inhibitor) and Sofosbuvir (NS5B polymerase inhibitor) treatment as well as to fit our model to data from IFN-α and Daclatasvir (NS5A phosphoprotein inhibitor) treatment. To account for inhibitor effects, we included IC_{50} or E_{Max} terms indicated with red font in the corresponding equations.

(a)
$$k_1 \cdot \frac{1}{1 + \left(\frac{c_{ISG}}{IC50_k}\right)^n} \cdot R_P^{cyt} \cdot (Ribo - T_c)$$

(b)
$$\mu_x \cdot \left(1 + \left(\frac{E_{Max} \cdot [ISG]^n}{[ISG]^n + EC50^n}\right)^n\right) \cdot [R_x]$$

(c)
$$k_c \cdot \frac{1}{1 + \left(\frac{C_{Tel}}{IC50_{Tel}}\right)^n} \cdot P$$

(d)
$$k_{4m} \cdot \frac{1}{1 + \left(\frac{C_{Sof}}{IC50_{Sof}}\right)^n} \cdot R_{IP}$$

(e)
$$k_{4p} \cdot \frac{1}{1 + \left(\frac{C_{Sof}}{IC50_{Sof}}\right)^n} \cdot R_{IdS}$$

METHODS

4. RESULTS

We made use of the robust and well-established transient HCV replication assay in highly permissive Huh7-Lunet cells to analyze the effects of therapeutic intervention. Huh7-Lunet cells were electroporated with *in vitro* transcripts of a subgenomic HCV genotype 2a reporter RNA (sgJFH) and replication was monitored via luciferase activity as a surrogate for viral protein levels. The luciferase reporter gene has replaced the information for the structural genes in this RNA. This allows the analysis of effects exclusively on viral RNA translation and replication as no viral particles are produced.

4.1. Deciphering the mode of action of IFN-α and hepatitis C virus (HCV) inhibitors using an intracellular model for HCV replication

This section describes HCV replication and the effects of IFN-α treatment or the use of direct-acting antivirals against HCV on its replication. We used mathematical modeling to describe and decipher the highly complex virus-host interactions. The modeling part was performed by Darius Schweinoch (Kaderali lab, Greifswald) and modifications/extensions of the model as well as interpretation of the results were done in close collaboration between the Kaderali lab and us. All plots that show model simulations or model fits were produced and provided by Darius Schweinoch on basis of data provided by us. The collaborative project will be published soon with a shared first authorship.

IFN-α treatment has been the standard of care for chronic HCV infection for decades. However, the exact mode of action of viral replication inhibition remains elusive. Thus, we asked the question which step of intracellular HCV RNA replication is affected by IFN-α treatment and the induced antiviral response of the host cell. In a first step, we wanted to analyze the IFN-α-mediated effects on viral RNA translation. Therefore, we used a replication-defective version of the subgenomic reporter RNA, which harbors a 10 amino acid deletion in the catalytic center of the viral polymerase (sgJFH$^{\Delta GDD}$).

4.1.1. The IFN-α-triggered antiviral response primarily inhibits HCV RNA translation

We pre- and co-treated Huh7-Lunet cells with different concentrations of IFN-α, electroporated the cells with sgJFH$^{\Delta GDD}$ RNA and recorded luciferase activity over time. Already 1.5 hours post electroporation (hpe), luciferase activity was markedly lower in IFN-α-treated cells than in untreated cells (Figure 9A, abs), suggesting a strong translational inhibition of the transfected RNA. In addition, when normalizing to the initial value, RNA stability seemed to be decreased as well since luciferase signals declined faster in IFN-α-treated cells than in untreated cells (Figure 9A, rel). However, another explanation might be a faster decay of cellular proteins induced by the antiviral response. To underpin the notion of increased RNA decay upon IFN-α treatment, we used Northern blotting to assess RNA levels directly. RNA signals seemed quite similar in the different conditions. However, upon quantification, IFN-α treatment appeared to increase RNA decay in both concentrations used (Figure 9B). Non-linear regression of the signals revealed half-lives of 1 h 38 min and 1 h 15 min for the untreated and the IFN-α-treated conditions, respectively (Figure A1). To assure that not only excess RNA that sticks to the cells was measured, we electroporated samples without RNA and added RNA immediately afterwards. The rigorous washing steps
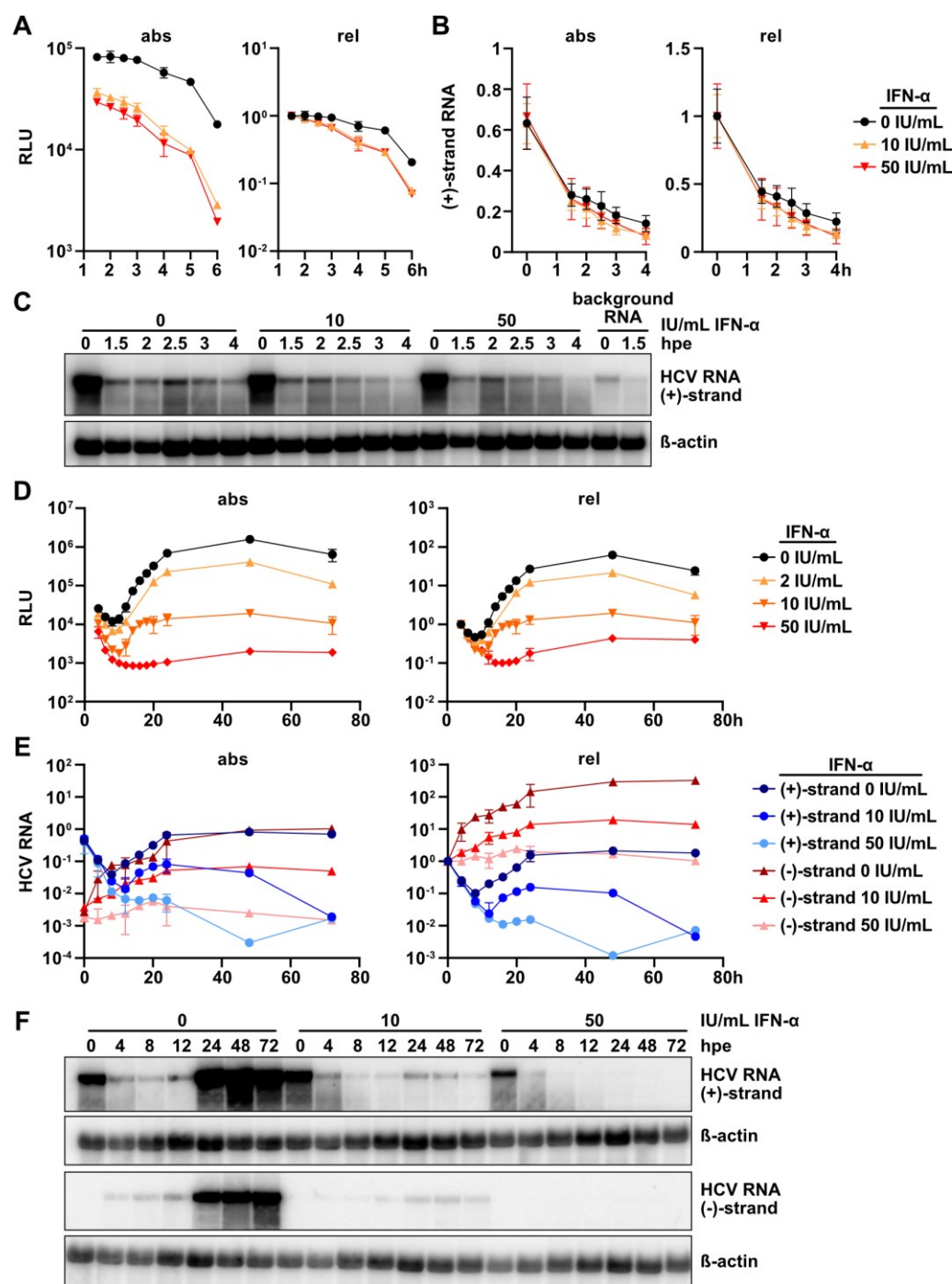
Figure 9 The antiviral response triggered by IFN-α inhibits HCV RNA translation and reduces HCV RNA half-life.
(A) Luciferase activity over time after electroporation of the replication-deficient subgenomic firefly luciferase-encoding HCV RNA sgJFH$^{\Delta GDD}$ into untreated or IFN-α pre- and co-treated Huh7-Lunet cells. **(B)** Quantification of HCV RNA levels from strand-specific Northern blot over time after electroporation as in (A). **(C)** Representative Northern blot used for quantification shown in (B). **(D)** Luciferase activity over time after electroporation of the subgenomic firefly luciferase-encoding HCV RNA sgJFH into untreated or IFN-α pre- and co-treated Huh7-Lunet cells. **(E)** Quantification of HCV RNA levels from strand-specific Northern blot (n=2) over time after electroporation as in (D). **(F)** Representative Northern used for quantification shown in (E). ß-actin served as a loading control and for normalization. Background RNA was not electroporated but only added to the cells to account for RNA that sticks to the cells and could not be washed off. The signal obtained from those lanes was subtracted from all other signals. Luciferase activity is given in relative light units (RLU) either in absolute values (abs) or relative to the first time-point obtained (rel). Northern blot quantification data is given normalized to ß-actin (abs) or normalized to ß-actin and relative to the first time-point obtained (rel). If not stated otherwise, data shows means +/- standard deviation from three independent experiments.

removed most of the input RNA and gave only a faint signal at 0 hours that vanished within 1.5 hours (Figure 9C). Thus, the IFN-α-triggered antiviral response raised by the host cell seems to largely suppress HCV IRES-mediated translation and only slightly reduce HCV RNA half-life.

We then used a replication-competent RNA (sgJFH) to examine possible additional effects of IFN-α treatment on HCV RNA replication. As IFN-α treatment with 10 or 50 IU/mL severely impaired HCV replication in this setting, we included a lower concentration of 2 IU/mL to better visualize the dose-dependence and the dynamics of the inhibition (Figure 9D). Similar to sgJFH$^{\Delta GDD}$ RNA, initial translation of sgJFH RNA was reduced already at 1.5 hpe and luciferase activity declined strongly in the 10 and 50 IU/mL condition during the initial phase (0–12 hpe) (Figure 9D, abs). Due to this translational inhibition, which delays the availability of viral proteins to start replication, onset of replication was delayed, especially visible in the 10 and 50 IU/mL IFN-α treatment conditions (Figure 9D, rel). Further, the slope of the curve did not seem to be reduced in the 2 and 10 IU/mL condition at first, but signals leveled off much faster with increasing IFN-α concentration and did not reach the plateau as defined by the untreated condition (Figure 9D). The 50 IU/mL IFN-α treatment allowed almost no HCV replication, making it impossible to analyze replication dynamics. Quantification of (+)-strand RNA levels directly assessed by Northern blot clearly resembled the luciferase signals (Figure 9E, -F). (+)-strand levels initially dropped lower in the IFN-α conditions (Figure 9E, abs), the increase in (+)-strand RNA levels reflected a delayed onset of replication, and the plateau as defined by the untreated sample was not reached (Figure 9E). The (-)-strand is the replication intermediate of HCV, which is only produced from transfected (+)-strands, and should not be not present at 0 hpe. Therefore, values measured at 0 hpe were technical background (normalized to ß-actin; see Figure 9 legend). Synthesis of (-)-strands first appeared at 4 hpe in the untreated condition, giving a very faint band (Figure 9F). In the 10 IU/mL IFN-α condition, (-)-strands appeared much later, at 12 hours. There was no visible (-)-strand band appearing in the 50 IU/mL IFN-α condition (Figure 9F). Overall, only the untreated condition gave strong signals for (+)- and (-)-strands from 24 to 72 hpe (Figure 9F). These pronounced effects on HCV replication were unlikely only a consequence of the initial and possibly sustained translational inhibition. However, we cannot distinguish between those and direct effects on replication in this system.

To clarify if there is another, distinct effect on viral replication, we made use of a mathematical model that is able to simulate intracellular HCV replication [277]. The model consists of ordinary differential equations (ODEs) that describe every central step of intracellular HCV replication, from translation of the genome to establishment of the replication compartment, and includes degradation rates for viral RNA and protein species. We generated a model fit using HCV replication without treatment or under 1 or 10 IU/mL IFN-α treatment (Figure 10). Since we knew already that IFN-α treatment severely impaired translation of HCV RNA, we pre-selected the translation initiation rate k_1 and modified it by including an ISG effect using an IC$_{50}$ term (see Methods section). The model was allowed to modify one or more additional parameters in the same way to generate the best fit. We achieved the best fit upon adjustment of the viral translation rate k_1 as well as viral RNA degradation rates μ (in the cytoplasm as well as in the
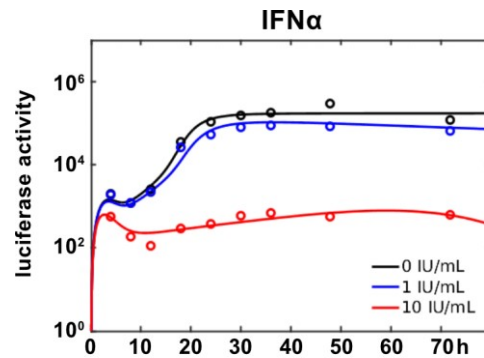
Figure 10 Model fit of the intracellular HCV model (Binder *et al.*, 2013) to HCV replication data under IFN-α treatment. Luciferase activity over time after electroporation of the subgenomic firefly luciferase-encoding HCV RNA sgJFH into untreated or IFN-α pre- and co-treated (1 or 10 IU/mL IFN-α) Huh7-Lunet cells. For the best fit, parameters k_1 (translation of the viral RNA in the cytoplasm) and viral RNA degradation rates μ (inside the replication compartment as well as in the cytoplasm) were adjusted. For details, see Methods section. Data produced by Aparna Pandey. Model implementation, fit and plot by Darius Schweinoch.

replication compartment (RC) (Figure 10, for details see Methods section). The model fit accurately described the biological data and confirmed our *in vitro* findings of increased viral RNA degradation upon IFN-α treatment. However, the adjustment of other parameter combinations yielded similarly good fits, suggesting an insufficient amount or variety of data used for model fitting. A shorter half-life of the RC might yield a similar outcome; however, this possibility is not covered in our model.

In conclusion, the antiviral response raised by the host cell upon IFN-α treatment strongly inhibits HCV RNA translation and slightly reduces HCV RNA half-life. A mathematical model describing intracellular HCV replication corroborated these findings by data fitting. Although we cannot rule out additional effects, for example on the establishment of RCs, those must be very small according to the near optimal fit. Since our system and the model are limited to intracellular HCV replication, we cannot address effects on particle assembly, release or infectivity, yet.

4.1.2. HCV inhibitors have distinct modes of action that the intracellular model can recapitulate

The antiviral response raised by IFN-α treatment is not the only treatment for HCV with an elusive mode of action. For a few years now, highly efficacious direct-acting antivirals (DAAs) against chronic HCV infection provide cure rates of ≥95 % [300]. Amongst those, the highly potent class of inhibitors of the multifunctional HCV phosphoprotein NS5A display half-maximal inhibitory concentrations (IC50s) in the picomolar range [301]. NS5A has no enzymatic function but forms dimers or even oligomers that bind HCV RNA [302], and is required for replication [152, 303, 304] as well as assembly [296]. One of the first clinically approved NS5A inhibitors was Daclatasvir (DCV) [305], sold under the market name Daklinza and discovered at Bristol-Myers Squibb [306-308]. Despite its efficacy in inhibiting NS5A, how exactly DCV affects HCV replication remains elusive. To understand which functions of NS5A DCV impairs, we recorded intracellular HCV replication dynamics under DCV treatment using our luciferase reporter construct sgJFH as described above and applied our intracellular model to identify the most likely affected parameters or steps in the viral life cycle. We used the NS3/4A protease inhibitor Telaprevir (TEL) and the NS5B polymerase

inhibitor Sofosbuvir (SOF), both possessing distinct and well-defined modes of action, to prove the ability of our model to predict viral replication under treatment.

We electroporated equal amounts of sgJFH RNA into Huh7-Lunet cells treated with the aforementioned inhibitors at different concentrations or left them untreated. We took samples at indicated time points (see Figure 11 legend) and measured luciferase activity as a surrogate for viral protein. TEL treatment resulted in a delayed onset of replication, starting at roughly 12 hpe compared to 8 hpe in the untreated setting (Figure 11A). This effect seemed to be dose-dependent as increasing the TEL concentration from 100 nM to 200 nM resulted in a substantial decrease in luciferase signal at 20 hpe. After replication onset, the luciferase signal increase over time was highly similar to the untreated setting leading to almost equal endpoint levels at 70 hpe. In contrast, SOF treatment showed no effect on onset of replication even in high concentrations of 800 nM, but led to a constantly reduced slope of the luciferase signal over the complete time course (Figure 11B). This led to a dose-dependent reduction of endpoint levels at 72 hpe. Treatment with DCV resulted in a delayed onset of replication, especially with higher concentrations (150 pM and 200 pM) as well as a reduced slope of the signal increase between 12 and 60 hpe (Figure 11C). At 70 hpe, only the lowest dose (75 pM) reached endpoint levels close to
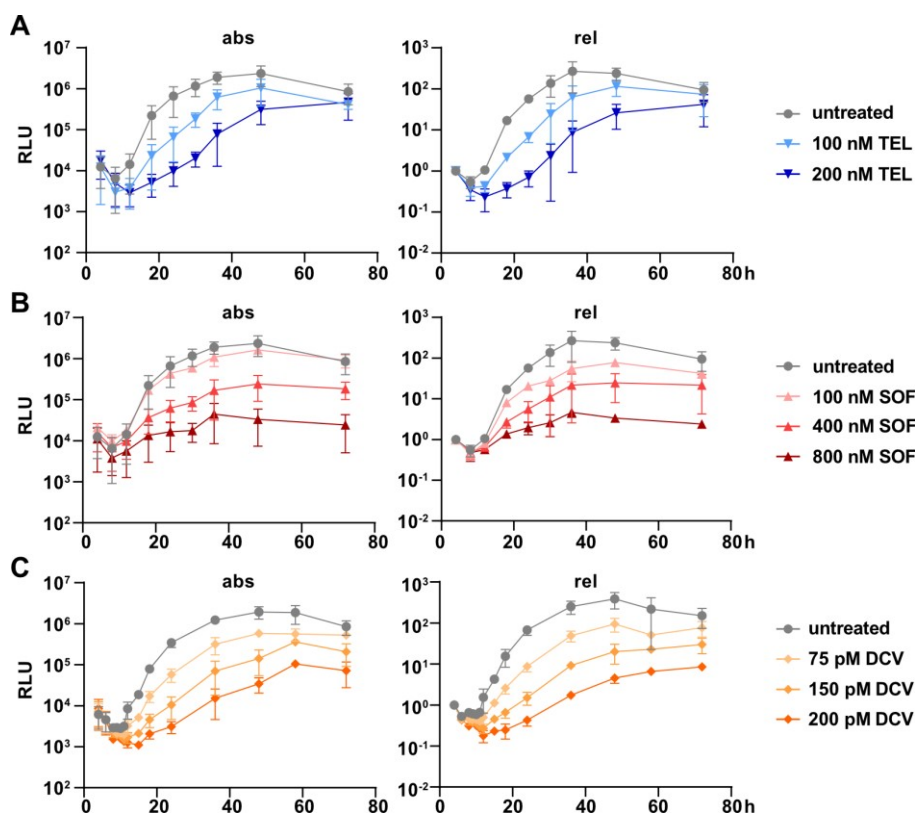
Figure 11 HCV direct-acting antivirals reveal distinct replication kinetics dependent on their mode of action. (A) Luciferase activity over time after electroporation of the subgenomic firefly luciferase-encoding HCV RNA sgJFH into Huh7-Lunet cells left untreated or treated with 100 or 200 nM Telaprevir (TEL) **(A)**, 100, 400 or 800 nM Sofosbuvir (SOF) **(B)** or 75, 150 or 200 pM Daclatasvir (DCV) **(C)**. Luciferase activity is given in relative light units (RLU), either in absolute values (abs) or relative to the first time-point obtained (4h, rel). Time point captured were 4, 8, 12, 18, 24, 30, 36, 48, 72 hours for (A) and (B), and 4, 6, 8, 9, 10, 11, 12, 15, 18, 24, 36, 48, 58, 72 hours for **(C)**. Data shows means +/- standard deviation from at least three independent experiments, except for 100 and 800 nM SOF (n=2). Note that the untreated data for (C) is different from that in (A) and (B). Data produced by Aparna Pandey.

the untreated condition. Higher doses of 150 pM or 200 pM DCV resulted in markedly reduced endpoint levels with more than one log reduction for the highest dose of 200 pM DCV.

Our intracellular model is able to describe HCV replication in Huh7-Lunet cells, a low permissive Huh7 variant (Huh7-LP), and even using manipulated replicons that are impaired in (+)- or (-)-strand replication initiation [277]. We challenged our model to predict intracellular HCV replication upon targeted intervention using HCV inhibitors with distinct modes of action to see if we can use it to identify the unknown mode of action of DCV. We used TEL and SOF as such inhibitors and adapted the corresponding steps in our mathematical model to account for the drug effect. TEL inhibits the NS3/4A protease, so we included an IC_{50} term in the polyprotein processing step $k_c \cdot P$, in which k is the rate constant and P is the amount of polyprotein (see also Methods section). The model prediction described our biological data upon adjustment of k_c only quite well, although it overestimated the drug effect in the 100 nM setting (Figure 12A). To account for the SOF effect, we modified the RNA synthesis steps k_{4m} and k_{4p}, exerted by the viral polymerase NS5B, by including IC_{50} terms (see also Methods section). The resulting model prediction fit the HCV replication data under SOF treatment quite good as well (Figure **12**A). Importantly, the model is able to recapitulate the two very different modes of action of TEL and SOF, which resulted in two very distinct model predictions. Thus, our model proved to be capable of predicting HCV replication even under drug treatment.

We went on and used our model to fit data obtained from HCV replication dynamics under DCV treatment. As done before for IFN-α, we allowed the model to modify one or more parameters to gain the best fit. The model revealed the best fit upon adjustment of k_1 (translation initiation) as well as k_{4p} and k_{4m} (RNA synthesis in the RC) (Figure 12C, see also Methods section), and was able to describe HCV replication in all the three tested DCV concentrations. Only at 70 hpe, the model was not able to capture the pronounced reduction in luciferase activity. As NS5A reportedly binds HCV RNA, is part of the replicase complex, and is involved in formation of the RC, our modeling outcome seemed reasonable. However, closer monitoring of the replication dynamics and
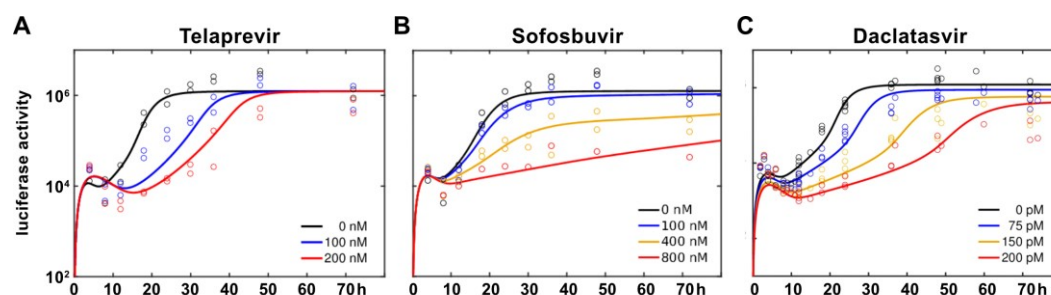
Figure 12 Model predictions (A, B) and model fit (C) correctly reflect HCV intracellular replications dynamics under drug treatment. (A) We used our intracellular model to predict viral replication dynamics after electroporation of our subgenomic reporter replicon sgJFH into Huh7-Lunet cells. To account for the drug effect, we inserted IC_{50} terms in the corresponding equations: describing the polyprotein cleavage step in case of Telaprevir ($k_c \cdot P$) **(A)** or the RNA synthesis steps in the RC involving k_{4m} and k_{4p} in case of Sofosbuvir **(B)**. **(C)** We used our biological data to fit the model and allow adjustment of parameters to achieve the best fit. In the end, adjusting k_1 and the RNA synthesis steps involving k_{4m} and k_{4p} revealed the best fit. Model predictions, fit, and plots generated and provided by Darius Schweinoch.

additional concentrations might yield deeper insights. Since NS5A is also crucial for virion assembly, our model and experimental setting need to be extended to the full viral life cycle to get a comprehensive view of the DCV effects on NS5A function and thus on HCV replication.

Overall, our model proved to not only be able to simulate HCV replication in unchallenged settings, but also successfully fitted HCV replication data under IFN-α treatment, thereby corroborating our *in vitro* findings and proving itself capable of identifying the steps in HCV replication affected by a specific treatment. It further correctly predicted HCV replication under NS3/4A or NS5B inhibitor treatment and was eventually able to fit HCV replication data under DCV treatment. The DCV model fit revealed insights into the possibly affected steps by NS5A inhibition and provides a basis for further investigations into this direction.

4.2. Extension of the intracellular model to the full HCV life cycle

This section describes the extension of our intracellular to the full life-cycle model on the biological as well as mathematical side, of which the latter represents the PhD project of our close collaborator Darius Schweinoch (Kaderali lab, Greifswald). The content regarding the modeling part is thus mostly his intellectual property that he communicated and that we commonly discussed in many interactive meetings and presentations. The collaborative project will be published soon with a shared first authorship.

The intracellular model has proven its capability to describe HCV replication in different settings and even under drug treatment. However, its limitation to the inside of the cell forbids addressing questions about particle assembly, release, infectivity, or spread of the infection. In order to gain those insights, we expanded our model in collaboration with Darius Schweinoch (Kaderali lab, Greifswald) and extended our experimental setting accordingly to the full viral life cycle. The obstacles we had to overcome to achieve our goal were the following. First, we needed to find a cell line that was sufficiently similar to Huh7-Lunet cells (which our intracellular model is based on) and that supported the full viral life cycle, *i.e.* is susceptible to cell culture-produced HCV (HCV$_{cc}$) infection. Second, we had to replace our subgenomic reporter replicon sgJFH with a full-length version that is able to produce infectious particles and has similar replication dynamics. In addition, we replaced our strand-specific Northern blot, which requires 5–10 µg RNA per lane, with the much more sensitive strand-specific RT-qPCR that was recently established in the group of Volker Lohmann and only requires around 1 µg of RNA [295].

4.2.1. Jc1 replication dynamics resemble those of sgJFH and sgJFH replication is not affected by CD81 overexpression

Addressing the first obstacle, we compared replication dynamics of the subgenomic firefly luciferase-encoding sgJFH replicon with the full-length reporter version JcR2a, encoding a renilla luciferase gene. The renilla luciferase gene is inserted into the very N-terminus of the HCV genome and is liberated from the HCV polyprotein by a C-terminal foot-and-mouth-disease virus 2a peptide [104]. Although the two constructs harbor 5'-UTRs including IRES sequences from two different isolates (JFH-1 for sgJFH, J6CF for JcR2a), both belong to genotype 2a and translation efficiency should be comparable. Figure 13A shows intracellular replication dynamics of both constructs electroporated into Huh7-Lunet, where only replication but no infection and thus no spread was possible. We adjusted the amount of RNA electroporated according to genome length to assure that the same number of molecules was transfected. The renilla luciferase dynamics lacked the sharp drop in signal during the first 12 hours that was apparent for sgJFH and reflects degradation of most of the transfected RNA where only few molecules start replicating successfully (Figure 13A). This might have been caused by the higher stability of the renilla (t$_{1/2}$ 4.5 hours) compared to the firefly luciferase (t$_{1/2}$ 3 hours) [309] and posed a problem since we used the luciferase signal as a direct proxy for viral protein and model parameters would have needed adjustment in this case. Overall replication dynamics appeared delayed for JcR2a and not as fast as for sgJFH, which reached almost 100-fold levels 72 hpe (relative to 4h) in contrast to only 10-fold for JcR2a (Figure 13A). We thus went on and tested a non-reporter full-length version of HCV RNA, named Jc1. Jc1 is a chimera cloned from two different genotype 2a isolates, J6CF and JFH-1 [283], and was one of the first clones that efficiently replicated and produced sufficient

amounts of progeny virus in cell culture. Jc1 is identical to JcR2a but lacks the renilla luciferase reporter gene. Thus, we made use of our well-established Northern blot to detect viral (+)-strands. Figure 13B shows the quantification of two independent Northern blots after electroporating the depicted constructs into Huh7-Lunet as described above. Jc1 resembled sgJFH replication dynamics and appeared to replicate even faster and to higher levels than sgJFH (Figure 13B, -C). JcR2a failed to replicate as efficiently as sgJFH or Jc1 as the luciferase data already suggested, proving that the observed differences between sgJFH and JcR2a luciferase activities were not due to different translation efficiencies. Despite the lack of a luciferase gene to monitor replication easily, we decided to use Jc1 for downstream experiments due to its robust replication.
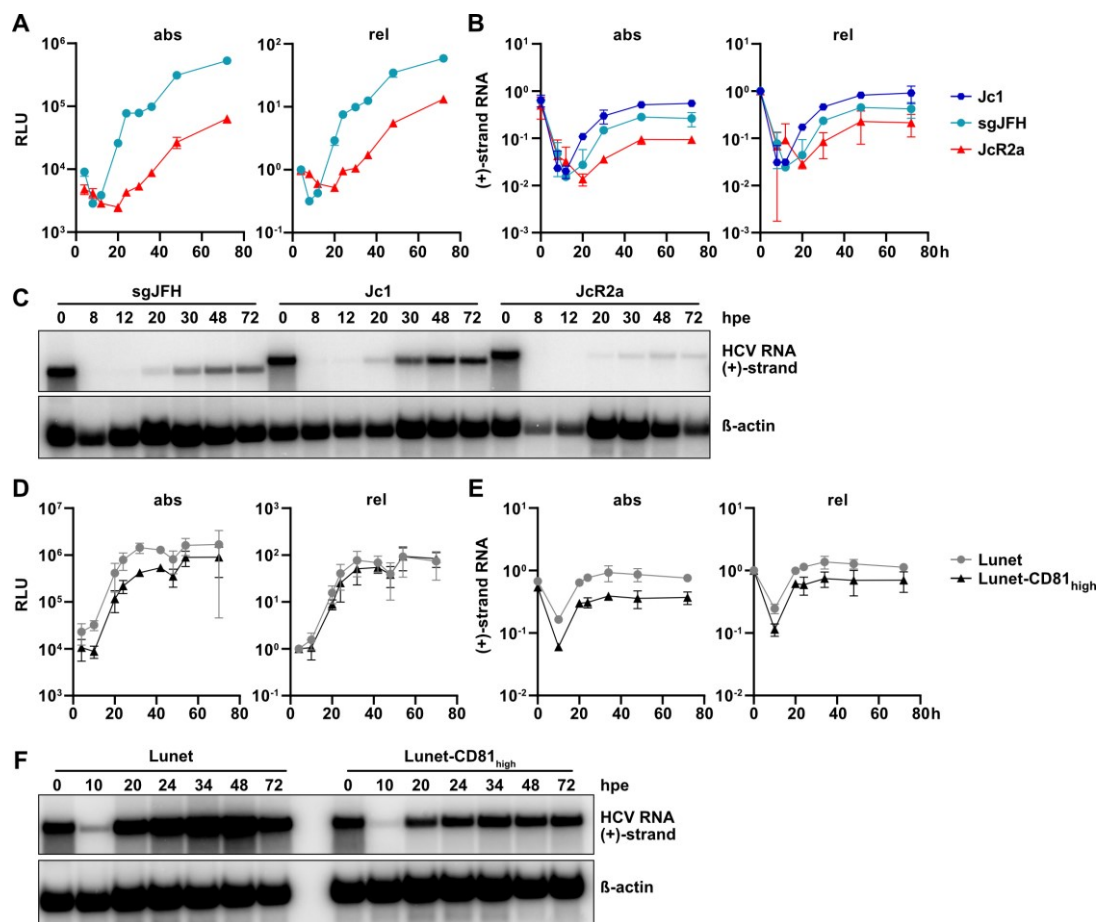
Figure 13 Full-length Jc1 replicates with similar kinetics as subgenomic sgJFH and CD81 overexpression does not change sgJFH replication kinetics. (A) Luciferase activity over time after electroporation of the subgenomic firefly luciferase-encoding HCV RNA sgJFH or the full-length renilla luciferase-encoding HCV RNA JcR2a into Huh7-Lunet cells. **(B)** Quantification of HCV RNA levels from strand-specific Northern blot over time (n=2) after electroporation of the subgenomic firefly luciferase-encoding HCV RNA sgJFH, the full-length version Jc1 or the full-length renilla luciferase-encoding HCV RNA JcR2a into Huh7-Lunet cells. **(C)** Representative Northern used for quantification shown in (B). **(D)** Luciferase activity over time after electroporation of the subgenomic firefly luciferase-encoding HCV RNA sgJFH into Huh7-Lunet or -Lunet-CD81$_{high}$ cells. **(E)** Quantification of HCV RNA levels from strand-specific Northern blot over time (n=2) after electroporation as in (D). **(F)** Representative Northern used for quantification shown in (E). Luciferase activity is given in relative light units (RLU), either in absolute values (abs) or relative to the first time-point obtained (rel). ß-actin was used as a loading control and for normalization in Northern blot experiments. Northern blot quantification data was normalized to ß-actin (abs) or normalized to ß-actin and relative to the first time-point obtained (rel). If not stated otherwise, data shows means +/- standard deviation from three independent experiments.

The second hurdle we needed to overcome was to find a susceptible cell line as a replacement for Huh7-Lunet cells. Studies on HCV entry successfully identified a number of receptors and co-receptors involved in HCV infection of host cells (reviewed in [143]). Among the first ones identified was the tetraspanin CD81 that binds the HCV glycoprotein E2 [145] and that could block infection of cells by HCV$_{cc}$ when added to the medium as a soluble, recombinant peptide [310] or when using an α-CD81 antibody [132, 133, 283, 310]. Huh7-Lunet cells do not express sufficient amounts of CD81 to support HCV$_{cc}$ infection, however, stable CD81 overexpression allows infection levels comparable to Huh7.5, another highly permissive Huh7 clone [279]. We compared replication dynamics in Huh7-Lunet versus Huh7-Lunet-CD81$_{high}$ cells using our subgenomic reporter replicon sgJFH. Figure 13D shows luciferase activity after electroporation of sgJFH into both cell lines. Absolute values revealed a lower baseline of replication in Huh7-Lunet-CD81$_{high}$ cells. However, relative to the initial luciferase activity 4 hpe, replication was identical in both cell lines, reaching almost 100-fold at 72 hpe (rel. to 4h; Figure 13D, rel). Northern blot quantification showed that indeed HCV RNA levels were consistently lower in Huh7-Lunet-CD81$_{high}$ compared to Huh7-Lunet cells despite equal starting values (Figure 13E, -F). This might have, however, been caused by independent cellular properties, as for example passage number, in which the cell lines differed.

In summary, subgenomic sgJFH and full-length Jc1 replication dynamics were qualitatively highly similar in Huh7-Lunet cells and CD81 overexpression did not change sgJFH replication dynamics in Huh7-Lunet cells. Thus, we used Huh7-Lunet-CD81$_{high}$ cells and the full-length construct Jc1 for further experiments.

In order to accurately monitor spread of the infection in our cell culture and quantify the number of infected cells in an automated fashion, we utilized two cellular reporters that we stably transduced in Huh7-Lunet-CD81$_{high}$ cells. First, an eGFP reporter where the SV40 nuclear localization sequence (NLS) and the C-terminal (mitochondrial) transmembrane domain of the signaling protein MAVS (also known as CARDIF, IPS-1, or VISA; [311]) were fused to the eGFP C-terminus [290]. After stable transduction, naïve cells thus show a punctate, mitochondrial pattern, whereas upon HCV infection, the viral NS3/4A protease cleaves the MAVS transmembrane domain [86, 254, 312] and the eGFP$_{NLS}$ shuttles into the nucleus, giving a sharp nuclear signal (see below). Second, in order to quantify total cell numbers, we used an mCherry-tagged histone protein H2B for a constitutive nuclear signal. In the course of this study, we call these triple transduced cells Lunet-CGM (Lunet-C̲D81$_{high}$-e̲GFP$_{NLS-MAVS}$-H2B-m̲Cherry).

4.2.2. Quantification of viral determinants during infection

Having a full-length construct and a susceptible reporter cell line at hand, we went on to quantify viral and cellular determinants in a tight time-course to equilibrate and test our extended mathematical model (details to the model extension are provided in the next section).

We infected Lunet-CGM cells with cell culture-produced Jc1 (see 3. Methods, 3.12. Virus stocks preparation) at an MOI of 2.42 using a "cold infection" protocol to achieve simultaneous entry and onset of replication (see 3. Methods, 3.14. "Cold" infection of Lunet-CGM cells) (Figure 14A). For this,

we pre-cooled cells at 4°C for 30 minutes (min), added the pre-cooled virus inoculum and allowed attachment of viral particles on cell surfaces for one hour at 4°C. We aspirated the inoculum and incubated at 37°C with pre-warmed medium for one hour to allow entry of the attached particles. After that, we removed excess particles by an acidic washing step and started the time-course with taking the 0 hpi sample. Subsequent samples were then taken as depicted in Figure 14A and analyzed for the percentage of infected cells by fluorescence microscopy, viral titer by limiting dilution assay, and viral RNA by strand-specific RT-qPCR at each time-point. Before taking RNA samples, we washed the cells with the same acidic wash protocol as right after the infection to remove extracellular particles or vesicles attached to the cell surface.

Jc1 replication dynamics after infection of Lunet-CGM cells resembled those of the subgenomic replicon sgJFH. After an initial drop in viral RNA levels, replication started and RNA levels increased steadily until the assay endpoint at 70 hpi (Figure 14B). In contrast to the intracellular system where infection could not spread, RNA levels did not reach a plateau at the assay endpoint in this setting. RT-qPCR of an earlier batch of Jc1 virus stock revealed that the (+)-strand content exceeds the number of infectious (+)-strand RNA molecules as given by its $TCID_{50}$ by roughly 3000-fold and contains around $5 \cdot 10^8$ (-)-strand molecules per mL (Figure A2). Since infectious HCV particles contain only one copy of their (+)-strand genome, all the excess (+)- and (-)-strand were probably derived from dsRNA secreted in extracellular vesicles [295]. Thus, the majority of HCV RNA molecules we detected in the initial phase were probably non-infectious RNAs that were degraded and did not start replicating. Newly synthesized (+)-strands could be detected from roughly 4–8 hpi on and (-)-strands from 12 hpi on (Figure A3). To calibrate our mathematical model, we counted only that fraction of (+)-strands as infectious that we measured via infectivity assay ($TCID_{50}$). We modeled all the excess RNAs as non-infectious as they did probably originate from inactivated viral particles or extracellular vesicles that possessed similar biophysical properties as virions and precipitated along with them during the stock preparation process. We detected released infectious particles from 20 hpi on and their number steadily increased until 70 hpi. Since the infection could spread in this system and we started with a very low number of infected cells, not all of the cells were infected even at 70 hpi (Figure 14C). We could readily detect infected cells, marked by their nuclear GFP signal, from 12 hpi on (Figure 14D, middle panel, white arrow). Their number increased steadily and reached between 60 and almost 80% at the assay endpoint (Figure 14C, -D), varying largely between independent experiments.
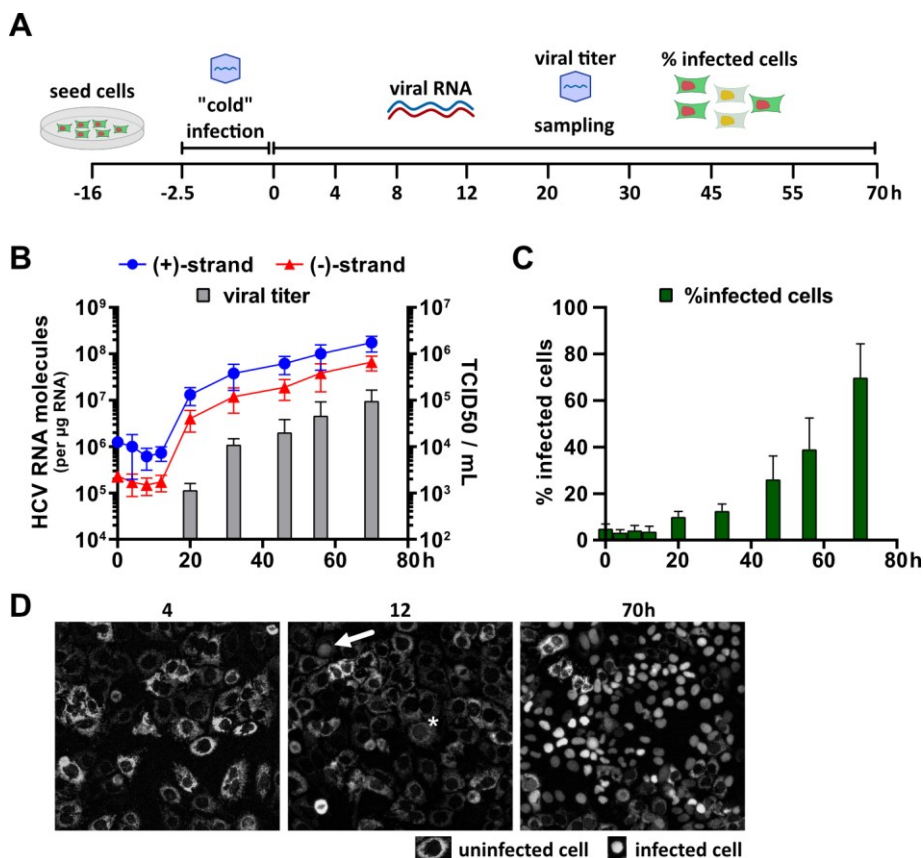
Figure 14 Full-length HCV$_{cc}$ (Jc1) replication kinetics after infection of Lunet-CGM cells. (A) Workflow of Jc1 infection experiments. Lunet-CGM cells were seeded 16 hours prior to "cold infection" and samples were taken in a tight time-course as depicted in the scheme and analyzed for viral RNA, viral titer and the percentage of infected cells via fluorescence microscopy. **(B)** Jc1 replication dynamics after infection of Lunet-CGM cells at an MOI of 2.42. Viral RNA levels were assessed via strand-specific RT-qPCR and viral titers were measured using an end-point dilution assay (TCID$_{50}$). **(C)** The percentage of infected cells per time-point was determined by quantification of fluorescence microscopy images (D). **(D)** Representative images taken at 4, 12 and 70 hpi in the green channel (470 nm). The cellular eGFP marker localizes to mitochondria, giving a punctate cytoplasmic pattern, until the cell is infected and the eGFP shuttles to the nucleus, giving a sharp nuclear signal. Arrow in the 12h image shows an infected cell. Asterisk indicates a newly infected cell with cytoplasmic and nuclear eGFP signal. Uninfected as well as infected cells are exemplified and were counted via an H2B$_{mCherry}$ marker. Images were quantified using Fiji. Data in (B) and (C) shows means +/- standard deviation from five (viral RNA, % infected cells) and four (viral titer) independent experiments, respectively. 226 images in total were quantified for (C). Quantification presented in (C) was performed with the help of Christoph Harmel.

4.2.3. Model simulation of full-length HCV replication

This section describes the extension of our intracellular to the full life-cycle model on the mathematical side, which represents the PhD project of our close collaborator Darius Schweinoch (Kaderali lab, Greifswald). The content is thus mostly his intellectual property that we commonly discussed in many interactive meetings and presentations. The collaborative project will be published soon with a shared first authorship.

After setting up the experimental system to measure viral determinants in the course of a full-length HCV$_{cc}$ infection, we extended our mathematical model accordingly to be able to describe viral infection, the production and release of infectious particles, and spread in this new experimental setting. Figure 15 shows model schemes for both, our intracellular (A) as well as our extended full life cycle model (B). The intracellular model was developed in our lab and published many years ago [277]. It describes all key steps in the HCV replication cycle after electro-transfection of Huh7-Lunet cells with the subgenomic reporter replicon sgJFH. Those are: processing of the transfected RNA (R_P^{unp} to R_P^{cyt}, (1)), translation of the processed RNA (2), processing of the synthesized polyprotein (3), establishment of the replication compartment and initiation of (-)-strand synthesis (4), synthesis of (-)-strands (5) as well as progeny (+)-strands (6), and output of the (+)-strand RNA back into the cytoplasm (7) (Figure 15A). We made few adaptations and introduced new species to account for the novel experimental system. Since target cells (*TU*) are now infected by authentic viral particles, step (1) was replaced and represents infection by viral particles (V_a) with rate (β) now (Figure 15B). The number of ribosomes that can simultaneously bind one (+)-strand RNA molecule as well as the RNA synthesis rates k_{4p} and k_{4m} were adapted to the increased length of the HCV RNA used. The production and release of infectious particles was calculated by the total amount of (+)-strand RNA ($R_{P,tot}$) and structural protein $E_{S,tot}$ with the assembly and release rate *p* (8). The unknown infection rate β and assembly rate *p* were fitted together with several other parameters. All the parameters were identifiable, which confirmed that our model includes no redundant parameterization and allows for mechanistic interpretation of model simulations. The new age-based model takes into account the period a cell is infected and the time-dependent production of viral RNA as well as infectious particles. This age-based model is linked to a population model describing the number of infected cells to account for viral spread.

Figure 15 Model schemes of the intracellular (A) and full life cycle model (B) of HCV replication. (A) The intracellular model is based on the electroporation of a subgenomic reporter version of the HCV RNA genome (sgJFH) into Huh7-Lunet cells. The transfected RNA ($R_P{}^{unp}$) is processed in a first step (k_0) to become translation-competent. The model scheme is adapted from and based on the Binder model [277]. **(B)** The full life cycle model is based on infection of Lunet-CGM cells with cell culture-derived full-length Jc1. Cells (*TU*) are infected by viral particles (*V_a*) with infection rate β and turn into infected cells (*TI*). Total cellular (+)-strand RNA ($R_{P,tot}$) and structural proteins ($E_{S,tot}$) are used for assembly (assembly rate *p*) of infectious particles (*V_a*). *k* are rate constants and *μ* are degradation rates.

Figure 16 shows Jc1 infections dynamics data (as already presented in Figure 14 as means +/- standard deviation) plus the new model simulations. We used the recorded data to fit adapted or new parameters in our new full life cycle model, which was eventually able to simulate viral RNA and infectious particle kinetics as well as infection spread in Lunet-CGM cells after Jc1 infection (Figure 16A–D). The variations we observed were of technical nature or caused by cellular properties that changed with passage number and affected viral replication. Passage number is the one determinant that reportedly most fundamentally affects HCV replication efficiency [280]. The percentage of infected cells appeared to vary the most; however, note that all other parameters are on logarithmic scale. The model quite accurately fit (+)-strand RNA dynamics despite the huge excess of non-infectious (+)-strand RNA in the virus inoculum (Figure 16A and Figure A2B). The immense drop in (+)-strand RNA levels between 0 and 8 hpi could also represent, at least in part, the minor portion of infectious viral (+)-strands that manage to establish a productive infection in the host cell. (-)-strand RNA levels were overrepresented in the first 4 hpi as compared to the model fit (Figure 16B). However, this probably owes to the immense excess of (-)-strand RNAs in the virus inoculum that was non-infectious and degraded over time as well (see above and Figure A3). In the model simulation, we assumed that there is a 12-hour delay in the time from a cell being infected to being detected as such. This is based on the nature of our eGFP reporter system in which the viral protease NS3/4A needs first to be produced in the infected cell so it can cleave the MAVS mitochondrial membrane anchor of eGFP, which then needs to translocate to the nucleus in sufficient amounts. The cells that were counted in an automated
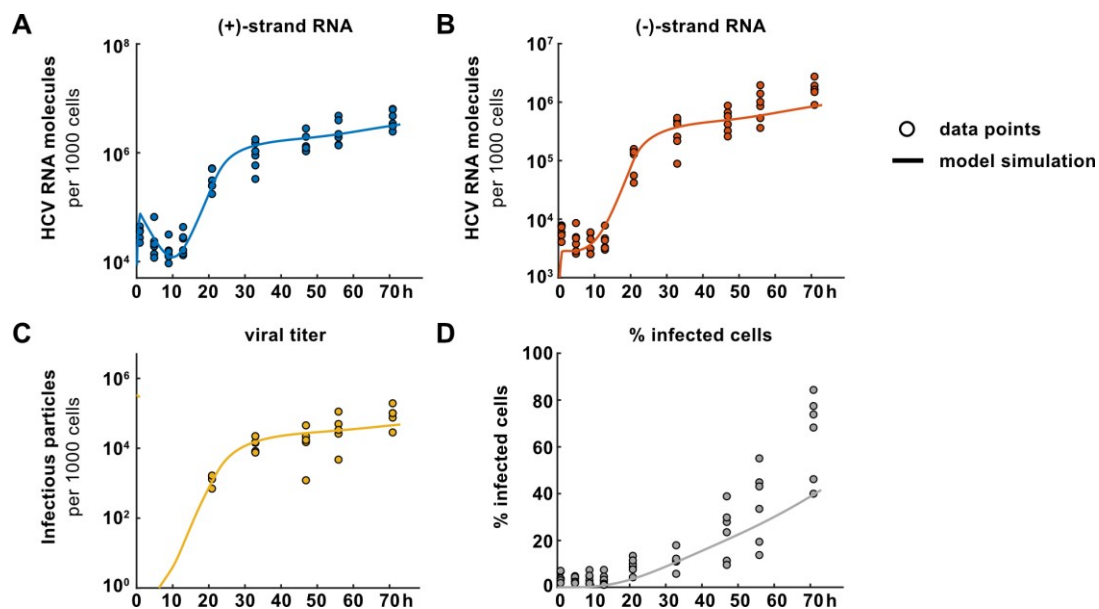
Figure 16 HCV$_{cc}$ (Jc1) replication dynamics in Lunet-CGM cells and model fits of the new full life-cycle model. Lunet-CGM cells were infected with HCV$_{cc}$ (Jc1) at an MOI of 2.42 and viral and cellular determinants were measured in a tight time-course. A strand-specific RT-qPCR was used to determine the absolute numbers of (+)- **(A)** and (-)-strand RNA molecules **(B)**. Viral titers were determined using an endpoint dilution assay (TCID$_{50}$) **(C)**. Fluorescent microscopy images were used to quantify the percentage of infected cells **(D)**. Data points are represented by circles and model simulations by lines. Model simulations and plots were generated and provided by Darius Schweinoch. Figures show data from six independent biological experiments.

manner as infected between 0 and 12 hpi were mostly dead cells that looked highly similar to infected cells and were hard to discriminate from the latter by the image quantification software.

4.2.4. Model simulation of Jc1 dynamics under DAA treatment

After fitting our new full life-cycle model to the highly time-resolved and quantitative data and seeing that it is able to describe viral replication and spread in this setting quite well, we went on to validate our model using targeted intervention. For several years now, direct-acting antivirals (DAAs) are available on the market and used in the clinics to treat chronic HCV infection with remarkable efficacy and only mild side effects. Mainly three classes of DAAs exist: inhibitors of the NS3/4A protease (dubbed -previr), the NS5B polymerase (-buvir), and the NS5A phosphoprotein (-asvir) (reviewed in [313]). As described above, the mode of action of NS5A inhibitors is still elusive due to the many functions of NS5A in the viral life cycle. In contrast, NS3/4A protease and NS5B polymerase inhibitors have rather specific modes of action as determined by the functions of their targets. Thus, we set out to validate our model by challenging it with HCV replication data under treatment with the NS3/4A inhibitor Telaprevir (TEL) and the NS5B inhibitor Sofosbuvir (SOF) as we did before with the intracellular model. We determined the IC_{50}s of all three inhibitors in the full life-cycle setting and used exactly those to achieve inhibition but no complete eradication of viral infection (Figure A4).

4.2.4.1. The NS3/4A inhibitor Telaprevir (TEL)

Figure 17 shows Jc1 replication dynamics upon TEL treatment. As expected, TEL treatment led to reduced viral replication by inhibiting the polyprotein processing step exerted by NS3/4A. As already observed in the intracellular setting, onset of replication was delayed as (+)- and (-)-strand levels increased from only 20 hpi on compared to 12 hpi for the untreated condition (Figure 17A). In contrast to the intracellular system, RNA levels in the TEL condition did not reach similar levels at the assay point as in the untreated condition. RNA levels only reached 20% of untreated at 70 hpi in this setting (see also Figure A5A). The delayed onset of replication might have impaired particle production resulting in less infection spread and thus lower total RNA levels at the assay

Figure 17 Jc1 replication dynamics under Telaprevir (TEL) treatment. (A–C) Jc1 replication dynamics after infection of Lunet-CGM cells with an MOI of 2.42 under TEL inhibition (IC_{50}, 182 nM) or untreated. Viral RNA was assessed via strand-specific RT-qPCR (A) and viral titers were measured using an end-point dilution assay ($TCID_{50}$) (B). The percentage of infected cells was quantified from fluorescence microscopy images (C). Data in (A) shows means +/- standard deviation from five (untreated) and two (TEL), data in (B) from four (untreated) and two (TEL), and data in (C) from five (untreated) and two (TEL) independent experiments, respectively. Total images quantified for (C) were 226 for untreated and 71 for TEL. Image quantification was performed with the help of Christoph Harmel.
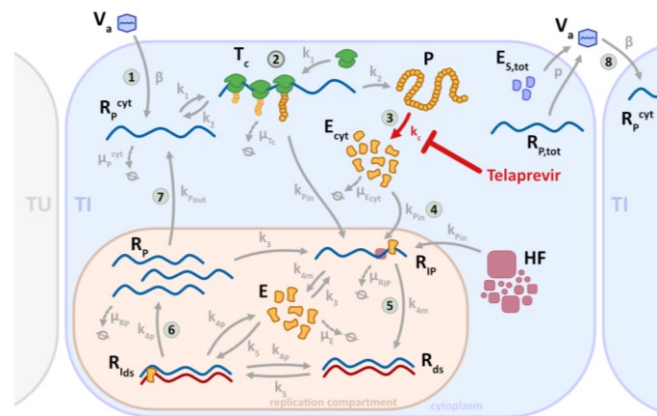
Figure 18 Model scheme with highlighted mode of action of the NS3/4A inhibitor TEL. TEL inhibits the NS3/4A protease, which processes the HCV polyprotein and cleaves it into the mature proteins (k_c). Details are provided in the Methods section.

endpoint. Indeed, viral titers were reduced during the whole time course (Figure 17B). Compared to the decline in RNA levels (down to 20%), viral titers seemed reduced even more, reaching only 10% of untreated at later time-points (Figure A5A), suggesting an additional effect of TEL on particle production on top of polyprotein cleavage. Image quantification revealed a strong decrease in the percentage of infected cells in the culture dish as well (Figure 17C). This probably only partly originated from a real reduced number of infected cells, though, since the NS3/4A inhibition by TEL not only impairs polyprotein processing but also cleavage of our eGFP reporter, which at least slows down if not partly abrogates translocation of the same into the nucleus and thus detection and counting of the cell as infected. Hence, we probably underestimate the number of infected cells in this case. Collectively, it seems that TEL not only inhibited polyprotein cleavage by targeting NS3/4A, which delayed the onset of replication. The even more pronounced effect on viral titer reduction suggests a yet undefined additional impairment of infectious particle production or release.

We wanted to test our new extended and calibrated model if it was able to predict Jc1 replication dynamics in the full-length context under drug treatment. We implemented the inhibition term of TEL at the polyprotein processing step k_c (Figure 18) as we did before in the intracellular setting, resulting in a good model prediction (Figure 12A). Unfortunately, the model now underestimated the inhibitory effect of TEL treatment on Jc1 replication dynamics (Figure 19, dotted lines). The reason for this might be that TEL indeed inhibits additional steps in the viral life cycle besides polyprotein processing (k_c) that we did not account for in the model, for example particle assembly or release. The dramatic decrease in viral titers that we observed in the biological data might support this notion. As our subgenomic setup and the intracellular model did not include any of these steps, the model prediction for the TEL treatment was quite good (see Figure 12A). However, it might as well be that the establishment of a productive replication/infection is much more sensitive in the infection setting than it is in the electroporation setting, where hundreds to thousands of RNA molecules per cell are present at the assay start. Model predictions including a TEL effect on the assembly rate p should reveal if there is an additional effect on top of the polyprotein processing rate reduction. Those predictions should resemble the biological data

Figure 19 Model simulations of Jc1 replication dynamics in Lunet-CGM cells under Telaprevir (TEL) treatment. The model was calibrated on data from the untreated condition and predicted viral replication dynamics by only adapting k_c, the polyprotein cleavage step exerted by NS3/4A, which was inhibited by TEL. **(A)** (+)-strand RNA levels, **(B)** (-)-strand RNA levels, **(C)** infectious titers, **(D)** percentage of infected cells. Model fit for the untreated condition is in lines, data points for the treatment (TEL) condition are in circles, and model prediction for the treatment setting is in dotted lines. Model simulations and plots were generated and provided by Darius Schweinoch. Figures show data from two independent biological experiments.

better than the prediction taking into account only k_c as a target step of TEL treatment. Still, to find out which step in the viral life cycle is affected on top of k_c in an unbiased way, we could use the model to fit the data allowing only one additional parameter to change at a time. This would give an answer if assembly or any other step in the viral life cycle is possibly affected by inhibiting the NS3/4A protease using TEL.

4.2.4.2. The NS5B inhibitor Sofosbuvir (SOF)

After decades of standard of care for chronic hepatitis C with PEG-IFN-α and ribavirin, resulting in only 50% cured patients along with severe side effects, Sofosbuvir (SOF) was among the first direct-acting antivirals (DAAs) to get approval and hit the US market in 2013 [189]. It was the first direct-acting antiviral that was administered (together with the NS5A inhibitor ledipasvir) as an all-oral, IFN-free, single tablet regimen in 2014 in the US [189]. Its high tolerability, efficacy, and low risk for drug-drug interactions made it indispensable for HCV treatment since then [189]. SOF is a pro-drug that is metabolized in the liver to its active uridine triphosphate analogue form and is incorporated into the nascent RNA strand by NS5B, which leads to chain termination [188, 314].

We used SOF to validate our newly extended full life cycle model for HCV replication as described before for TEL. Since SOF is a prodrug and needs activation first, we started treatment 16 hours prior to infection and continued it throughout the experiment as for TEL. As already observed in the intracellular setting, SOF treatment reduced the slope of RNA level increase, whereas onset of replication was not delayed (Figure 21A). This eventually resulted in about 50% reduction in (+)- and (-)-strand RNA levels at the assay endpoint (70 hpi, see also Figure A5B). The data showed a consistent drop in (+)-strand RNA levels at 45 hpi, the cause of which is hard to explain though.
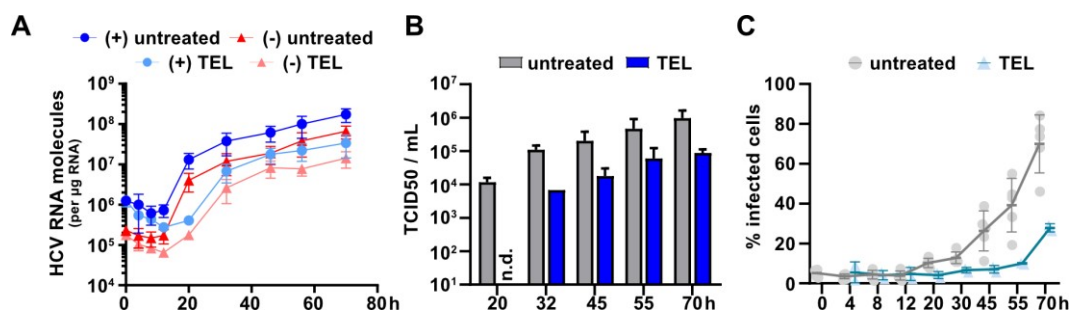
Figure 21 Jc1 replication dynamics under Sofosbuvir (SOF) treatment. (A–C) Jc1 replication dynamics after infection of Lunet-CGM cells at an MOI of 2.42 under SOF inhibition (IC_{50}, 37 nM) or untreated. Viral RNA was assessed via strand-specific RT-qPCR (A) and viral titers were measured using an end-point dilution assay ($TCID_{50}$) (B). The percentage of infected cells was quantified from fluorescence microscopy images (C). Data in (A) shows means +/- standard deviation from five (untreated) and two (SOF), data in (B) from four (untreated) and two (SOF), and data in (C) from five (untreated) and two (SOF) independent experiments, respectively. Total images quantified for (C) were 226 for untreated and 83 for SOF. Image quantification was performed with the help of Christoph Harmel.

Infectious titers were reduced throughout the experiment but only to a slight extent (Figure 21B). Quantification of fluorescence images revealed a minor reduction in the number of infected cells (Figure 21C).

We then wanted to test if our new model was able to predict Jc1 replication dynamics upon SOF treatment. We incorporated the SOF effect in our model using IC_{50} inhibition terms at the rate constants k_{4p} and k_{4m} as done before with the intracellular model (Figure 20, see also Methods section). The model predicted Jc1 replication dynamics under SOF treatment quite well, although the difference to the untreated condition was very small (Figure 22). The data points for (+)-strand RNA levels at 45 and 55 hpi were not covered by the model prediction (Figure 22A), although they might be outliers as well. The model prediction also missed the (-)-strand RNA data points at 32 and 45 hpi (Figure 22B). The infectious titer prediction fit quite well although there was a high variation in the biological data for few time points (Figure 22C). Due to the high variance of the percentage of infected cells data in the untreated condition (n=5, see Figure 21C), the model prediction was quite off for the SOF condition, especially at late time points (Figure 22D). In the SOF replicates, the percentage of infected cells was comparably high and the model allows only a
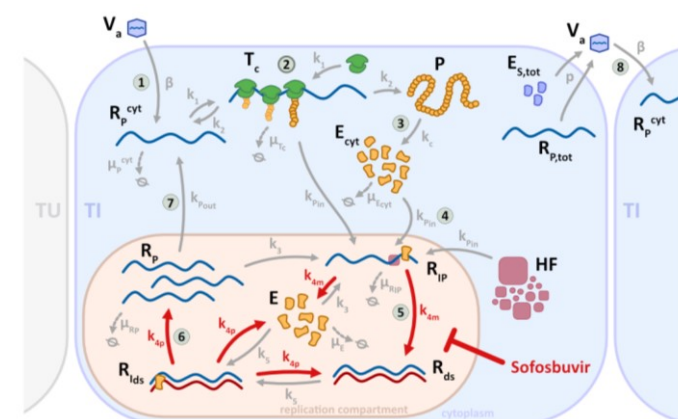
Figure 20 Model scheme with highlighted mode of action of the NS5B inhibitor SOF. SOF inhibits the NS5B polymerase, which synthesizes (+)- and (-)-strands in the replication compartment (k_{4p} and k_{4m}). Details are provided in the Methods section.
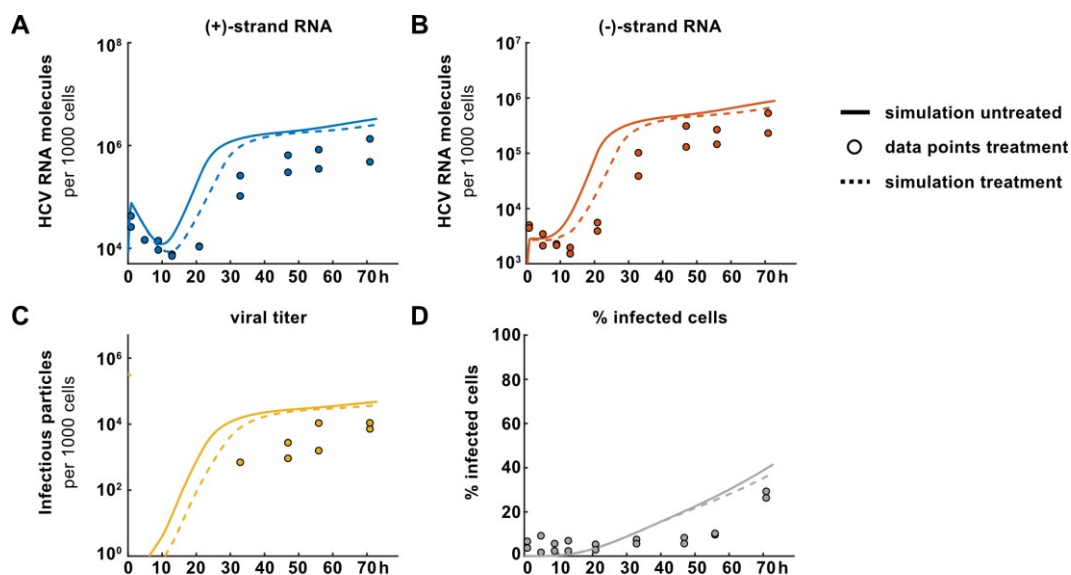
Figure 22 Model simulations of Jc1 replication dynamics in Lunet-CGM cells under Sofosbuvir (SOF) treatment. The model was calibrated on data from the untreated condition and predicts viral replication dynamics by only adapting k_{4p} and k_{4m}, the RNA synthesis steps exerted by NS5B, which is inhibited by SOF. **(A)** (+)-strand RNA levels, **(B)** (-)-strand RNA levels, **(C)** infectious titers, **(D)** percentage of infected cells. Model fit for the untreated condition is in lines, data points for the treatment (SOF) condition are in circles, and model prediction for the treatment setting is in dotted lines. Model simulations and plots were generated and provided by Darius Schweinoch. Figures show data from two independent biological experiments.

reduction upon treatment (Figure 22D). Overall, the model prediction of Jc1 replication dynamics under SOF treatment resembled the biological data adequately, although the effect of SOF inhibition was rather small.

In conclusion, our newly extended full life cycle model is able to predict Jc1 replication dynamics even under treatment with inhibitors with a known mode of action. In order to improve the TEL prediction, we might need to include an additional effect on a step in the viral life cycle besides polyprotein cleavage. Using different drug concentrations should confirm our findings and help in refining the model. Still, based on the finding that our model is in principal able to recapitulate drug effects in the full-length system, we went on to analyze the effect of DCV treatment on Jc1 replication in the biological data as well as in the model prediction.

4.2.4.3. The NS5A inhibitor Daclatasvir (DCV)

Our model fit of intracellular HCV replication dynamics under DCV treatment revealed k_1 as well as k_{4m} and k_{4p} as the steps most probably affected by DCV treatment (Figure 12). Except for late time points, the model was able to fit the actual data quite well. We used the very same set of parameters in order to predict now full-length Jc1 replication dynamics and to see if it was necessary to include additional effects on assembly or other steps in the viral life cycle to produce an accurate prediction.

As already observed in the intracellular system, Jc1 replication dynamics under DCV showed features of TEL and SOF inhibition at one time. Clearly visible for (+)-strand dynamics, onset of replication was delayed by 4 hours under DCV treatment (12 vs. 8 hpi, Figure 23A). The following
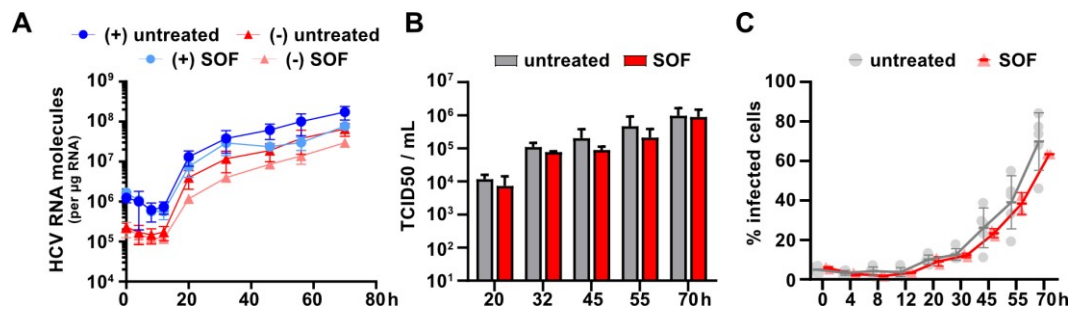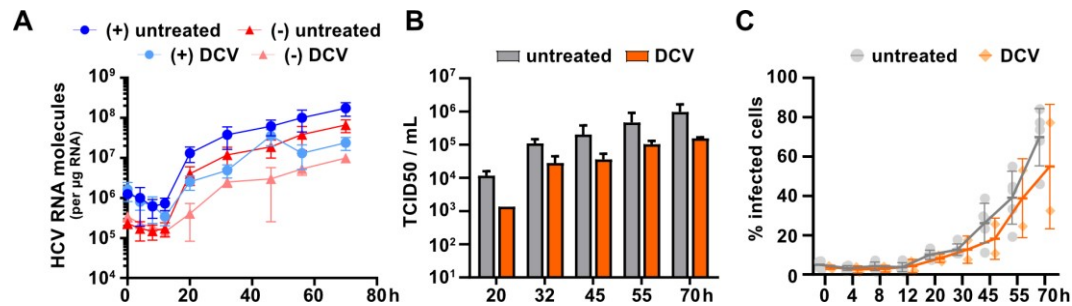
Figure 23 Jc1 replication dynamics under Daclatasvir (DCV) treatment. (A–C) Jc1 replication dynamics after infection of Lunet-CGM cells at an MOI of 2.42 under DCV inhibition (IC_{50}, 82 pM) or untreated. Viral RNA was assessed via strand-specific RT-qPCR (A) and viral titers were measured using an end-point dilution assay ($TCID_{50}$) (B). The percentage of infected cells was quantified from fluorescence microscopy images (C). Data in (A) shows means +/- standard deviation from five (untreated) and two (DCV), data in (B) from four (untreated) and two (DCV), and data in (C) from five (untreated) and two (DCV) independent experiments, respectively. Total images quantified for (C) were 226 for untreated and 71 for DCV. Image quantification was performed with the help of Christoph Harmel.

increase in RNA levels was not as steep as for the untreated condition and RNA levels reached only about 15% of untreated levels at 70 hpi (see also Figure A5C). Infectious titers were markedly reduced (Figure 23B), however, not exceeding the reduction in RNA levels as during TEL treatment (see also Figure A5C). Despite the big standard deviation due to the high variance in the two replicates, the percentage of infected cells under DCV treatment appeared to be lower compared to untreated as well (Figure 23C).

We used our extended full life cycle model to predict Jc1 replication dynamics under DCV treatment, assuming that the same set of parameters (k_1, k_{4p}, and k_{4m}) as found by model fit in the intracellular system is affected here (depiction of affected parameters in Figure 24). RNA level predictions fit quite well and reflected what we observed in the biological data: a delayed onset of replication that is more pronounced for the (+)-strand than for the (-)-strand, and a less steep increase in RNA levels leading to lower plateaus and endpoint levels at 70 hpi (Figure 25A, -B). Unfortunately, RNA levels seemed to be off for few time points. This was true for especially one
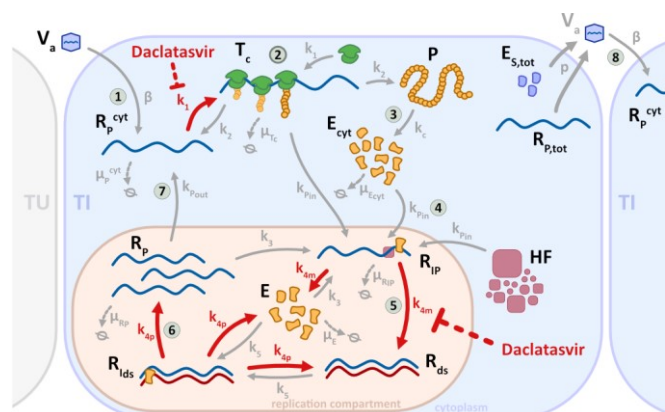
Figure 24 Model scheme with steps affected by DCV treatment as revealed by model fitting in the intracellular setting. DCV inhibits the NS5A phosphoprotein, which binds HCV RNA and is involved in building the replication compartment and assembly of virions. Upon fitting our intracellular model to HCV replication data, it revealed adjustment of k_1, k_{4m}, and k_{4p} to give the best fit. Details are provided in the Methods section. See also Figure 12C.
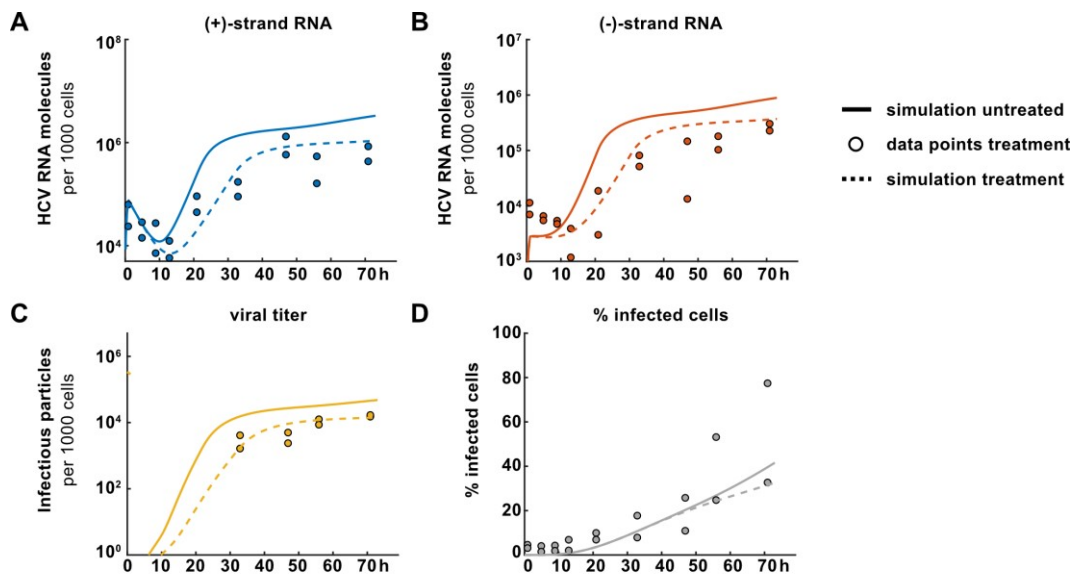
Figure 25 Model simulations for Jc1 replication dynamics in Lunet-CGM cells under Daclatasvir (DCV) treatment. The model was calibrated on data from the untreated condition and predicts viral replication dynamics by adapting k_1, k_{4p} and k_{4m}. Those parameters 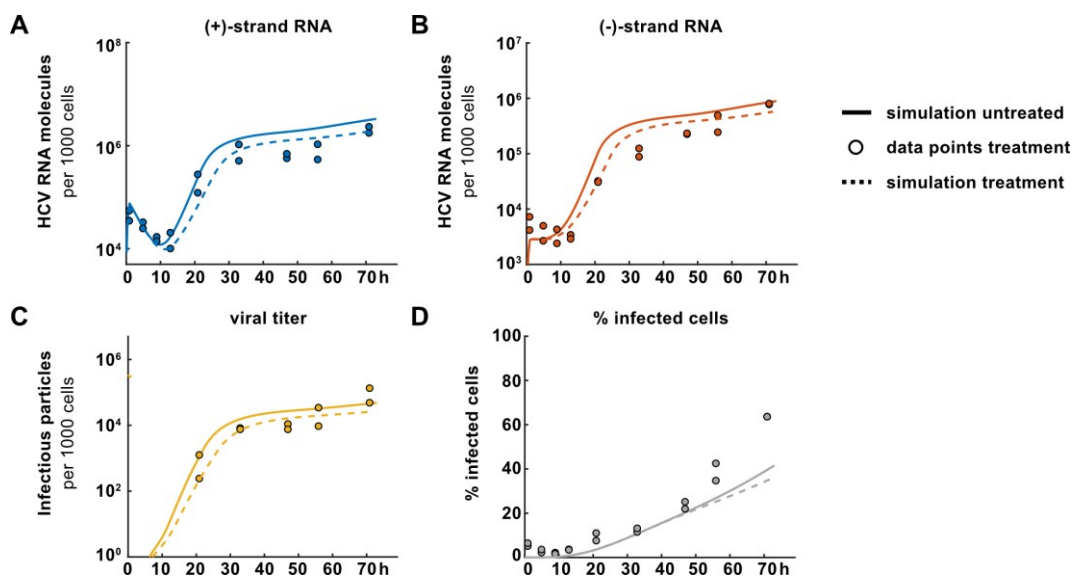revealed to be affected using our intracellular model fit. **(A)** (+)-strand RNA levels, **(B)** (-)-strand RNA levels, **(C)** infectious titers, **(D)** percentage of infected cells. Model fit for the untreated condition is in lines, data points for the treatment (DCV) condition are in circles, and model prediction for the treatment setting is in dotted lines. Model simulations and plots were generated and provided by Darius Schweinoch. Figures show data from two independent biological experiments.

replicate and its 20 and 45 hpi time points, where reproducibly (+)-strand RNA levels were too high and (-)-strand levels too low, respectively. The model slightly overestimated endpoint RNA levels for both strands. This might be a hint that modeling inhibition of only the described parameters is not sufficient to predict the impact exerted by DCV treatment. However, virus titer predictions are near perfect, except at 45 hours where the biological data shows a slight drop in infectious titers (Figure 25C). The number of infected cells was hard to predict as we observed a strong variation between our two biological replicates (Figure 23C). The model simulation resembled more closely the replicate with a much lower percentage of infected cells than the other replicate and was not able to reflect the sharp increase in the percentage of infected cells between 45 and 55 hours (Figure 25D). This might in part be due to reasons discussed for the percentage of infected cells in the SOF treatment (see above). Eventually, model predictions upon adjustment of only k_1, k_{4m}, and k_{4p}, fit the biological data quite well and qualitatively resembled Jc1 replication dynamics under DCV treatment. It was not necessary to include additional effects on particle production, although this might further improve the predictions. A next step would be to completely block HCV replication in the steady state with a sufficient dose of DCV and to monitor and model infectious titers as well as intra- and extracellular RNA. This would certainly reveal if DCV immediately halts particle release or renders particles less or non-infectious.

Overall, we successfully extended our intracellular HCV replication model to cover the full viral life during Jc1 infection of Lunet-CGM cells. We provide an experimental platform to accurately measure viral (+)- and (-)-strands, infectious titers as well as the percentage of infected cells in the culture dish. The data basis as well as the model extension are sufficient to identify and fit newly

introduced parameters. The new model is able to simulate (+)- and (-)-strand RNA levels, viral titers, and spread in the cell culture during the course of infection. In addition, it is capable of predicting the impact of drugs with a known mode of action on HCV replication. The model prediction of Jc1 replication dynamics under DCV treatment resembled the data quite well by only adjusting parameters that were identifying using the intracellular model. We did not have the chance to improve this prediction or generate a model fit to Jc1 replication dynamics data under DCV treatment. This, clearly, would give deeper insights into the mode of action of DCV. Nevertheless, as such, our new full life cycle model poses the first detailed model of its kind and can now be used the study the effect of drugs, including IFN-α and DCV, on HCV replication in an infection setting. Furthermore, the model can reveal insights into the molecular origin of permissiveness for HCV, the differences in virulence among HCV genotypes, and the impact or the nature of host factors governing HCV replication.

4.3. The intracellular model proposes a host factor that is involved in replication complex formation determines permissiveness

The findings presented in this part are already published [278] and figures depicted here are taken from the publication with minor modifications as indicated in the figure legends.

The intracellular model could simulate HCV replication in an Huh7 variant with high HCV replication efficiency, termed permissiveness, (Huh7-Lunet) as well as in a low permissive Huh7 variant (Huh7-LP), with roughly 10-fold lower HCV replication efficiency [277]. By doing so, it revealed that formation of the replication compartment (RC) is the most probable step for the involvement of a host factor (HF) that determines cellular permissiveness [277]. As the model further suggested, this HF appears to be limiting for replication in Huh7-LP cells, but not so in Huh7-Lunet cells [277]. This HF could be a single protein, a protein complex, or a host process.

4.3.1. Gene expression profiling suggests potential host factors for HCV

To identify potential candidates qualifying as such a HF, gene expression data from microarrays of eight different Huh7 variants were correlated with their respective HCV permissiveness [277]. Those eight different Huh7 variants differed up to 1000-fold in their permissiveness for HCV (Figure 26A). Functional annotation of the hits revealed an enrichment for genes involved in "cell growth and proliferation" [277]. To exclude that permissiveness for HCV is solely based on different growth kinetics of the analyzed Huh7 variants, we quantified proliferation of three of them using the IncuCyte™ live cell imaging platform, and found no major differences (Figure 26B). We teamed up with Evgeny Gladilin (IPK, Gatersleben) who re-analyzed the microarray data and came up with 34 novel candidate genes that we decided to follow up regarding their biological relevance for HCV replication (Figure 26C). Those candidate genes showed rather low differential expressions but constantly high correlation coefficients with HCV permissiveness across the eight tested Huh7 variants (Figure 26C). Raw expression values from microarray data confirmed the results from the statistical analysis and showed increasing levels of candidate mRNAs with increasing permissiveness for HCV among the tested Huh7 variants (Figure 26D).

4.3.2. Knockdown of proposed host factor candidates restricts HCV replication

We used highly permissive Huh7-Lunet cells with presumably high expression of all our candidate genes to test for their role in HCV replication. We reverse-transfected three different siRNAs per gene and infected the cells with our full-length reporter virus JcR2a 24 hours later to see if their knockdown affects HCV replication. 72 hours post infection (hpi), we measured luciferase activity and tested for cytotoxicity in in parallel mock-infected plates. Twelve candidate genes targeted by 14 siRNAs (two siRNA for two of the genes) showed a robust reduction of JcR2a replication (Figure 27A) from roughly 60–90% without affecting cell viability (except ZNF512B, cut-off 75% viability, Figure A6A). The full list of candidates with their effects on HCV replication and cell viability are provided in the Appendix (Figure A7, Table A1). We used siRNAs targeting the well-described host factor phosphatidylinositol-4 kinase III alpha (PI4KIIIα) as a positive control and an siGFP as a negative control. To confirm these results in a different and more robust system, we used a cell line that stably replicates a subgenomic reporter version of HCV RNA in its cytoplasm, called
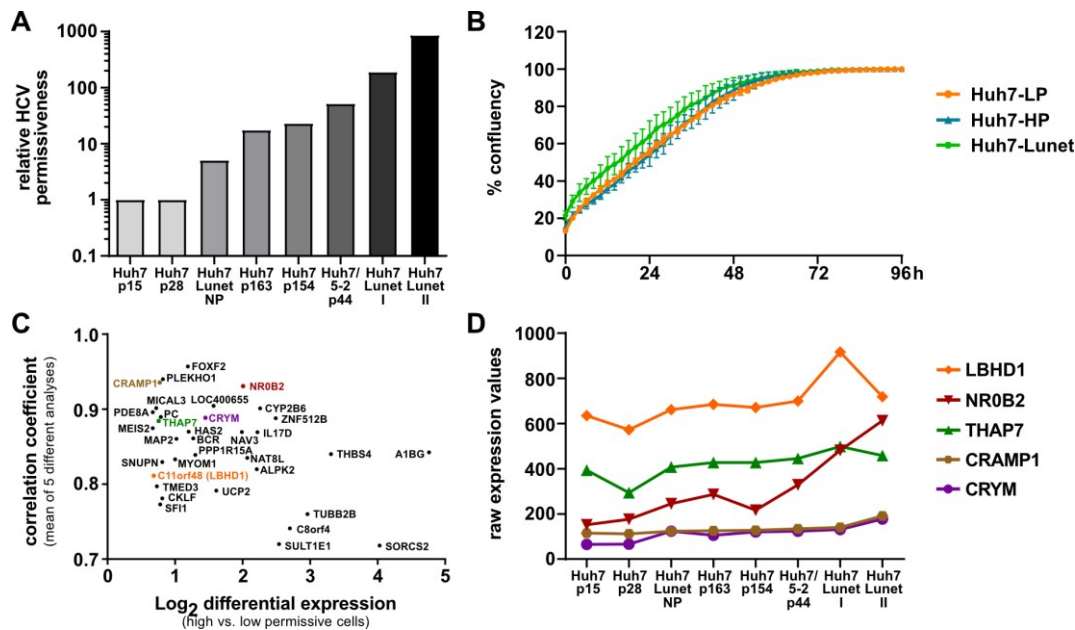
Figure 26 Correlation of gene expression profiling with HCV permissiveness in eight different Huh7 variants reveals novel HF candidate genes. (A) Relative HCV replication efficiency in eight different Huh7 variants based on the replication of the subgenomic firefly luciferase reporter replicon Con1-ET (genotype 1b) at 48 hpe vs. 4 hpe. Data was normalized to the two low permissive variants Huh7 p15 and -p28. **(B)** 7500 (Huh7-LP) or 5000 (Huh7-HP, Huh7-Lunet) cells were seeded in 96-well plates and imaged every two hours in an IncuCyte machine. Images were quantified with the IncuCyte™ ZOOM software and its confluence mask. Data shows means +/- standard deviation from technical quadruplicates and one independent experiment. **(C)** 34 selected candidates after statistical filtering for the correlation of their expression with HCV permissiveness in the eight Huh7 variants. Followed-up candidates are in color. **(D)** Raw expression values from microarray data for five candidates that showed promising results and were followed up further. Statistical analysis for filtering candidate genes (C) was performed by Evgeny Gladilin. Data shown in (A) was produced by Marco Binder [277]. Figure adapted from [278].

Huh7-LucUbiNeo-JFH [136]. This clonal cell line is kept under constant selection pressure by G418 (neomycin) to which resistance is conferred by the replicon. The selection process and further passaging conferred robust replication of the HCV replicon and possible adaptations on the host side. This system allowed us to simply reverse-transfect siRNAs as before without the need of transfection of or infection with viral genomes. Luciferase measurements 96 hours post siRNA transfection confirmed five of the 14 tested siRNAs to reduce HCV replication even in this system (Figure 27B). As expected, the effects of gene knockdown on HCV replication were not as pronounced as during JcR2a infection (Figure 27A). This might either be caused by roles of the knocked down genes in steps not represented in the subgenomic replicon setting, like assembly or release of viral particles, or originate from the robustness of the replicon system as described above. In addition, transfection efficiencies could be lower in the replicon cell line, but we have not tested for this. However, the knockdown effects of PI4KIIIα seemed more robust than those of our candidate genes and impaired HCV replication severely. None of the confirmed siRNAs showed strong cytotoxic effects in this system (Figure A6B).

Conclusively, the statistical analysis and filtering of genes that correlated in their expression levels with HCV permissiveness in eight different Huh7 variants, revealed several promising candidates that upon knockdown impaired HCV replication efficiency. This impairment was found upon infection with the reporter virus JcR2a as well as in a stable replicon cell lines with robust replication of a subgenomic HCV reporter RNA. The five most promising candidates were LBH domain containing 1 (LBHD1, also known as C11orf48), cramped chromatin regulator homolog 1 (CRAMP1), crystalline μ (CRYM), THAP domain containing 7 (THAP7), and nuclear receptor subfamily 0 group B member 2 (NR0B2, also known as SHP). The former two are barely characterized and the latter three are a nuclear receptors or transcriptional (co-)repressors, respectively. However, before characterizing those genes functionally, we sought to further analyze the role of their expression levels for HCV replication.

4.3.3. Overexpression of host factor candidates in a low permissive Huh7 variant boosts HCV replication

Since the model proposed that the HF is of limiting abundance in low permissive Huh7-LP cells [277], we speculated that upon overexpression of our candidate genes HCV replication might increase. Therefore, we cloned their cDNAs into N-terminally HA- or C-terminally FLAG-tagged expression vectors and stably transduced Huh7-LP cells. All the candidate genes were robustly
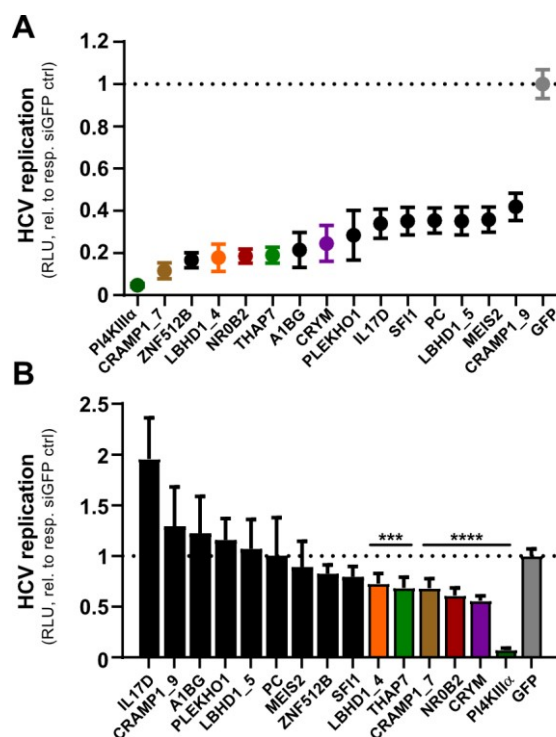
Figure 27 HCV replication upon siRNA-mediated knockdown of candidate genes using the full-length reporter virus JcR2a (A) or the stable replicon cell line Huh7-LucUbiNeo-JFH (B). (A) Huh7-Lunet cells were reverse-transfected with indicated siRNAs 24 hours prior to JcR2a infection (MOI ~0.1). 72 hours post infection, cells were lysed and luciferase activity was measured. Data is shown relative to an siGFP control. **(B)** Huh7-LucUbiNeo-JFH cells were reverse-transfected and luciferase activity of the subgenomic replicon was measured 96 hours later. Data is shown relative to an siGFP control. Candidates that were followed-up further are in color. Data shows means +/- standard deviation from three (A) and two (B) independent experiments, respectively. *** p ≤ 0.001, **** p ≤ 0.0001. Adapted from [278].

expressed and could be detected on mRNA level via qPCR as well as on protein level as assessed by immunoblotting against the corresponding tags or their own epitopes (except for NR0B2-FLAG using an α-FLAG antibody, Figure A8, Figure A9, Figure A10). We measured mRNA expression levels of CRAMP1, CRYM, and LBHD1 only in the FLAG-tagged versions. However, measurements of THAP7 and NR0B2 overexpressing cells showed that HA-tagged versions are at least similarly if not more robustly overexpressed than the corresponding FLAG-tagged ones (Figure A9, Figure A10). We used our subgenomic reporter replicon sgCon1-ET and our full-length reporter virus JcR2a to assess the effect of overexpression on HCV replication.

CRAMP1 overexpression showed no significant effect on sgCon1-ET replication neither with the N-terminal HA- nor the C-terminal FLAG-tag (Figure 28A). However, we observed a slight but statistically significant boost of HCV replication in the infection setting (Figure 28B). CRYM overexpression led to a 2-fold increase in sgCon1-ET replication at 72 hpe, which was limited to the HA-tagged version though (Figure 28C). Again, overexpression of CRYM showed a stronger effect on JcR2a replication than on sgCon1-ET replication that reached almost 5-fold levels compared to the empty control at 72 hpi (Figure 28D). LBHD1 overexpression effects were ambiguous: HA-LBHD1 increased sgCon1-ET replication at 48 and 72 hpe to more than 2-fold; however, LBHD1-FLAG reduced HCV by almost 2-fold at those time points (Figure 28E). JcR2a infection confirmed the positive effect of HA-LBHD1 overexpression in an infection setting and
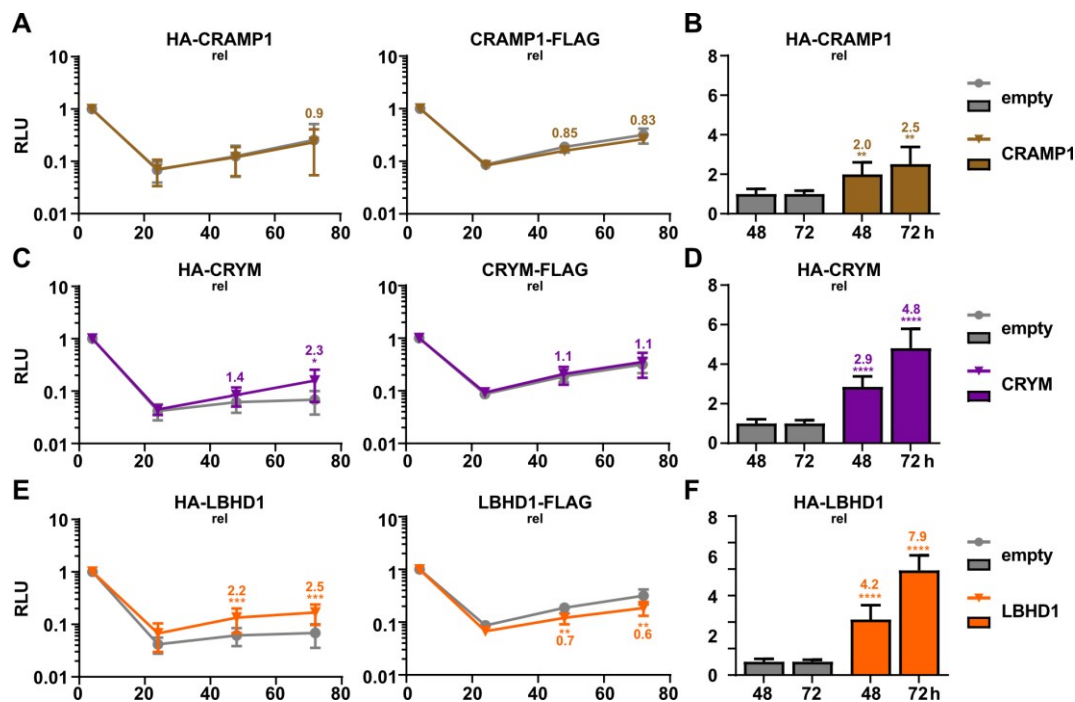
Figure 28 HCV replication after electroporation of sgCon1-ET (A, C, E) or infection with JcR2a (B, D, F) in HF candidate overexpressing cells. (A, C, E) Huh7-LP cells overexpressing either N-terminally HA- (left panels) or C-terminally FLAG-tagged (right panels) versions of CRAMP1 (A), CRYM (C), LBHD1 (E), or the corresponding controls (HA-empty, empty-FLAG) were electroporated with the subgenomic reporter replicon sgCon1-ET (gt1b) and luciferase activity was measured at 4, 24, 48, and 72 hpe. **(B, D, F)** Huh7-Lunet cells overexpressing N-terminally HA-tagged CRAMP1 (A), CRYM (D), or LBHD1 (F), or their respective controls (HA-empty) were infected with JcR2a (MOI ~0.1) and luciferase activity was measured at 48 and 72 hpi. Data shows means +/- standard deviation from three independent experiments (except (B) and (F), n=2) each and is relative to 4 hpe (A, C, E) or relative to the empty control (B, D, F). * p ≤ 0.05, ** p ≤ 0.005, *** p ≤ 0.001, **** p ≤ 0.0001. Adapted from [278].

showed an almost 8-fold increase in HCV replication at 72 hpi (Figure 28F). The contrary results with the FLAG-tagged LBHD1 might stem from a functional impairment of the protein by a C-terminal tag or by sterical hindrance of its interaction with other proteins. Changing the tags would reveal if the position or the tag itself causes the observed difference, but we did not follow up on this. The consistently more pronounced effect on JcR2a compared to sgCon1-ET replication might simply be explained by the role of the HF suggested by our model, the formation of replication compartments. Those are already established in the replicon cell line but need to be formed *de novo* in JcR2a infection. Further, the difference might stem from the genotype difference (gt1b vs. gt2a) and the consequent disparate reliance on host factor proteins or processes. Another reason might be that the candidate genes have an additional role in particle assembly or release and might therefore exert a stronger function in the full-length context. It should be noted that overexpression of the host factor candidates literally rescued HCV replication in Huh7-LP cells, since without overexpression, JcR2a replication is close to background levels and barely detectable.

Among the tested candidates, THAP7 overexpression posed the strongest and most consistent effect on HCV replication. Besides proper expression, we could also detect THAP7 by immunofluorescence and confirm its correct subcellular localization in the nucleus as THAP7 is reported to be a transcriptional repressor [315, 316]. In the subgenomic sgCon1-ET setting, we observed a more than 5-fold and in the JcR2a infection a more than one $\log_{10}$ increase in HCV replication upon HA-THAP7 overexpression (Figure 29A, -B). The C-terminally FLAG-tagged version showed the same effect in sgCon1-ET replication, although not as pronounced as the HA-tagged version (Figure A9A). As the model suggested the HF to be limiting in Huh7-LP cells but not so in highly permissive Huh7-Lunet cells, we wanted to challenge this hypothesis and overexpressed HA-THAP7 in this highly permissive cell line. HA-THAP7 overexpression had no effect on HCV replication in Huh7-Lunet cells, despite robust expression and correct localization (Figure A9F–H), consistent with the model prediction (Figure 29C).
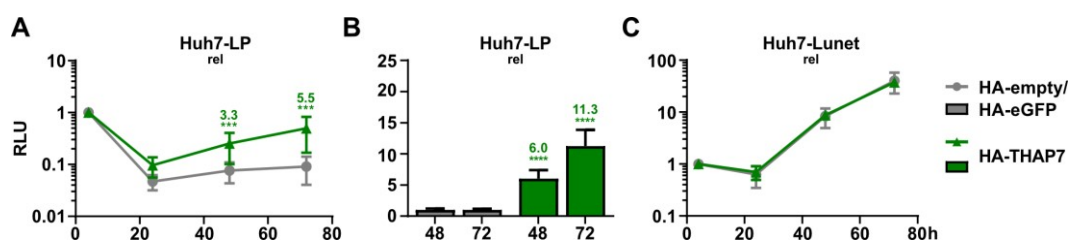
Figure 29 THAP7 overexpression boosts HCV replication in Huh7-LP cells. (A) Huh7-LP cells overexpressing N-terminally HA-tagged THAP7 or the corresponding control (HA-empty) were electroporated with the subgenomic reporter replicon sgCon1-ET (gt1b) and luciferase activity was measured at 4, 24, 48, and 72 hpe. **(B)** Huh7-Lunet cells overexpressing N-terminally HA-tagged THAP7 or the corresponding control (HA-empty) were infected with JcR2a (MOI ~0.1) and luciferase activity was measured at 48 and 72 hpi. **(C)** Huh7-Lunet cells overexpressing N-terminally HA-tagged THAP7 or the corresponding control (HA-eGFP) were electroporated with the subgenomic reporter replicon sgCon1-ET (gt1b) and luciferase activity was measured at 4, 24, 48, and 72 hpe. Data shows means +/- standard deviation from at least three independent experiments each and is relative to 4 hpe (A, C) or relative to the empty control (B). *** p ≤ 0.001, **** p ≤ 0.0001. Adapted from [278].

4.3.4. Strong NR0B2 overexpression inhibits HCV replication in Huh7-LP and -Lunet cells

Surprisingly, NR0B2 overexpression led to a moderate to strong inhibition of HCV replication instead of the expected increase. Replication of sgCon1-ET was impaired in Huh7-LP cells overexpressing HA-NR0B2 (Figure 30A) as well as NR0B2-FLAG by more than 50% (Figure A10A). This held true for JcR2a replication as well, of which replication levels dropped by 30–40% (Figure 30B). Inhibition of HCV replication was even stronger in the highly permissive Huh7-Lunet cells. Upon overexpression of HA-NR0B2 in Huh7-Lunet cells, sgCon1-ET replication declined almost 1000-fold at 72 hpe (Figure 30C), rendering HCV replication basically dead. We confirmed proper as well as similar overexpression in Huh7-LP and -Lunet cells via qPCR, immunoblotting, and immunofluorescence (Figure A10C–H). NR0B2 localization in the nucleus is in line with its reported role as a nuclear receptor and transcriptional co-repressor [317]. However, we also found a diffuse cytoplasmic signal and rarely distinct speckles in NR0B2 overexpressing cells (Figure A10E). Although this might be an artefact upon the massive overexpression, it aligns with the finding of a direct interaction between NR0B2 and NS5A reported by another group [318]. The suppression of HCV replication upon overexpression was not limited to genotype 1b (Con1-ET) but also held true for genotype 2a (JFH) (Figure 31A), although to a lesser extent. As these findings were in sharp contrast to what we expected and to what we found for the other host factor candidates, we were wondering if the massive overexpression of NR0B2 caused the observed effects. The basal fold expression of NR0B2 in Huh7-Lunet compared to Huh7-LP cells, possibly causing the higher permissiveness, was only 2.5-fold (Figure 31B). Overexpression in contrast, caused fold expressions of several orders of magnitude (Figure A10). We thus diluted the lentiviral particles we used for stable transduction of target cells to reach lower expression levels of NR0B2. Additionally, we used the weak ROSA26 promoter to induce overexpression of NR0B2 only very mildly (Figure 31B). Reduced NR0B2 levels indeed rescued HCV replication, suggesting a dose-dependent effect (Figure 31C). By using the ROSA26 promoter for NR0B2 overexpression, leading to only 8-fold NR0B2 mRNA levels compared to the control, we could even increase HCV replication slightly (Figure 31C).
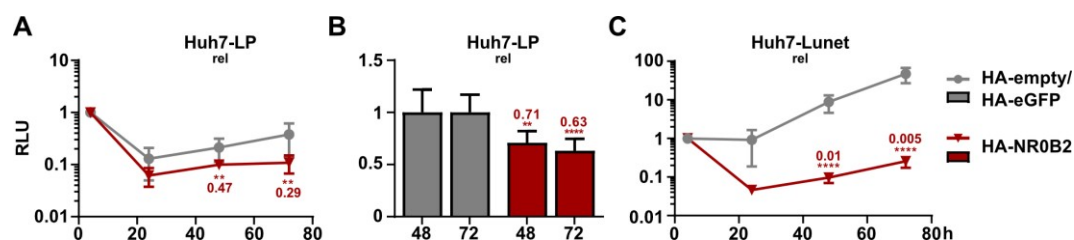
Figure 30 NR0B2 overexpression inhibits HCV replication in different settings. (A) Huh7-LP cells overexpressing N-terminally HA-tagged NR0B2 or the corresponding control (HA-empty) were electroporated with the subgenomic reporter replicon sgCon1-ET (gt1b) and luciferase activity was measured at 4, 24, 48, and 72 hpe. **(B)** Huh7-Lunet cells overexpressing N-terminally HA-tagged NR0B2 or the corresponding control (HA-empty) were infected with JcR2a (MOI ~0.1) and luciferase activity was measured at 48 and 72 hpi. **(C)** Huh7-Lunet cells overexpressing N-terminally HA-tagged NR0B2 or the corresponding control (HA-eGFP) were electroporated with the subgenomic reporter replicon sgCon1-ET (gt1b) and luciferase activity was measured at 4, 24, 48, and 72 hpe. Data shows means +/- standard deviation from three independent experiments each and is relative to 4 hpe (A, C) or relative to the empty control (B). ** p ≤ 0.005, **** p ≤ 0.0001. Adapted from [278].
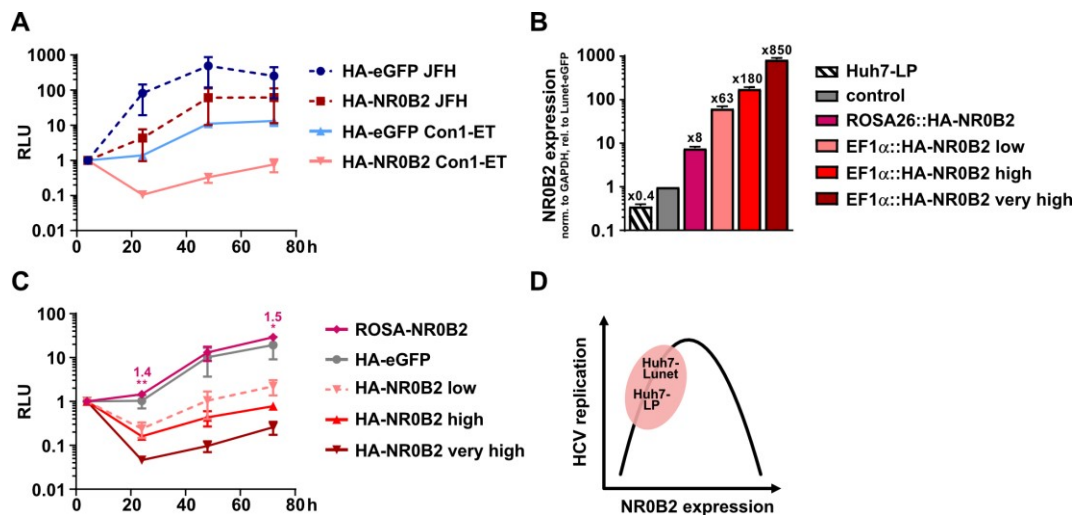
Figure 31 Effects of NR0B2 overexpression on HCV replication are genotype-independent but highly dose-dependent. (A) Huh7-LP cells overexpressing N-terminally HA-tagged NR0B2 or the corresponding control (HA-empty) were electroporated with the subgenomic reporter replicons sgJFH (JFH) or sgCon1-ET (Con1-ET) and luciferase activity was measured at 4, 24, 48, and 72 hpe. **(B)** Huh7-Lunet cells were stably transduced using increasing dilutions of lentiviral particles carrying overexpression constructs under the EF1α or ROSA26 promoter. Expression levels were determined by qPCR. **(C)** Huh7-Lunet cells expressing different amounts of HA-NR0B2 under the EF1α or ROSA26 promoter were electroporated with the subgenomic reporter replicon sgCon1-ET and luciferase activity was measured at 4, 24, 48, and 72 hours post electroporation. **(D)** Proposed model for the dose-dependent impact of NR0B2 levels on HCV replication. Adapted from [278].

These results let us hypothesize that there was a sensitive optimum curve of NR0B2 levels dictating HCV replication (Figure 31D). The higher NR0B2 expression levels in Huh7-Lunet compared to Huh7-LP cells seemed to be beneficial for HCV replication as was a slight overexpression in Huh7-Lunet cells using the ROSA26 promoter. In line with this, we also found that Jc1 infection of Huh7-Lunet cells led to a more than 2-fold upregulation of NR0B2 expression (Figure A11). However, upon exceeding the peak, NR0B2 levels seemed to be detrimental to HCV replication, as shown by our overexpression experiments. On the other side, reducing NR0B2 levels in Huh7-Lunet or -LP cells by siRNA knockdown suppressed HCV replication as well (see above). These intriguing findings prompted us to investigate further how NR0B2 manages to regulate HCV replication in such an intricate fashion.

4.3.5. The FXR-NR0B2 axis regulates HCV replication in Huh7-Lunet cells

Nuclear receptors are ligand-activated transcription factors that play important roles in development, homeostasis, and metabolic processes. To investigate if the effects of NR0B2 levels on HCV replication are part of its nuclear receptor activity regulating bile acid synthesis, we focused on the NR0B2 activator farnesoid X receptor (FXR). FXR (also NR1H4) constitutes the major bile acid sensor in the liver and intestines and is activated predominantly by chenodeoxycholic acid (CDCA) [319-322]. Bile acids are not only required for solubilization of nutrients in the intestinal tract, but also play central roles as signaling molecules in gene regulation [323]. Upon ligand-mediated activation, FXR activates the expression of NR0B2 (formerly SHP), which in turn suppresses the expression of CYP7A1, the rate-limiting enzyme in bile acid formation from cholesterol [324-326] (Figure 32A). We thus used available FXR modulators to analyze their

effects on HCV replication. The non-steroidal and highly selective FXR agonist GW4064 [327, 328] increased replication of sgCon1-ET in Huh7-Lunet cells around 2-fold (Figure 32B). This might correspond to the slight activation effect of NR0B2 that we observed upon overexpression using the ROSA26 promoter. On the contrary, the natural FXR antagonist (Z)-Guggulsterone [329, 330] inhibited HCV replication markedly, mirroring the effect of NR0B2 knockdown (Figure 32B). Still, we did not measure expression levels of the targeted nuclear receptors and affected downstream targets to corroborate our findings and exclude off-target or unspecific effects. Interestingly though, we found that FXR levels negatively correlated with NR0B2 levels in our NR0B2 overexpressing cell lines (Figure 32C). This might either pose an indirect feedback loop due to the stalled production of bile acids that would activate FXR or a novel direct feedback loop via NR0B2 itself that has not been reported, yet. According to the reported role of NR0B2 in bile acid synthesis, we assessed total bile acid contents and found indeed a 50% reduction in HA-NR0B2 overexpressing Huh7-Lunet compared to control cells (Figure A12). It should be noted though that the bile acid content in HA-NR0B2 cells was very low and around the detection limit of the assay kit. As stalling bile acid production not only lowers bile acid levels but also interferes with the catabolism of its precursor cholesterol, we used the fluorescent polyene Filipin-III [331], which binds cholesterol and thus allows a direct visualization of its cellular distribution. In contrast to a strong punctate pattern and ER-like localization in Huh7-LP HA-empty cells, HA-NR0B2 overexpression disrupted this pattern and showed a rather diffuse cytoplasmic distribution with distinct membrane boundaries, suggesting a transport or localization defect (Figure 32D). Since cholesterol is a major component of HCV RCs [155, 169], the disrupted supply with and recruitment of it might be another reason for the severe impairment of HCV replication upon strong NR0B2 overexpression. More specific visualization and co-localization studies are needed to reveal if and how cholesterol distribution or its recruitment to replication organelles is altered in NR0B2 overexpressing cells. In addition, ultrastructural and biochemical analyses should examine the fate of HCV RCs upon NR0B2 overexpression or knockdown. Identifying the host factors involved in these processes could give important insights into the pathways usurped by HCV to build its membranous web.
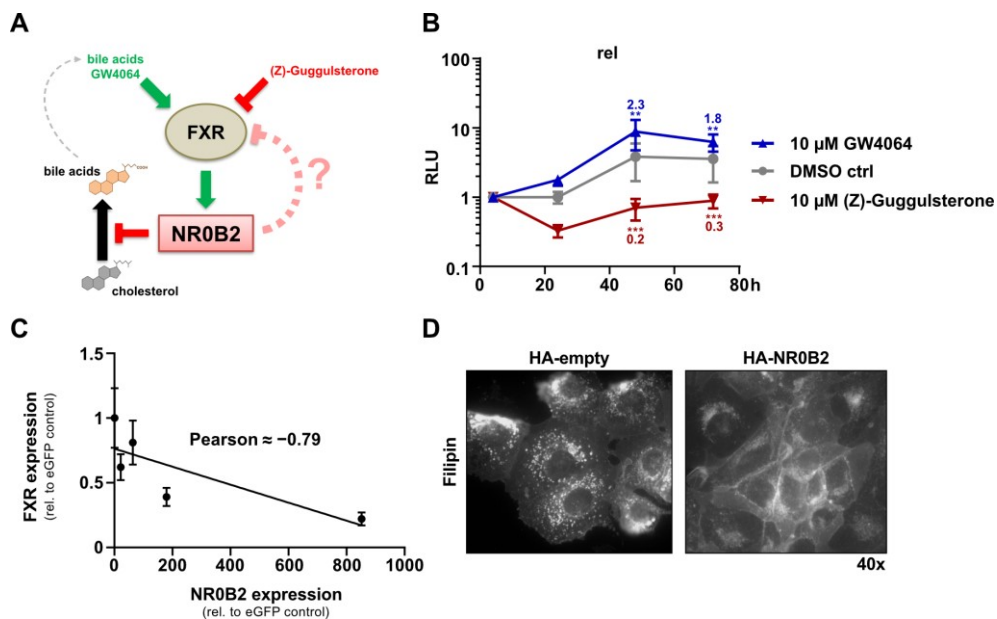
Figure 32 The FXR-NR0B2 axis modulates HCV replication and cholesterol distribution in Huh7-Lunet cells.
(A) Schematic of the FXR-NR0B2 axis in the liver. FXR is activated by bile acids and the non-steroidal agonist GW4064, and is suppressed by its antagonist (Z)-Guggulsterone. FXR activates NR0B2 expression, which in turn represses the rate-limiting step in the formation of bile acids from cholesterol. It is unclear if there is a direct inhibition of FXR by NR0B2. **(B)** Huh7-Lunet cells were electroporated with sgCon1-ET and either treated with 10 µM GW4064, 10 µM (Z)-Guggulsterone, or vehicle only. Luciferase activity as a surrogate for HCV replication was measured at 4, 24, 48, and 72 hpe. **(C)** NR0B2 and FXR mRNA levels were assessed via qPCR in NR0B2 overexpressing cell lines. **(D)** Immunofluorescent images of Huh7-LP cells overexpressing HA-NR0B2 or a control using Filipin-III in a 40x magnification. Data in (B) shows means +/- standard deviation from three independent biological experiments. ** p ≤ 0.005, *** p ≤ 0.001. Adapted from [278].

4.3.6. NR0B2 overexpression specifically impairs HCV replication

Since the strong inhibition of HCV replication by high overexpression of NR0B2 poses a possible option for treatment and many other human pathogenic viruses rely on membrane-derived replication organelles as HCV does, we investigated if this effect is limited to HCV only or holds true for other disease-causing viruses as well. We chose the rather closely related Dengue (DENV, *Flavivirus*) and the less related Rift Valley Fever virus (RVFV, *Phlebovirus*) to test this. We used reporter viruses and infected HA-NR0B2 overexpressing Huh7-Lunet cells. Strong HA-NR0B2 overexpression severely impaired HCV replication but not so much DENV or RVFV replication (Figure 33). Interestingly, we observed the same dose-dependence for DENV as for HCV, although much less pronounced (Figure 33). This insensitivity of DENV is surprising, as both, DENV and HCV, highly depend on cholesterol and other cellular lipids for their replication [332, 333]. Thus, either there are fine-tuned differences in the dependence on cholesterol and possibly involved host factors between HCV and DENV, or this argues for a rather specific, cholesterol-independent role of NR0B2 in HCV replication. RVFV replication, which does not rely on cholesterol or lipids to the extent *Flaviviridae* do, did not show much alteration and no such optimum curve regarding NR0B2 levels [334].
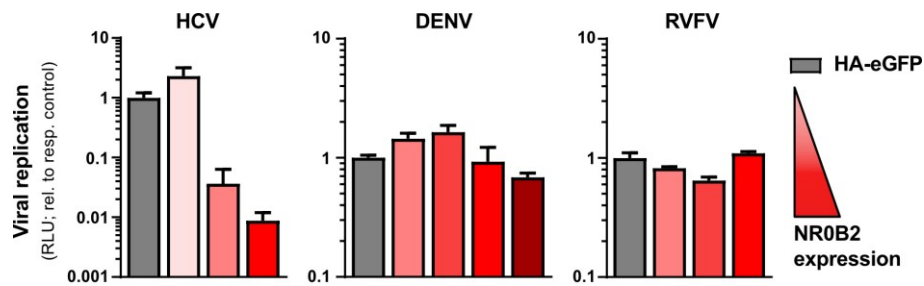
Figure 33 NR0B2 overexpression specifically impairs HCV replication. Huh7-Lunet cells overexpressing different amounts of HA-NR0B2 or HA-eGFP as a control were infected with luciferase reporter versions of the indicated viruses: JcR2a (HCV, MOI ~0.1) for 72 hours, DenR2a (DENV, MOI 1) for 48 hours, and a ΔNSs rift valley renilla reporter virus (RVFV, MOI 0.01) for 48 hours. Cells were lysed at the indicated time points and luciferase activities were measured. Data shows means +/- standard deviations from two to three (HCV), two (DENV), and one to two (RVFV) independent biological experiments, respectively. Adapted from [278].

In conclusion, our search for novel HCV host factors determining cellular permissiveness in different Huh7 variants by correlating gene expression with HCV replication efficiency, yielded several promising candidates. We could confirm their role in HCV replication by knockdown and overexpression studies, in the latter of which we could confirm what the model proposed: the limiting abundance of the HF for HCV replication in Huh7-LP but not in Huh7-Lunet cells. Upon overexpression of the putative HFs, HCV replication, especially in the full-length setting with JcR2a, increased. This increase was most dramatic for THAP7, of which overexpression caused a more than 10-fold increase in JcR2a replication in Huh7-LP cells but had no effect in Huh7-Lunet cells. Functional analyses of the candidate genes should reveal insights into the cause of these increases in HCV replication. Since several of them appear to be transcriptional regulators, further transcriptional analyses should give insights into the regulated genes. The one very intriguing HF candidate for HCV replication that we identified is the nuclear receptor and transcriptional co-repressor NR0B2. The dose-dependent regulation of HCV replication suggests an intricate interplay with the HCV life cycle. Further, the involvement of cholesterol and its disturbed localization upon NR0B2 overexpression hints towards defects in RC formation or particle assembly of HCV. Since many other human pathogenic viruses, e.g. DENV, ZIKV, SARS-CoV, and many more, use similar replication organelles to amplify their genomes, elucidation of the host factor involved in their formation and homeostasis is highly warranted. Thus, findings from HCV could be extended and possibly help to understand basic principles of RC formation during (+)-RNA virus infection.

In conclusion, we showed that the intracellular model for HCV replication is able to recapitulate HCV replication even under drug treatment. The model was able to identify steps in the viral replication cycle affected by the antiviral response raised by the host cell upon IFN-α treatment, which were corroborated by *in vitro* findings. Furthermore, the model correctly predicted intracellular HCV replication dynamics under TEL and SOF treatment and revealed possible steps affected by DCV treatment, an inhibitor of the elusive multifunctional HCV NS5A protein. We extended the intracellular model for HCV replication to the full HCV life cycle and validated the new model using Jc1 infection dynamics in a Huh7-Lunet-based cell line. The new full life cycle model is able to i) simulate HCV infection and spread in this setting and ii) incorporate drug effects and correctly predict viral replication dynamics under drug treatment in a full-length setting. It can now be used to deepen our understanding of the mode of action of the highly potent class of NS5A inhibitors, exemplified by DCV, by further experiments and model analyses. However, questions regarding genotypic differences in replication dynamics, the mode of action of other drugs or the best drug combinations, as well as the role of host factors involved in HCV replication, can be addressed as well. We could confirm several novel host factors for HCV replication that might contribute to cellular permissiveness for HCV. This finding is based on a model prediction and confirms the validity of such an approach. Interestingly, the impact of those host factors on HCV replication was consistently more pronounced in the full-length setting, suggesting involvement of those factors in infectious particle production steps. We can now use our new full life cycle model now to determine the steps in which those host factors are possibly involved and gain answers into their mode of action during replication compartment establishment and maybe others.

5. DISCUSSION

Our lab has previously published a mathematical model for intracellular HCV replication after electro-transfection of Huh7 cells with a subgenomic HCV reporter RNA [277]. The model was able to simulate HCV replication in two Huh7 variants that markedly differed in their HCV replication efficiency, *i.e.* permissiveness: viral RNA reached at least one $\log_{10}$ higher steady state levels in the high versus the low permissive Huh7 variant [277]. Remarkably, the model revealed that the level of a host factor species (HF) that is involved in establishing the HCV replication compartment (RC) and initiating (-)-strand RNA synthesis was responsible for the observed differences in permissiveness. In this study, we sought to identify this HF species in order to elucidate the cause for the differences in permissiveness between various Huh7 variants.

5.1. Host factors determining permissiveness for HCV

The search for determinants of HCV permissiveness started soon after the first successful replication of HCV in cell culture [124]. Subsequent studies revealed that not only determinants on the viral side, but also host determinants played a crucial role in the replication efficiency of HCV [138, 280]. Indeed, different passages of the host cell line Huh7 showed up to 200-fold differences in HCV permissiveness [280]. One highly permissive cell clone was generated by treating a stable replicon cell line (Huh7-LucUbiNeo-ET, [129]) with a selective HCV inhibitor until the replicon was no longer detectable [137]. This "cured" cell line, designated Huh7-Lunet, was highly permissive and possessed remarkable replication efficiency for HCV [137, 335]. The reasons for its high permissiveness, however, remain elusive. A similarly generated and permissive cell line, Huh7.5, was found to have a defective RIG-I, thus, the absent immune response seemed to be responsible for its high permissiveness [336]. However, a later study showed no reduction of permissiveness upon reconstitution of functional RIG-I and no general correlation between the innate antiviral response and permissiveness for HCV [337].

5.1.1. Gene expression profiling reveals promising HF candidates

Based on the suggestion of our intracellular model, we used microarrays to determine the gene expression profiles of eight different Huh7 variants and correlated expression levels of all genes with permissiveness for HCV across all those variants. Statistical analyses and filtering revealed 34 hits that we sought to investigate for their role in HCV replication. As the intracellular model for HCV replication [277] and early elegant *in vitro* approaches [280] suggested, the host gene product or process was of limiting abundance in low permissive cells but not so in high permissive cells. Thus, we analyzed the effects of knockdown of those 34 candidate genes on HCV replication in an infection setting in high permissive cells and in a stable replicon cell line. We selected the five most promising candidate genes and sought to confirm the model prediction by overexpressing them in the low permissive Huh7-LP variant. Indeed, all the five HF candidates increased JcR2a replication in Huh7-LP cells. This confirms the model prediction that HF is of limiting abundance in low permissive cells and reveals novel candidates that might explain the huge differences in HCV permissiveness among different Huh7 variants.

Although we saw a maximal increase of HCV permissiveness of around 10-fold (THAP7, Figure 29), a combination of two or more of the candidate genes might yield additive or synergistic effects to reach the two to three orders of magnitude difference between the lowest and highest Huh7 variants [277]. The fact that at least four of them (CRAMP1, CRYM, NR0B2, and THAP7) are reportedly involved in gene expression and regulation, underlines this notion. However, an initial attempt combining THAP7 and NR0B2 (under control of the ROSA26 promoter) overexpression did not result in an additive effect (data not shown). Still, we have not investigated all the remaining combinations.

5.1.2. Dually decoded genes and LBHD1 (C11orf48)

Interestingly, THAP7 and LBHD1 (C11orf48), the latter of which showed the second strongest (up to 8-fold) increase in HCV replication upon overexpression (Figure 28), have both been reported to be dually decoded [338]. THAP7 seems to encode an alternative peptide from an upstream ORF (uORF), whereas LBHD1 forms an alternative transcript that leads to a frameshift [338]. The THAP7 uORF might as well have only regulatory function in translation of the regular ORF [338]; however, the alternative LBHD1 peptide was detected in a mass spectrometry study [339]. In addition, LBHD1 was reported to be a tumor antigen in a bladder cancer cell line [340]. Given the pro-proliferative properties of oncogenes, this might give a rationale for the increased HCV replication efficiency in LBHD1 overexpressing cells as HCV replication is known to depend on proliferation in Huh7 cell [281]. However, using live cell imaging to quantify cell proliferation, we did not observe increased cell growth of LBHD1 overexpressing cells (data not shown). The positive effect of LBHD1 overexpression on HCV replication was abrogated and overexpression even inhibited HCV replication upon C-terminal tagging of the protein (Figure 28). Interestingly, the alternative peptide originating from the alternatively spliced LBHD1 transcript, seems to be translated from the rather 3'-region of the mRNA [338, 339]. The C-terminal tag might thus have interfered with the function of the regular or even the alternative peptide. Future experiments should assess THAP7 and LBHD1 expression levels upon HCV infection and address the question which forms of the peptides are possibly upregulated and exert the positive effect on HCV replication.

5.1.3. CRAMP1 (HN1L, TCE4)

The uncharacterized CRAMP1 (also called CRAMP1L, HN1L, or TCE4) exerted the smallest effect on HCV replication and did so only during JcR2a infection but not after electroporation of sgCon1-ET (Figure 28). CRAMP1 seems to have played a role in chicken domestication as revealed by SNP analysis [341] and its homolog was reported as a regulator of epigenetic marks in *Drosophila melanogaster* [342]. Thus, it would be interesting to investigate possible transcriptional changes upon CRAMP1 overexpression as well as its own expression upon HCV infection.

5.1.4. CRYM

Crystalline μ (CRYM) increased HCV replication only when overexpressed with an N-terminal but not with a C-terminal tag (Figure 28). Its positive effect was more pronounced during JcR2a infection than after electroporation with sgCon1-ET. The C-terminal tag might have interfered with its function. CRYM is the main cytosolic thyroid hormone binding protein [343] and has a well described ketimine reductase function in the brain [344]. It has been associated with insulin

sensitivity in adipose tissue [345] and mutations in CRYM in fibrocytes of the cochlea cause deafness [346]. Thyroid hormones are important players in lipogenesis, cholesterol synthesis, and insulin regulation [347, 348]. The fact that HCV disturbs the glucose metabolism [349] and frequently leads to insulin resistance and type 2 diabetes mellitus in patients [350] might represent a link to CRYM. Very recently, a study linked the loss of CRYM expression in mice to the development of obesity and fatty liver upon a high-fat diet [351]. Thus, it would be highly interesting to analyze CRYM expression levels upon HCV infection or in chronically infected patients. However, HCV infection might as well alter the activity or substrate availability for CRYM and thereby exert an effect without changing CRYM expression levels. In addition, the lipid content of infected cells and produced viral particles as well as their infectivity should be investigated. The functional impact of CRYM overexpression might also stem from transcriptional changes related to its nuclear receptor activity and could be revealed by transcriptional analyses [352].

5.1.5. THAP7

THAP7 is well characterized and offers a sound basis for explanation of its regulatory effect on HCV replication. THAP7 is a member of the Thanatos-associated protein family that comprises at least 12 members [315, 316]. Only few of them are characterized to date, though [316]. THAP12, for example, which is also known as THAP0 or DAP4, reportedly binds to and inhibits PKR activity [353] as well as stabilizes RIG-I by preventing its polyubiquitination [354]. Thus, THAP12 seems to preserve an antiviral state in the cell and consequently inhibit viral replication. No such antiviral function has been described for THAP7. THAP7 is a transcriptional repressor and binds to histone tails [315]. It acts by recruiting template-activating factor-Iβ (TAF-1β), nuclear receptor corepressor (NCOR1, also known as N-CoR), or histone deacetylase 3 (HDAC3) to histones, and thereby induce transcriptional inhibition of the target sequence by hypoacetylation [316]. The regulated target genes of THAP7 are not known. Interestingly, the N-terminal domain of TAF-1β inhibits protein phosphatase 2a (PTPA, also known as PP2A) [355], which in turn is upregulated during HCV infection, possibly by NS5A [356]. Exploitation of PTPA activity poses several possible advantages for HCV. For example, the protein arginine methyltransferase 1 (PRMT1), which methylates and thus inhibits NS3 helicase function, is repressed by PTPA [357]. Further, PTPA reduces STAT1 phosphorylation and thereby inhibits IFNα-mediated JAK/STAT signaling. One could speculate that THAP7 sequestrates TAF-1β from the cytosol and thus increases PTPA activity, which would be advantageous for HCV. However, MacFarlan *et al.* reported no effect on PTPA activity upon THAP7 overexpression [316]. A recent study showed that HDAC3 inhibitors suppressed HCV replication by increasing levels of hepcidin antimicrobial peptide (HAMP, also known as LEAP-1) and reducing levels of apolipoprotein apoA1 [358], which is reported to be required for HCV particle production [359]. Thus, future experiments should investigate if HAMP and APOA1 are target genes of THAP7 and how THAP7 overexpression affects their expression levels. Notably, to the best of our knowledge, the degree of the THAP7-mediated increase in HCV replication is unprecedented as a host factor and provides a solid basis for further investigations.

5.1.6. NR0B2 (SHP)

The atypical, orphan nuclear hormone receptor NR0B2 (also called SHP or SHP1) exhibited dose-dependent effects on HCV replication. Strong overexpression led to inhibition of HCV replication in low as well as high permissive cells. In the latter, HCV replication was reduced by almost three $\log_{10}$ (Figure 30). We could show that this inhibitory effect is genotype independent and can be titrated (Figure 31). Minor overexpression of only 8-fold of NR0B2 in Huh7-Lunet cells even increased HCV replication slightly (Figure 31). The ligands of NR0B2 remain elusive and it lacks a DNA-binding domain, making it a co-repressor [317]. However, there is a plethora of target genes and nuclear receptors co-repressed by NR0B2, complicating it in cholesterol, bile acid, glucose metabolism and many more [360]. Its activator is the main bile acid (BA) sensor FXR, which itself is activated by BAs [324, 361]. We observed an increase and decrease in HCV replication by modulating FXR activity with an agonist and antagonist, respectively (Figure 31B). These effects might mimic the slight overexpression and the knockdown of NR0B2 that similarly affected HCV replication. Hence, the NR0B2-mediated regulation of HCV replication is probably attributable to its authentic function as a nuclear receptor. Upon BA- or agonist-mediated activation by FXR, NR0B2 suppresses the expression of cytochrome P450 family member CYP7A1 by binding to the trans-activator NR5A2 (also known as LRH-1) [360]. CYP7A1 performs the first and rate-limiting step in the catabolism of cholesterol [360]. Thus, strong overexpression of NR0B2 presumably leads to a block of BA synthesis and cholesterol accumulation. Indeed, we found reduced total BA content in NR0B2 overexpressing cells (Figure A12) as well as disturbed subcellular cholesterol distribution (Figure 32D). Still, BA contents were near the lower limit of detection of the assay kit and the cholesterol distribution, especially its transport to the HCV replication compartment and possible co-localization with HCV proteins, needs further assessment. Previous reports already showed that BAs could stimulate replication of subgenomic HCV genotype (gt) 1b, but not gt2a, replicons [362, 363], although no mechanism was proposed. A subsequent study revealed that the refractoriness to BA stimulation of the gt2a replicon was probably due to its already extraordinary replication efficiency [364]. The authors showed that an attenuated version of the gt2a replicon indeed was sensitive to BA stimulation. In addition, they reported that also full-length gt1b as well as gt2a replication profited from BA supplementation. Interestingly, besides an effect on replication, the authors observed a slight increase in infectivity of gt2a particles. Lipids, apolipoproteins, cholesterol, and cholesteryl esters make up a substantial portion of HCV particles [142], thus it would be highly interesting to measure the lipid composition and infectivity of released viral particles from NR0B2 overexpressing cells. One follow-up study of the above mentioned found the EGFR/ERK pathway to be responsible for the bile acid-mediated increase in HCV replication [365]. With NR0B2 and its nuclear receptor as well as transcriptional co-repressor activities, we present a number of possible pathways involved in the regulation of HCV replication by NR0B2 levels.

NR0B2 has been implicated in HCV infection and its regulation before, however the findings are controversial. Two reports showed reduced NR0B2 levels upon HCV infection *in vitro* as well as in liver specimen of chronically HCV-infected patients [366, 367], and a concomitant progression of liver disease. Surprisingly, both studies reported no effect on HCV replication upon NR0B2

knockdown or overexpression. Along the same lines, but without the involvement of HCV, NR0B2 was reported to have a protective effect on the progression from non-alcoholic fatty liver (NAFL) to non-alcoholic steatohepatitis (NASH) [368]. In contrast to these findings, an Italian group reported increased NR0B2 levels upon HCV infection *in vitro* as well as in liver specimen, a relocalization of NR0B2 into the cytoplasm, and a direct interaction of NR0B2 with NS5A via co-IP [318]. Further, they showed a strong reduction of HCV replication upon siRNA-mediated NR0B2 knockdown. These findings are in line with our observations of increased NR0B2 levels upon HCV infection (Figure A11), a reduction in HCV replication upon knockdown of NR0B2 (Figure 27), and a localization of overexpressed NR0B2 into speckles in the cytosol (Figure A10E), which might allow a direct interaction with HCV proteins. The differences to the findings above might be the use of a J6/JFH chimera in our hands and in [318], versus JFH in [366, 367], pointing to a role of the structural proteins in the NR0B2-mediated effects.

Interestingly, NR0B2 controls the expression of miRNAs and lncRNAs [369] that could possibly affect HCV RNA directly or indirectly via host dependency factors. However, we could not detect consistent changes at least in miR-122 levels, dependent on NR0B2 expression (data not shown).

Lastly, we showed that the dose-dependent strong impact of NR0B2 expression levels was specific to HCV replication, as DENV was much less and RVFV not at all affected in a dose-dependent manner (Figure 33). The insensitivity of DENV was surprising since both, HCV and DENV, heavily rely on cholesterol and lipids [333]. However, DENV replication did show a dose-dependent effect of NR0B2 overexpression, but much less pronounced than HCV. This might allude different host pathways and dependency factors involved in the cholesterol and lipid supply of HCV and DENV replication and assembly, or point towards other regulatory pathways triggered by NR0B2 that affect HCV more specifically.

NR0B2 seems to dictate HCV replication in a fashion reminiscent of that of PI4KIIIα [370], with severe effects. The multifaceted roles of NR0B2 make it difficult but at the same intriguing to elucidate the underlying mechanisms of HCV replication regulation. Follow-up studies should identify the functions of NR0B2 crucial for HCV replication. This will not only give insights into the molecular virology but also into liver disease progression upon chronic HCV infection.

Overall, we identified five candidates that open up new venues to explain the huge differences in host cell permissiveness for HCV. We did so by combining findings from a mathematical model with *in vitro* validation experiments. This underpins the capability of mathematical models to help in better understanding and elucidating molecular aspects of viral replication. It will be intriguing to analyze the effects of those candidates with a model that supports the full viral life cycle.

5.2. The intracellular and the new full life cycle model of HCV replication

The Binder model proved fit in simulating replication of HCV subgenomes in low as well as high permissive Huh7 cells [277]. It could fit replication of attenuated subgenomic HCV RNA versions and predicted a HF species involved in RC formation and (-)-strand synthesis initiation to dictate HCV replication efficiency in two different Huh7 variants. We could confirm this model prediction and found HF candidates that increased HCV replication upon overexpression in low permissive Huh7-LP cells and decreased HCV replication upon siRNA-mediated knockdown in high permissive Huh7-Lunet cells. The intracellular mode further revealed the most sensitive steps in the intracellular HCV life cycle upon targeted intervention [277]. To prove if the model was also able to identify those steps in intracellular HCV replication that are targeted by a specific treatment, we recorded HCV replication dynamics under IFN-α treatment.

5.2.1. The intracellular model reveals the mode of action of IFN-α

IFN-α has been the standard of care as a recombinant protein, PEGylated, and in combination with ribavirin for decades [22]. Sustained virologic response (SVR) rates upon IFN-α treatment largely depend on HCV genotype and progression of liver disease, but did not exceed 40–50% on average, and IFN-α treatment came along with severe side effects [22]. Today, DAAs have mostly replaced IFN-α as the standard of care for HCV infection. However, the exact mode of action of IFN-α treatment remains largely unsolved. Understanding the effects of IFN-α treatment on HCV replication not only reveals insights into the viral life cycle but also in the antiviral response of the host cell. IFN-α triggers a signaling cascade via the JAK-STAT pathway and leads to the expression of hundreds of ISGs [371]. Several of those ISGs have proved to possess anti-HCV activity but only for few of them, the molecular mode of action has been described (reviewed in [371, 372]), *e.g.* the OAS/RNaseL system which leads to endonucleolytic cleavage of HCV RNA [252, 373] or ISG20, which has exonuclease activity [372]. However, no comprehensive picture of or the contribution of different ISGs on intracellular HCV replication inhibition exists. We used our intracellular HCV replication model to decipher the mode of action of an IFN-α-triggered antiviral response on HCV replication and to determine the steps most probably affected by the antiviral response of the host cell.

In order to do so, we monitored translation and replication of subgenomic HCV reporter replicons under treatment of different doses of recombinant IFN-α. We observed that translation of HCV RNA was severely impaired upon IFN-α treatment in Huh7-Lunet cells (Figure 9). This is in line with earlier findings, which also showed that HCV IRES-mediated translation is even stronger affected by IFN treatment than (cellular) cap-dependent translation [250, 374, 375]. However, a major limitation to these studies was that they only used bicistronic luciferase reporter plasmids instead of replicons. Thus, possible counteractions or stabilizing effects of viral proteins or secondary RNA structures on HCV IRES-mediated translation could not apply. Possible suggested mechanisms for the observed translational shutdown were inhibition of eIF2 activity by phosphorylation of its α subunit through PKR, sequestration of eIF3 by IFIT1, or reduced supply of ribosomes by upregulation of the OAS/RNase L system, which has been shown to cleave 28S ribosomal RNA ([250] and references therein). However, in a later siRNA-screen study, PKR did not appear as a hit

and was subsequently confirmed to play no major role in the IFN-α-mediated suppression of HCV replication [244]. The same study also revealed that singular knockdown or overexpression of ISGs exerted only moderate effects on HCV replication. However, upon combination, the authors observed additive and even synergistic effects on HCV replication upon knockdown of the investigated ISGs [244]. Similar findings were obtained upon combinatorial overexpression of ISGs [242]. This argues for a concerted action of ISGs against HCV and gives a rationale for the plethora of ISGs upregulated by IFN treatment. Besides classical ISGs, miRNAs as well as interferon effector genes (IEGs) that are not transcriptionally upregulated upon IFN treatment have been reported to possess anti-HCV activity [376, 377]. Large screening studies using either siRNA knockdown or overexpression of putative ISGs confirmed the early findings of translation inhibition of HCV RNA and revealed many genes involved in mRNA processing and translation initiation or showed translational inhibition of HCV RNA directly, respectively [242, 243]. Thus, inhibition of HCV IRES-mediated translation is clearly a major effect of the antiviral response raised by the host cell upon IFN-α treatment. The host factors responsible for this strong inhibition and their relative contribution, however, remain to be determined.

We also found that HCV RNA stability was decreased upon IFN-α treatment (Figure 9), arguing for a faster degradation, possibly by RNase L, ISG20, or other nucleases. HCV RNA is usually protected from 5'-3'-exonucleases by miR-122 binding to its 5'-UTR and by its 5'-triphosphate [60, 378, 379]. However, a possible reduction of miR-122 levels upon IFN treatment [376] could ease the access of pyrophosphatases to the 5'-end of HCV RNA, trimming it and consequently allowing Xrn1/2-mediated degradation [59, 378, 380]. Although HCV replication and later steps in its life cycle have been described to be targeted by ISGs [247, 371], our intracellular model could very accurately fit intracellular HCV replication data under IFN treatment by only incorporating effects on translation and RNA degradation (Figure 10). That means that potential additional effects would be only minor and could not improve the model fit much further. However, our system was solely based on intracellular HCV replication after electroporation of *in vitro* transcripts. It would be intriguing to test the impact of IFN-α treatment on HCV replication in the full-length setting with a full life cycle model to fit the data. Possibly then, effects on replication compartment formation, assembly or release of viral particles need to be taken into account to generate a good fit.

5.2.2. Both models are able to predict viral replication dynamics under drug treatment

The Binder model revealed promising therapeutical intervention steps in the intracellular HCV replication cycle [277]. To investigate if the model was also able to predict viral replication under therapeutic intervention, we recorded replication dynamics of a subgenomic reporter RNA under treatment with direct-acting antivirals (DAAs). DAAs are the new standard of care for chronic HCV infection [20]. They exhibit cure rates of 95–100%, have mild to no side effects, and are recommended for most comorbidities or stages of liver disease. The three main classes of DAAs against HCV are NS3/4A inhibitors (-previr), NS5B inhibitors (-buvir), and NS5A inhibitors (-asvir). Administered regimens are usually combinations of at least two of them [20]. The former two have distinct and well-defined modes of action, whereas the mode of action of NS5A inhibitors is more elusive. We used Telaprevir (TEL) and Sofosbuvir (SOF) to prove the capability of our

intracellular model to predict HCV replication under DAA treatment. TEL and SOF have distinct and well-defined modes of action, which allowed us to pre-select the steps in the HCV replication cycle targeted by the respective drug. However, to reflect the situation in an infected patient more closely, the model needed extension the full viral life cycle. Such a model would include viral particle production and infection of target cells, representing spread of the infection.

Therefore, we have extended the Binder model for intracellular HCV replication, which is based on the transfection of reporter replicons, to the full HCV life cycle (Figure 15), represented by infection of Lunet-CGM cells with cell culture-produced full-length Jc1 particles. We have added novel parameters to the intracellular model that represent crucial steps in an authentic infection, as for example rates for infection and assembly of viral particles. In addition, the model now takes into account the age of an infected cell, meaning the time it is already infected and thus produces more (+)-strand RNA and viral progeny. Moreover, the model is linked to a population model that accounts for the number of infected cells. The resulting multilevel model is able to predict intra- and extracellular viral determinants as well as spread of the infection. We confirmed the validity of our model extension with data obtained from the infection of Lunet-CGM cells with cell culture-produced Jc1. We assessed viral (+)- and (-)-strand RNA, viral titers, and the percentage of infected cells in the culture dish. All the newly introduced parameters were identifiable and could be fitted based on the recorded data. The model simulation closely resembled the biological data for all the assessed parameters. Thus, our model proved valid and could be used to predict viral replication under drug treatment in a more authentic infection setting.

We started with the intracellular model and predicted intracellular HCV RNA replication by only adapting the steps directly affected by the respective drug (polyprotein processing rate k_c by TEL and RNA synthesis rates k_{4m} and k_{4p} by SOF). The model generated predictions that correctly reflected viral replication dynamics under different concentrations of the respective drug (Figure 12). Although the predictions did not precisely match all the data points and could possibly be improved, they, importantly, qualitatively resembled the two very distinct replication dynamics of HCV under treatment with these two different classes of inhibitors. Briefly, TEL led to a later onset of replication but a similar slope and HCV replication reached the same levels as in the untreated condition at the assay endpoint at 72 hpe. SOF in contrast, slowed down HCV replication dynamics markedly, which resulted in lower steady state levels of HCV RNA replication. These results confirmed that the intracellular HCV replication model was in principle capable of implementing drug effects and predicting HCV replication under treatment. Thus, we were tempted to analyze the drug effects of Daclatasvir on HCV replication by generating a model fit that could suggest the most probably affected steps in the intracellular life cycle of HCV by the treatment.

5.2.2.1. Mode of action of the NS5A inhibitor Daclatasvir (DCV)

Daclatasvir (DCV) was approved for HCV treatment by the FDA in 2015 [305] and exhibits inhibitory potency in the replicon system in the low picomolar range [307]. Due to the many functions of NS5A in the HCV life cycle, the mechanism of action of DCV remains elusive, especially because NS5A has no enzymatic function [381]. NS5A consists of an N-terminal amphipathic helix that allows membrane anchoring, a structured domain 1 (D1) that coordinates a Zn^{2+} ion, and two

highly unstructured domains, D2 and D3 [382]. Whereas D1 and D2 are required for replication, D3 is not; however, D3 is essential for viral assembly [381]. Importantly, the first crystal structure of NS5A D1 showed a dimer with a potential groove for RNA binding [99]. Interestingly, other D1 crystallization studies revealed alternative dimer forms [383, 384], suggesting NS5A could form large oligomers [383]. Later studies showed that NS5A indeed is an RNA-binding protein [100, 385, 386] and dimerization, and possibly oligomerization, is required for efficient HCV replication [387]. DCV resistance mutations suggested early on that the compound directly binds to D1 and later *in vitro* experiments confirmed this notion [388, 389]. However, instead of disrupting, DCV was shown to stabilize the dimer upon binding and thereby exclude RNA binding of NS5A [388].

We used our intracellular model to fit HCV replication data under DCV treatment. The model achieved the best fit upon including inhibitory drug effects on the translation rate k_1 and the RNA synthesis rates k_{4m} and k_{4p} (Figure 12). Although NS5B, which is not targeted by DCV [307], is the viral polymerase that synthesizes (+)- and (-)-strands, NS5A has been shown to bind HCV RNA [100, 386] and is probably part of the replicase complex [64]. This gives a rationale for our finding of RNA synthesis steps being a target of DCV inhibition. In addition, the D1 mutation Y93H confers partial resistance to DCV but reduces RNA levels during replication by 10-fold [390]. There is no evidence of a direct involvement of NS5A in HCV RNA translation. However, NS5A reportedly binds PKR and leads to its activation, which in turn leads to eIF2α phosphorylation and translational shutdown in the cell. A cyclophilin A (CypA) inhibitor was shown to revert this phenotype, probably by blocking the interaction of CypA and NS5A, which enables the NS5A-PKR interaction [391]. The same might hold true for DCV, but this needs experimental evidence. Instead, delivery of HCV RNA to the cytoplasm might be affected by the DCV-mediated NS5A inhibition, which would eventually result in lower translation rates. Kinetic analyses of another group have also shown a direct effect of DCV on RNA synthesis [392]. This effect was immediate, but could interestingly block RNA synthesis only to maximal 50% within the first 12 hours. This argues for different pools of NS5A inside the cell, some accessible to DCV and others not [392], and supports a model in which DCV blocks formation of new replication compartments, but has no effect on pre-existing ones [303, 393].

Our intracellular model and the corresponding experimental system were limited to intracellular replication of an HCV subgenome and did not account for effects on the production of infectious particles or their release. NS5A, though, reportedly plays an essential role in assembly and particle production and localizes together with Core to LDs [95, 96, 394]. Consequently, the kinetic study on DCV inhibition mentioned above indeed showed a rapid (≤ 3 hours) abrogation of release of infectious viral particles as well as formation of intracellular infectious particles upon DCV treatment [392]. A mathematical modeling study using patient data showed that in order to fit serum viral load, DCV must exert a direct inhibition of both, replication and assembly [395]. The LD-binding motif of NS5A is located in D1 [381], which might be masked or disrupted upon DCV binding, leading to an abrogation of LD localization of NS5A, explaining the assembly defect [394].

We therefore used our new full life cycle model to predict full-length HCV replication under DCV treatment. We adjusted the parameters that the intracellular model revealed upon fitting HCV

replication data under DCV treatment: inhibition of the translation rate k_1 and RNA synthesis rates k_{4m} and k_{4p}. The resulting prediction closely resembled Jc1 replication dynamics, although (+)- and (-)-strand RNA data posed a high variation in the two biological replicates (Figure 25). Interestingly, viral titer data and model prediction fit very well, without changing assembly rate p in the model. Overall, the model prediction of Jc1 dynamics under DCV accurately fit the data, even when only including effects on k_1, k_{4m}, and k_{4p}. However, we did only test one, relatively low (82 pM) concentration of DCV and the variance in our biological data was quite high. Still, the implementation of an assembly effect of DCV seemed not necessary in our experimental system. However, we did not perform a systematic fit of the model to the DCV data, yet. Maybe this would result in a different set of adjusted parameters that include the assembly rate. In addition, it would be highly interesting to analyze the effect of DCV when steady state levels have been reached, *e.g.* at 72 hpi or later, and monitor the decay in infectious titers and RNA levels upon high doses of DCV, to see if the model can fit the data with or without adjusting assembly rate p. This approach would more closely reflect an authentic therapeutic intervention.

5.2.2.2. Mode of action of the NS3/4A protease inhibitor Telaprevir (TEL)

NS3 is a multifunctional protein due to its protease and helicase domain [81]. The protease function is essential for processing of the viral polyprotein and for blunting the antiviral response of the host cell by cleaving important adaptor proteins. TEL is a peptidomimetic α-ketoamid that blocks the active site of the NS3 protease by covalent binding [396].

We used TEL to validate that our intracellular model is capable of predicting HCV replication even under drug treatment. We recorded intracellular subgenomic HCV RNA replication under treatment with two different TEL concentrations (100 and 200 nM), and generated a model prediction after including an IC_{50} term in the polyprotein processing rate k_c. The model prediction accurately resembled the qualitative changes in HCV replication dynamics upon TEL treatment. Those were a later onset of replication but no reduction in the slope of amplification (Figure 12). However, our system did not account for later steps in the HCV life cycle, like assembly and release of viral particles, in which NS3/4A reportedly plays essential roles as well [84, 397-400]. We extended our intracellular model to the full viral life cycle and used the new model to predict Jc1 replication dynamics under TEL treatment, again only considering a drug effect on k_c (Figure 19). The model prediction in this setting strongly underestimated the TEL effect on Jc1 replication, including RNA levels as well as infectious titers. This might allude to effects of TEL on steps besides polyprotein processing, that we did not account for in the model prediction. However, it might as well be that HCV replication during an infection is much more sensitive and relies stronger on viral protein production, *e.g.* for establishing the RC or producing virions for spread, than HCV replication of viral subgenomes after electroporation into cells. In case not only the polyprotein processing function is affected, TEL might stabilize NS3 in a distinct confirmation – as shown for the DCV-NS5A interaction [388] – that renders it refractory to interact with other (viral or host) proteins, or disturbs its recruitment or localization, and thereby exert its inhibitory effect.

NS3, like NS5A, is probably involved in RNA synthesis and part of the replicase complex [43, 64]. The helicase domain might function in resolving RNA secondary structures or unwinding dsRNA

intermediates to allow access or higher processivity of NS5B ([43] and references therein). McGivern *et al.* claim a direct effect of TEL on HCV RNA synthesis as they observed a rapid (≤ 12 hours) decrease in newly synthesized RNA upon treatment at a point where NS5B levels are not yet decreased [401]. However, there is evidence that NS5B acts only in *cis*, meaning it synthesizes (-)-strands only directly after translation from its very own (+)-strand it has been translated from [402]. This would immediately stop RNA synthesis upon halted production of NS5B. In addition, blockage of the formation of new replication complexes as a consequence of inhibited polyprotein processing might explain such a phenotype as well. It has been described that the protease domain is needed for helicase function [403], giving a rationale for the immediate effect McGivern *et al.* saw on RNA synthesis [401]; however, this is probably attributable to an allosteric effect and evidence for the need of the NS3 protease enzyme activity for helicase function is lacking. Moreover, TEL was reported to not impair the helicase function of NS3 [404]. This complicates the explanation of possible further effects of protease inhibition on virion assembly, because it suggests a direct involvement of the protease function in these processes.

NS3/4A plays an essential role in HCV assembly (reviewed in [75]). Inhibitor treatment as well as NS3 resistance mutations to TEL show specific defects in assembly independent of impaired RNA replication [405]. Guedj *et al.* show with their mathematical modeling of patient serum viral load that TEL also impairs viral assembly/secretion [395]. This is supported by the kinetic *in vitro* studies of McGivern *et al.* that show a dramatic loss in viral titers, exceeding the reduction in RNA levels upon TEL or boceprevir (a similar NS3/4A inhibitor) treatment [392, 401]. This is also reflected in our data, especially at 32 and 45 hpi (Figure A5A). These effects may not necessarily stem from a loss of function of the NS3 protease itself though, but rather from the NS3 helicase or the co-factor NS4A upon loss of stimulation by the NS3 protease (their functions in assembly are reviewed in [81]). There is solid evidence for the NS3 helicase domain to function in virion assembly [84] and that the NS3 protease domain (but not its enzymatic activity) is needed for the helicase to function properly [403]. The N-terminal amphipathic helix α_0 of NS3 as well as the linker domain between the NS3 protease and helicase are required for assembly as well [397, 406]. Still, neither of those domains or their functions should be affected directly by TEL. The NS3/4A assembly defect upon TEL treatment could also be exerted via its reported interaction and co-recruitment with NS5A to lipid droplets [394].

Overall, there is solid evidence for a role in virion assembly for all NS3/4A domains, but not yet for NS3 protease activity. Still, others and we found that infectious titers are decreased to a level that exceeds the reduction in RNA levels. These findings strongly support a role for the NS3 protease function in virion assembly or release. However, it is hard to address this question experimentally since NS3 protease function is required for replication and cannot be separated from its function in assembly easily. Further analyses with our new full life cycle model and additional kinetics data should allow to gain new insights into this second role of the NS3 protease and help us understand the TEL effect on viral particle production.

We used the NS5B polymerase inhibitor Sofosbuvir (SOF) as a DAA with distinct and known mechanism of action to validate our intracellular model. The intracellular model prediction upon

adjustment of the RNA synthesis rates k_{4m} and k_{4p} revealed a good fit and resembled replication dynamics under the inhibitor (Figure 12). The full life cycle model prediction fit the data quite well, although the drug effect was very small (Figure 22). Importantly, and in contrast to TEL and DCV, SOF did not specifically affect infectious particle production and titers dropped just according to reductions in RNA levels (Figure A5). Since SOF is a pro-drug, we had to implement an activation model to make the model prediction resemble the data closely.

We extended the intracellular HCV replication model to the full life cycle. This included the addition of parameters for yet uncovered steps by the model, *e.g.* the infection rate β. Those, yet unknown, parameters needed to be estimated and fitted based on the available set of data. We detected a huge excess of HCV (+)- and (-)-strands in the viral stock that we used for the infection dynamics. In order to be able to fit the above mentioned parameter, we had to make the assumption that all of those were non-infectious. The following section gives insights into the possible origin of these excess (+)- and (-)-strand RNAs.

5.2.3. Extracellular, non-infectious vesicles

The cell culture-derived Jc1 particle stocks used in this study were produced by PEG-precipitation of culture supernatants after electroporation of cells with *in vitro*-transcribed Jc1 RNA [283]. Strand-specific RT-qPCR of one stock revealed a huge excess of viral (+)- as well as (-)-strands compared to infectious particles as determined by limiting dilution assay (Figure A2B). Remarkably, because HCV is a (+)-strand RNA virus, (-)-strands should not be present in the viral stock at all. We did not attempt to clarify the origin of these excess (+)- and (-)-strands, but they probably derived from secreted extracellular vesicles (EVs). Initially, EVs were thought to simply dispose of unneeded cellular content [407]. However, it became clear that EVs fulfill various functions in intercellular signaling and communication [407]. Very early it became apparent that Huh7 cells secrete membranous particles that contain HCV (sub)genomes, independent of particle production [408]. However, the transferred nucleic acids largely failed to establish a productive replication [408]. Later, it was shown that such HCV (sub)genomes transferred by EVs are able to elicit an immune response in professional immune cells [221, 409], and can even establish a productive infection in target cells [410, 411]. Although Bukong *et al.* [410] provided evidence for the establishment of a productive infection by HCV RNA-containing EVs, the amount of those in cell culture supernatants was at least three $\log_{10}$ lower compared to infectious viral particles [410]. This was corroborated by another study that reported only 0.1% of EVs contained HCV RNA and in which the authors failed to establish a productive replication in target cells with unpurified EVs containing subgenomic replicons [411]. Further, it was reported that the transmission of such HCV RNA-containing EVs requires cell-to-cell contacts [221, 411]. Thus, "infection" with EVs might be possible, but only after purification or upon cell-to-cell contact, and might be negligible in an authentic infection. In addition, purification of such EVs and thereby excluding a cross-contamination with authentic HCV particles is difficult due to their highly similar size and buoyant density [407]. Immuno-purification of exosomes (a subfraction of EVs) via the exosome marker CD63 might represent an alternative approach and has been done before [410]; however, another exosome marker, CD81 [412], is a HCV co-receptor and thus cross-purification of attached viral

particles cannot be excluded. Still, HCV RNA-containing EVs have been isolated from patient serum and shown to contain not only (+)- but also (-)-strand RNA [295, 410]. Grünvogel and colleagues found that (-)-strands are even enriched in EVs compared to the intracellular milieu, concluding that EVs mostly contain dsRNA and secretion of dsRNA-containing EVs poses a way of evading the immune response of the host cell by avoiding detection by TLR3 [295]. The ratio of (+)- to (-)-strands in one of our Jc1 stock preparations was roughly 10:1 in contrast to 4:1 as Grünvogel *et al.* reported [295]. This might be caused by cellular or culture differences, although both studies used Huh7-Lunet-CD81$_{high}$ cells, or by the different purification methods: PEG-precipitation in our study versus ultra-centrifugation and Exo-spin columns in [295]. The higher amount of (+)-strands in our virus stock could also suggest that the purification method or the one freeze-thaw cycle during stock preparation rendered viral particles non-infectious. In our mathematical model, we assumed that all those excess (+)- and (-)-strand RNAs in the virus stock were non-infectious. The good fit of the model simulation to the actual data supports the notion that most if not all of the detected excess (+)- and (-)-strands were non-infectious.

In conclusion, we extended our intracellular model to the full viral life cycle and showed that is capable of simulating HCV replication dynamics in the full-length context. In addition, the model has proven fit to incorporate drug effects and predict HCV replication dynamics under treatment with different DAAs against HCV. It is the first such detailed model of its kind that is based on solid experimental data. Our model will be useful in understanding the mode of action of DAAs against HCV in detail, and can be used to address various other questions in HCV biology. These might regard the differences in replication efficiencies of HCV genotypes or isolates on the viral side or qualitative and quantitative host factor involvement on the other side.

To conclude, we used an intracellular HCV replication model to identify novel HCV host factors that possibly contribute to the huge differences in permissiveness between Huh7 variants and thus constitute important pillars of HCV replication. By doing so, we confirmed the model prediction that a host factors species involved in determining permissiveness is limiting in low permissive cells. We further used the model to shed light on the mechanism of action of IFN-α treatment on HCV replication and provided a basis for a comprehensive understanding of the mode of action of the NS5A inhibitor DCV. We extended the intracellular model and developed a multilevel model that covers the full HCV life cycle, including infection of target cells, viral particle production, and spread of the infection. The new model can simulate (+)- and (-)-strand RNA levels, infectious titers in the supernatant, and spread of the infection in the culture. This new full life cycle model allows a comprehensive assessment of drug effects, including IFN-α, DCV, or TEL, on the full life cycle of HCV, including particle production and spread. It might serve in solving the role and explaining the impact of our newly identified host factor candidates for HCV replication in an authentic infection setting. Thus, this study provides a better understanding of HCV permissiveness and lays the foundation for gaining further insights into HCV replication as well as liver disease progression.

6. REFERENCES

1. Parvez, M. K.; Parveen, S., Evolution and Emergence of Pathogenic Viruses: Past, Present, and Future. *Intervirology* **2017,** 60, (1-2), 1-7.
2. Fields, B. N.; Knipe, D. M.; Howley, P. M., *Fields virology*. Wolters Kluwer Health/Lippincott Williams & Wilkins: Philadelphia, 2007.
3. Woolhouse, M.; Scott, F.; Hudson, Z.; Howey, R.; Chase-Topping, M., Human viruses: discovery and emergence. *Philos Trans R Soc Lond B Biol Sci* **2012,** 367, (1604), 2864-2871.
4. Dowdle, W. R.; Cochi, S. L., The principles and feasibility of disease eradication. *Vaccine* **2011,** 29, D70-D73.
5. Goodson, J. L.; Alexander, J. P.; Linkins, R. W.; Orenstein, W. A., Measles and rubella elimination: learning from polio eradication and moving forward with a diagonal approach. *Expert review of vaccines* **2017,** 16, (12), 1203-1216.
6. Holmes, K.; Bertozzi, S.; Bloom, B.; et, a., Major Infectious Diseases: Key Messages from Disease Control Priorities, Third Edition. In *Major Infectious Diseases. 3rd edition.*, 3rd ed.; The International Bank for Reconstruction and Development / The World Bank: Washington (DC).
7. Plummer, M.; de Martel, C.; Vignat, J.; Ferlay, J.; Bray, F.; Franceschi, S., Global burden of cancers attributable to infections in 2012: a synthetic analysis. *The Lancet Global Health* **2016,** 4, (9), e609-e616.
8. Ritchie, H.; Roser, M. Causes of Death. https://ourworldindata.org/causes-of-death (retrieved 01.04.2020),
9. Global, regional, and national age–sex specific all-cause and cause-specific mortality for 240 causes of death, 1990–2013: a systematic analysis for the Global Burden of Disease Study 2013. *The Lancet* **2015,** 385, (9963), 117-171.
10. IARC, World Cancer Report 2014. In Stewart, B.; Wild, C., Eds. 2014.
11. Stanaway, J. D.; Flaxman, A. D.; Naghavi, M.; Fitzmaurice, C.; Vos, T.; Abubakar, I.; Abu-Raddad, L. J.; Assadi, R.; Bhala, N.; Cowie, B.; Forouzanfour, M. H.; Groeger, J.; Hanafiah, K. M.; Jacobsen, K. H.; James, S. L.; MacLachlan, J.; Malekzadeh, R.; Martin, N. K.; Mokdad, A. A.; Mokdad, A. H.; Murray, C. J. L.; Plass, D.; Rana, S.; Rein, D. B.; Richardus, J. H.; Sanabria, J.; Saylan, M.; Shahraz, S.; So, S.; Vlassov, V. V.; Weiderpass, E.; Wiersma, S. T.; Younis, M.; Yu, C.; El Sayed Zaki, M.; Cooke, G. S., The global burden of viral hepatitis from 1990 to 2013: findings from the Global Burden of Disease Study 2013. *Lancet (London, England)* **2016,** 388, (10049), 1081-1088.
12. Polaris Observatory, H. C. V. C., Global prevalence and genotype distribution of hepatitis C virus infection in 2015: a modelling study. *The lancet. Gastroenterology & hepatology* **2017,** 2, (3), 161-176.
13. Smith, S.; Harmanci, H.; Hutin, Y.; Hess, S.; Bulterys, M.; Peck, R.; Rewari, B.; Mozalevskis, A.; Shibeshi, M.; Mumba, M.; Le, L.-V.; Ishikawa, N.; Nolna, D.; Sereno, L.; Gore, C.; Goldberg, D. J.; Hutchinson, S., Global progress on the elimination of viral hepatitis as a major public health threat: An analysis of WHO Member State responses 2017. *JHEP Reports* **2019,** 1, (2), 81-89.
14. WHO, WHO urges countries to invest in eliminating hepatitis. In media contacts; Namjilsuren, T.; Lindmeier, C., Eds. Online, 2019, retrieved 01.04.2020.
15. Pawlotsky, J. M., New Hepatitis C Therapies: The Toolbox, Strategies, and Challenges. *Gastroenterology* **2014,** 146, (5), 1176-1192.
16. Jin, F.; Matthews, G. V.; Grulich, A. E., Sexual transmission of hepatitis C virus among gay and bisexual men: a systematic review %J Sexual Health. **2017,** 14, (1), 28-41.
17. Thursz, M.; Fontanet, A., HCV transmission in industrialized countries and resource-constrained areas. *Nature reviews. Gastroenterology & hepatology* **2014,** 11, (1), 28-35.
18. Shiffman, M. L., The next wave of hepatitis C virus: The epidemic of intravenous drug use. *Liver international : official journal of the International Association for the Study of the Liver* **2018,** 38 Suppl 1, 34-39.
19. Arends, J. E.; Kracht, P. A. M.; Hoepelman, A. I. M., Performance of hepatitis C virus (HCV) direct-acting antivirals in clinical trials and daily practice. *Clinical Microbiology and Infection* **2016,** 22, (10), 846-852.
20. EASL Recommendations on Treatment of Hepatitis C 2018. *Journal of hepatology* **2018,** 69, (2), 461-511.
21. Sikavi, C.; Chen, P. H.; Lee, A. D.; Saab, E. G.; Choi, G.; Saab, S., Hepatitis C and human immunodeficiency virus coinfection in the era of direct-acting antiviral agents: No longer a difficult-to-treat population. *Hepatology* **2018,** 67, (3), 847-857.
22. Pawlotsky, J.-M.; Feld, J. J.; Zeuzem, S.; Hoofnagle, J. H., From non-A, non-B hepatitis to hepatitis C virus cure. *Journal of hepatology* **2015,** 62, (1, Supplement), S87-S99.
23. Bartenschlager, R.; Baumert, T. F.; Bukh, J.; Houghton, M.; Lemon, S. M.; Lindenbach, B. D.; Lohmann, V.; Moradpour, D.; Pietschmann, T.; Rice, C. M.; Thimme, R.; Wakita, T., Critical challenges and emerging opportunities in hepatitis C virus research in an era of potent antiviral therapy: Considerations for scientists and funding agencies. *Virus research* **2018,** 248, 53-62.
24. Falade-Nwulia, O.; Sulkowski, M. S.; Merkow, A.; Latkin, C.; Mehta, S. H., Understanding and addressing hepatitis C reinfection in the oral direct-acting antiviral era. *Journal of viral hepatitis* **2018,** 25, (3), 220-227.
25. Bartenschlager, R.; Urban, S.; Protzer, U., Towards curative therapy of chronic viral hepatitis. *Zeitschrift fur Gastroenterologie* **2019,** 57, (1), 61-73.
26. Hutin, Y. J.-F.; Bulterys, M.; Hirnschall, G. O., How far are we from viral hepatitis elimination service coverage targets? **2018,** 21, (S2), e25050.

REFERENCES

27.   Messina, J. P.; Humphreys, I.; Flaxman, A.; Brown, A.; Cooke, G. S.; Pybus, O. G.; Barnes, E., Global distribution and prevalence of hepatitis C virus genotypes. *Hepatology* **2015,** 61, (1), 77-87.

28.   Donald B. Smith, J. B., Carla Kuiken, A. Scott Muerhoff, Charles M. Rice, Jack T. Stapleton and Peter Simmonds Flaviviridae Study Group. https://talk.ictvonline.org/ictv_wikis/flaviviridae/w/sg_flavi/56/hcv-classification - retrieved 03.04.2020

29.   Simmonds, P.; Becher, P.; Bukh, J.; Gould, E. A.; Meyers, G.; Monath, T.; Muerhoff, S.; Pletnev, A.; Rico-Hesse, R.; Smith, D. B.; Stapleton, J. T.; Consortium, I. R., ICTV Virus Taxonomy Profile: Flaviviridae. **2017,** 98, (1), 2-3.

30.   Scheel, T. K.; Simmonds, P.; Kapoor, A., Surveying the global virome: identification and characterization of HCV-related animal hepaciviruses. *Antiviral research* **2015,** 115, 83-93.

31.   Stapleton, J. T.; Foung, S.; Muerhoff, A. S.; Bukh, J.; Simmonds, P., The GB viruses: a review and proposed classification of GBV-A, GBV-C (HGV), and GBV-D in genus Pegivirus within the family Flaviviridae. *The Journal of general virology* **2011,** 92, (Pt 2), 233-246.

32.   Bhattarai, N.; Stapleton, J. T., GB virus C: the good boy virus? *Trends in microbiology* **2012,** 20, (3), 124-30.

33.   Lauck, M.; Bailey, A. L.; Andersen, K. G.; Goldberg, T. L.; Sabeti, P. C.; O'Connor, D. H., GB virus C coinfections in west African Ebola patients. *Journal of virology* **2015,** 89, (4), 2425-9.

34.   Balcom, E. F.; Doan, M. A. L.; Branton, W. G.; Jovel, J.; Blevins, G.; Edguer, B.; Hobman, T. C.; Yacyshyn, E.; Emery, D.; Box, A.; van Landeghem, F. K. H.; Power, C., Human pegivirus-1 associated leukoencephalitis: Clinical and molecular features. **2018,** 84, (5), 781-787.

35.   Smith, D. B.; Bukh, J.; Kuiken, C.; Muerhoff, A. S.; Rice, C. M.; Stapleton, J. T.; Simmonds, P., Expanded classification of hepatitis C virus into 7 genotypes and 67 subtypes: Updated criteria and genotype assignment web resource. *Hepatology* **2014,** 59, (1), 318-327.

36.   Simmonds, P.; Bukh, J.; Combet, C.; Deléage, G.; Enomoto, N.; Feinstone, S.; Halfon, P.; Inchauspé, G.; Kuiken, C.; Maertens, G.; Mizokami, M.; Murphy, D. G.; Okamoto, H.; Pawlotsky, J. M.; Penin, F.; Sablon, E.; Shin, I. T.; Stuyver, L. J.; Thiel, H. J.; Viazov, S.; Weiner, A. J.; Widell, A., Consensus proposals for a unified system of nomenclature of hepatitis C virus genotypes. *Hepatology* **2005,** 42, (4), 962-73.

37.   Simmonds, P., The origin of hepatitis C virus. *Current topics in microbiology and immunology* **2013,** 369, 1-15.

38.   Mohd Hanafiah, K.; Groeger, J.; Flaxman, A. D.; Wiersma, S. T., Global epidemiology of hepatitis C virus infection: New estimates of age-specific antibody to HCV seroprevalence. **2013,** 57, (4), 1333-1342.

39.   Petruzziello, A.; Marigliano, S.; Loquercio, G.; Cozzolino, A.; Cacciapuoti, C., Global epidemiology of hepatitis C virus infection: An up-date of the distribution and circulation of hepatitis C virus genotypes. *World journal of gastroenterology* **2016,** 22, (34), 7824-40.

40.   Murphy, D. G.; Willems, B.; Deschênes, M.; Hilzenrat, N.; Mousseau, R.; Sabbah, S., Use of sequence analysis of the NS5B region for routine genotyping of hepatitis C virus with reference to C/E1 and 5' untranslated region sequences. *Journal of clinical microbiology* **2007,** 45, (4), 1102-12.

41.   Borgia, S. M.; Hedskog, C.; Parhy, B.; Hyland, R. H.; Stamm, L. M.; Brainard, D. M.; Subramanian, M. G.; McHutchison, J. G.; Mo, H.; Svarovskaia, E.; Shafran, S. D., Identification of a Novel Hepatitis C Virus Genotype From Punjab, India: Expanding Classification of Hepatitis C Virus Into 8 Genotypes. *The Journal of infectious diseases* **2018,** 218, (11), 1722-1729.

42.   Petruzziello, A.; Loquercio, G.; Sabatino, R.; Balaban, D. V.; Ullah Khan, N.; Piccirillo, M.; Rodrigo, L.; di Capua, L.; Guzzo, A.; Labonia, F.; Botti, G., Prevalence of Hepatitis C virus genotypes in nine selected European countries: A systematic review. *Journal of clinical laboratory analysis* **2019,** 33, (5), e22876.

43.   Lohmann, V., Hepatitis C Virus RNA Replication. In *Hepatitis C Virus: From Molecular Virology to Antiviral Therapy*, Bartenschlager, R., Ed. Springer Berlin Heidelberg: Berlin, Heidelberg, 2013; pp 167-198.

44.   Bartenschlager, R.; Lohmann, V.; Penin, F., The molecular and structural basis of advanced antiviral therapy for hepatitis C virus infection. *Nature Reviews Microbiology* **2013,** 11, 482.

45.   Tsukiyama-Kohara, K.; Iizuka, N.; Kohara, M.; Nomoto, A., Internal ribosome entry site within hepatitis C virus RNA. *Journal of virology* **1992,** 66, (3), 1476-1483.

46.   Niepmann, M.; Shalamova, L. A.; Gerresheim, G. K.; Rossbach, O., Signals Involved in Regulation of Hepatitis C Virus RNA Genome Translation and Replication. *Front Microbiol* **2018,** 9, 395.

47.   Wang, C.; Sarnow, P.; Siddiqui, A., Translation of human hepatitis C virus RNA in cultured cells is mediated by an internal ribosome-binding mechanism. *Journal of virology* **1993,** 67, (6), 3338-44.

48.   Kieft, J. S.; Zhou, K.; Jubin, R.; Doudna, J. A., Mechanism of ribosome recruitment by hepatitis C IRES RNA. *Rna* **2001,** 7, (2), 194-206.

49.   Spahn, C. M. T.; Kieft, J. S.; Grassucci, R. A.; Penczek, P. A.; Zhou, K.; Doudna, J. A.; Frank, J., Hepatitis C Virus IRES RNA-Induced Changes in the Conformation of the 40S Ribosomal Subunit. **2001,** 291, (5510), 1959-1962.

50.   Pestova, T. V.; Shatsky, I. N.; Fletcher, S. P.; Jackson, R. J.; Hellen, C. U., A prokaryotic-like mode of cytoplasmic eukaryotic ribosome binding to the initiation codon during internal translation initiation of hepatitis C and classical swine fever virus RNAs. *Genes & development* **1998,** 12, (1), 67-83.

51.   Niepmann, M., Hepatitis C Virus RNA Translation. In *Hepatitis C Virus: From Molecular Virology to Antiviral Therapy*, Bartenschlager, R., Ed. Springer Berlin Heidelberg: Berlin, Heidelberg, 2013; pp 143-166.

52.   Garaigorta, U.; Chisari, F. V., Hepatitis C virus blocks interferon effector function by inducing protein kinase R phosphorylation. *Cell Host Microbe* **2009,** 6, (6), 513-22.

53. Niepmann, M.; Shalamova, L. A.; Gerresheim, G. K.; Rossbach, O., Signals Involved in Regulation of Hepatitis C Virus RNA Genome Translation and Replication. *Front Microbiol* **2018,** 9, 395-395.

54. Jopling, C. L.; Schütz, S.; Sarnow, P., Position-dependent function for a tandem microRNA miR-122-binding site located in the hepatitis C virus RNA genome. *Cell Host Microbe* **2008,** 4, (1), 77-85.

55. Jopling, C. L.; Yi, M.; Lancaster, A. M.; Lemon, S. M.; Sarnow, P., Modulation of hepatitis C virus RNA abundance by a liver-specific MicroRNA. *Science* **2005,** 309, (5740), 1577-81.

56. Roberts, A. P.; Lewis, A. P.; Jopling, C. L., miR-122 activates hepatitis C virus translation by a specialized mechanism requiring particular RNA components. *Nucleic acids research* **2011,** 39, (17), 7716-29.

57. Bradrick, S. S.; Nagyal, S.; Novatt, H., A miRNA-responsive cell-free translation system facilitates isolation of hepatitis C virus miRNP complexes. *Rna* **2013,** 19, (8), 1159-69.

58. Schult, P.; Roth, H.; Adams, R. L.; Mas, C.; Imbert, L.; Orlik, C.; Ruggieri, A.; Pyle, A. M.; Lohmann, V., microRNA-122 amplifies hepatitis C virus translation by shaping the structure of the internal ribosomal entry site. *Nat Commun* **2018,** 9, (1), 2613-2613.

59. Sedano, C. D.; Sarnow, P., Hepatitis C virus subverts liver-specific miR-122 to protect the viral genome from exoribonuclease Xrn2. *Cell Host Microbe* **2014,** 16, (2), 257-264.

60. Li, Y.; Masaki, T.; Yamane, D.; McGivern, D. R.; Lemon, S. M., Competing and noncompeting activities of miR-122 and the 5' exonuclease Xrn1 in regulation of hepatitis C virus replication. *Proceedings of the National Academy of Sciences of the United States of America* **2013,** 110, (5), 1881-1886.

61. Shimakami, T.; Yamane, D.; Jangra, R. K.; Kempf, B. J.; Spaniel, C.; Barton, D. J.; Lemon, S. M., Stabilization of hepatitis C virus RNA by an Ago2-miR-122 complex. *Proceedings of the National Academy of Sciences of the United States of America* **2012,** 109, (3), 941-6.

62. Masaki, T.; Arend, K. C.; Li, Y.; Yamane, D.; McGivern, D. R.; Kato, T.; Wakita, T.; Moorman, N. J.; Lemon, S. M., miR-122 stimulates hepatitis C virus RNA synthesis by altering the balance of viral RNAs engaged in replication versus translation. *Cell Host Microbe* **2015,** 17, (2), 217-28.

63. Chang, J.; Nicolas, E.; Marks, D.; Sander, C.; Lerro, A.; Buendia, M. A.; Xu, C.; Mason, W. S.; Moloshok, T.; Bort, R.; Zaret, K. S.; Taylor, J. M., miR-122, a mammalian liver-specific microRNA, is processed from hcr mRNA and may downregulate the high affinity cationic amino acid transporter CAT-1. *RNA biology* **2004,** 1, (2), 106-13.

64. Binder, M.; Quinkert, D.; Bochkarova, O.; Klein, R.; Kezmic, N.; Bartenschlager, R.; Lohmann, V., Identification of determinants involved in initiation of hepatitis C virus RNA synthesis by using intergenotypic replicase chimeras. *Journal of virology* **2007,** 81, (10), 5270-83.

65. Bartenschlager, R.; Lohmann, V.; Penin, F., The molecular and structural basis of advanced antiviral therapy for hepatitis C virus infection. *Nature Reviews Microbiology* **2013,** 11, (7), 482-496.

66. Bartenschlager, R.; Penin, F.; Lohmann, V.; André, P., Assembly of infectious hepatitis C virus particles. *Trends in microbiology* **2011,** 19, (2), 95-103.

67. Moradpour, D.; Penin, F., Hepatitis C virus proteins: from structure to function. *Current topics in microbiology and immunology* **2013,** 369, 113-42.

68. Santolini, E.; Migliaccio, G.; La Monica, N., Biosynthesis and biochemical properties of the hepatitis C virus core protein. *Journal of virology* **1994,** 68, (6), 3631-41.

69. McLauchlan, J.; Lemberg, M. K.; Hope, G.; Martoglio, B., Intramembrane proteolysis promotes trafficking of hepatitis C virus core protein to lipid droplets. *The EMBO journal* **2002,** 21, (15), 3980-8.

70. Boulant, S.; Vanbelle, C.; Ebel, C.; Penin, F.; Lavergne, J.-P., Hepatitis C Virus Core Protein Is a Dimeric Alpha-Helical Protein Exhibiting Membrane Protein Features. **2005,** 79, (17), 11353-11365.

71. Cristofari, G. l.; Ivanyi-Nagy, R.; Gabus, C.; Boulant, S.; Lavergne, J. P.; Penin, F. o.; Darlix, J. L., The hepatitis C virus Core protein is a potent nucleic acid chaperone that directs dimerization of the viral (+) strand RNA in vitro. *Nucleic acids research* **2004,** 32, (8), 2623-2631.

72. Barba, G.; Harper, F.; Harada, T.; Kohara, M.; Goulinet, S.; Matsuura, Y.; Eder, G.; Schaff, Z.; Chapman, M. J.; Miyamura, T.; Bréchot, C., Hepatitis C virus core protein shows a cytoplasmic localization and associates to cellular lipid storage droplets. **1997,** 94, (4), 1200-1205.

73. Dubuisson, J.; Penin, F.; Moradpour, D., Interaction of hepatitis C virus proteins with host cell membranes and lipids. *Trends in Cell Biology* **2002,** 12, (11), 517-523.

74. Vieyres, G.; Thomas, X.; Descamps, V.; Duverlie, G.; Patel, A. H.; Dubuisson, J., Characterization of the envelope glycoproteins associated with infectious hepatitis C virus. *Journal of virology* **2010,** 84, (19), 10159-68.

75. Lindenbach, B. D., Virion Assembly and Release. In *Hepatitis C Virus: From Molecular Virology to Antiviral Therapy*, Bartenschlager, R., Ed. Springer Berlin Heidelberg: Berlin, Heidelberg, 2013; pp 199-218.

76. Wozniak, A. L.; Griffin, S.; Rowlands, D.; Harris, M.; Yi, M.; Lemon, S. M.; Weinman, S. A., Intracellular proton conductance of the hepatitis C virus p7 protein and its contribution to infectious virus production. *PLoS pathogens* **2010,** 6, (9), e1001087.

77. Steinmann, E.; Pietschmann, T., Hepatitis C virus p7-a viroporin crucial for virus assembly and an emerging target for antiviral therapy. *Viruses* **2010,** 2, (9), 2078-2095.

78. Jirasko, V.; Montserret, R.; Lee, J. Y.; Gouttenoire, J.; Moradpour, D.; Penin, F.; Bartenschlager, R., Structural and functional studies of nonstructural protein 2 of the hepatitis C virus reveal its key role as organizer of virion assembly. *PLoS pathogens* **2010,** 6, (12), e1001233.

79. Jirasko, V.; Montserret, R.; Appel, N.; Janvier, A.; Eustachi, L.; Brohm, C.; Steinmann, E.; Pietschmann, T.; Penin, F.; Bartenschlager, R., Structural and functional characterization of nonstructural protein 2 for its role in hepatitis C virus assembly. *The Journal of biological chemistry* **2008,** 283, (42), 28546-62.

80. Jones, C. T.; Murray, C. L.; Eastman, D. K.; Tassello, J.; Rice, C. M., Hepatitis C virus p7 and NS2 proteins are essential for production of infectious virus. *Journal of virology* **2007,** 81, (16), 8374-83.

81. Morikawa, K.; Lange, C. M.; Gouttenoire, J.; Meylan, E.; Brass, V.; Penin, F.; Moradpour, D., Nonstructural protein 3-4A: the Swiss army knife of hepatitis C virus. *Journal of viral hepatitis* **2011,** 18, (5), 305-15.

82. Steinkühler, C.; Urbani, A.; Tomei, L.; Biasiol, G.; Sardana, M.; Bianchi, E.; Pessi, A.; De Francesco, R., Activity of purified hepatitis C virus protease NS3 on peptide substrates. *Journal of virology* **1996,** 70, (10), 6694-700.

83. Lam, A. M. I.; Frick, D. N., Hepatitis C Virus Subgenomic Replicon Requires an Active NS3 RNA Helicase. **2006,** 80, (1), 404-411.

84. Ma, Y.; Yates, J.; Liang, Y.; Lemon, S. M.; Yi, M., NS3 Helicase Domains Involved in Infectious Intracellular Hepatitis C Virus Particle Assembly. **2008,** 82, (15), 7624-7639.

85. Pang, P. S.; Jankowsky, E.; Planet, P. J.; Pyle, A. M., The hepatitis C viral NS3 protein is a processive DNA helicase with cofactor enhanced RNA unwinding. **2002,** 21, (5), 1168-1176.

86. Meylan, E.; Curran, J.; Hofmann, K.; Moradpour, D.; Binder, M.; Bartenschlager, R.; Tschopp, J., Cardif is an adaptor protein in the RIG-I antiviral pathway and is targeted by hepatitis C virus. *Nature* **2005,** 437, (7062), 1167-72.

87. Li, K.; Foy, E.; Ferreon, J. C.; Nakamura, M.; Ferreon, A. C.; Ikeda, M.; Ray, S. C.; Gale, M., Jr.; Lemon, S. M., Immune evasion by hepatitis C virus NS3/4A protease-mediated cleavage of the Toll-like receptor 3 adaptor protein TRIF. *Proceedings of the National Academy of Sciences of the United States of America* **2005,** 102, (8), 2992-7.

88. Brass, V.; Berke, J. M.; Montserret, R.; Blum, H. E.; Penin, F.; Moradpour, D., Structural determinants for membrane association and dynamic organization of the hepatitis C virus NS3-4A complex. **2008,** 105, (38), 14545-14550.

89. Gouttenoire, J.; Penin, F.; Moradpour, D., Hepatitis C virus nonstructural protein 4B: a journey into unexplored territory. **2010,** 20, (2), 117-129.

90. Egger, D.; Wölk, B.; Gosert, R.; Bianchi, L.; Blum, H. E.; Moradpour, D.; Bienz, K., Expression of hepatitis C virus proteins induces distinct membrane alterations including a candidate viral replication complex. *Journal of virology* **2002,** 76, (12), 5974-5984.

91. Yu, G. Y.; Lee, K. J.; Gao, L.; Lai, M. M., Palmitoylation and polymerization of hepatitis C virus NS4B protein. *Journal of virology* **2006,** 80, (12), 6013-23.

92. Gouttenoire, J.; Roingeard, P.; Penin, F.; Moradpour, D., Amphipathic α-Helix AH2 Is a Major Determinant for the Oligomerization of Hepatitis C Virus Nonstructural Protein 4B. **2010,** 84, (24), 12529-12537.

93. Paul, D.; Romero-Brey, I.; Gouttenoire, J.; Stoitsova, S.; Krijnse-Locker, J.; Moradpour, D.; Bartenschlager, R., NS4B Self-Interaction through Conserved C-Terminal Elements Is Required for the Establishment of Functional Hepatitis C Virus Replication Complexes. **2011,** 85, (14), 6963-6976.

94. Kaneko, T.; Tanji, Y.; Satoh, S.; Hijikata, M.; Asabe, S.; Kimura, K.; Shimotohno, K., Production of Two Phosphoproteins from the NS5A Region of the Hepatitis C Viral Genome. *Biochem Biophys Res Commun* **1994,** 205, (1), 320-326.

95. Appel, N.; Zayas, M.; Miller, S.; Krijnse-Locker, J.; Schaller, T.; Friebe, P.; Kallis, S.; Engel, U.; Bartenschlager, R., Essential role of domain III of nonstructural protein 5A for hepatitis C virus infectious particle assembly. *PLoS pathogens* **2008,** 4, (3), e1000035.

96. Tellinghuisen, T. L.; Foss, K. L.; Treadaway, J., Regulation of hepatitis C virion production via phosphorylation of the NS5A protein. *PLoS pathogens* **2008,** 4, (3), e1000032-e1000032.

97. Appel, N.; Pietschmann, T.; Bartenschlager, R., Mutational analysis of hepatitis C virus nonstructural protein 5A: potential role of differential phosphorylation in RNA replication and identification of a genetically flexible domain. *Journal of virology* **2005,** 79, (5), 3187-94.

98. Tellinghuisen, T. L.; Foss, K. L.; Treadaway, J. C.; Rice, C. M., Identification of residues required for RNA replication in domains II and III of the hepatitis C virus NS5A protein. *Journal of virology* **2008,** 82, (3), 1073-83.

99. Tellinghuisen, T. L.; Marcotrigiano, J.; Rice, C. M., Structure of the zinc-binding domain of an essential component of the hepatitis C virus replicase. *Nature* **2005,** 435, (7040), 374-9.

100. Huang, L.; Hwang, J.; Sharma, S. D.; Hargittai, M. R.; Chen, Y.; Arnold, J. J.; Raney, K. D.; Cameron, C. E., Hepatitis C virus nonstructural protein 5A (NS5A) is an RNA-binding protein. *The Journal of biological chemistry* **2005,** 280, (43), 36417-28.

101. Quintavalle, M.; Sambucini, S.; Summa, V.; Orsatti, L.; Talamo, F.; De Francesco, R.; Neddermann, P., Hepatitis C virus NS5A is a direct substrate of casein kinase I-alpha, a cellular kinase identified by inhibitor affinity chromatography using specific NS5A hyperphosphorylation inhibitors. *The Journal of biological chemistry* **2007,** 282, (8), 5536-44.

102. Berger, K. L.; Kelly, S. M.; Jordan, T. X.; Tartell, M. A.; Randall, G., Hepatitis C virus stimulates the phosphatidylinositol 4-kinase III alpha-dependent phosphatidylinositol 4-phosphate production that is essential for its replication. *Journal of virology* **2011,** 85, (17), 8870-83.

103. Lim, Y. S.; Hwang, S. B., Hepatitis C virus NS5A protein interacts with phosphatidylinositol 4-kinase type IIIalpha and regulates viral propagation. *The Journal of biological chemistry* **2011,** 286, (13), 11290-8.

104. Reiss, S.; Rebhan, I.; Backes, P.; Romero-Brey, I.; Erfle, H.; Matula, P.; Kaderali, L.; Poenisch, M.; Blankenburg, H.; Hiet, M.-S.; Longerich, T.; Diehl, S.; Ramirez, F.; Balla, T.; Rohr, K.; Kaul, A.; Bühler, S.; Pepperkok, R.; Lengauer, T.; Albrecht, M.; Eils, R.; Schirmacher, P.; Lohmann, V.; Bartenschlager, R., Recruitment and activation of a lipid kinase by hepatitis C virus NS5A is essential for integrity of the membranous replication compartment. *Cell host & microbe* **2011,** 9, (1), 32-45.

105. Behrens, S. E.; Tomei, L.; De Francesco, R., Identification and properties of the RNA-dependent RNA polymerase of hepatitis C virus. *The EMBO journal* **1996,** 15, (1), 12-22.

106. Schmidt-Mende, J.; Bieck, E.; Hugle, T.; Penin, F.; Rice, C. M.; Blum, H. E.; Moradpour, D., Determinants for membrane association of the hepatitis C virus RNA-dependent RNA polymerase. *The Journal of biological chemistry* **2001,** 276, (47), 44052-63.

107. Moradpour, D.; Brass, V.; Bieck, E.; Friebe, P.; Gosert, R.; Blum, H. E.; Bartenschlager, R.; Penin, F.; Lohmann, V., Membrane association of the RNA-dependent RNA polymerase is essential for hepatitis C virus RNA replication. *Journal of virology* **2004,** 78, (23), 13278-84.

108. Ferrari, E.; Wright-Minogue, J.; Fang, J. W.; Baroudy, B. M.; Lau, J. Y.; Hong, Z., Characterization of soluble hepatitis C virus RNA-dependent RNA polymerase expressed in Escherichia coli. *Journal of virology* **1999,** 73, (2), 1649-54.

109. Lohmann, V.; Körner, F.; Herian, U.; Bartenschlager, R., Biochemical properties of hepatitis C virus NS5B RNA-dependent RNA polymerase and identification of amino acid sequence motifs essential for enzymatic activity. *Journal of virology* **1997,** 71, (11), 8416-28.

110. Ranjith-Kumar, C. T.; Kim, Y.-C.; Gutshall, L.; Silverman, C.; Khandekar, S.; Sarisky, R. T.; Kao, C. C., Mechanism of De Novo Initiation by the Hepatitis C Virus RNA-Dependent RNA Polymerase: Role of Divalent Metals. **2002,** 76, (24), 12513-12525.

111. Luo, G.; Hamatake, R. K.; Mathis, D. M.; Racela, J.; Rigat, K. L.; Lemm, J.; Colonno, R. J., De Novo Initiation of RNA Synthesis by the RNA-Dependent RNA Polymerase (NS5B) of Hepatitis C Virus. **2000,** 74, (2), 851-863.

112. O'Farrell, D.; Trowbridge, R.; Rowlands, D.; Jäger, J., Substrate Complexes of Hepatitis C Virus RNA Polymerase (HC-J4): Structural Evidence for Nucleotide Import and De-novo Initiation. *Journal of Molecular Biology* **2003,** 326, (4), 1025-1035.

113. Houghton, M., Discovery of the hepatitis C virus. **2009,** 29, (s1), 82-88.

114. Dienstag, J. L., Non-A, non-B hepatitis. I. Recognition, epidemiology, and clinical features. *Gastroenterology* **1983,** 85, (2), 439-462.

115. Choo, Q.; Kuo, G.; Weiner, A.; Overby, L.; Bradley, D.; Houghton, M., Isolation of a cDNA clone derived from a blood-borne non-A, non-B viral hepatitis genome. **1989,** 244, (4902), 359-362.

116. Kato, N.; Hijikata, M.; Ootsuyama, Y.; Nakagawa, M.; Ohkoshi, S.; Sugimura, T.; Shimotohno, K., Molecular cloning of the human hepatitis C virus genome from Japanese patients with non-A, non-B hepatitis. *Proceedings of the National Academy of Sciences of the United States of America* **1990,** 87, (24), 9524-9528.

117. Kuo, G.; Choo, Q. L.; Alter, H. J.; Gitnick, G. L.; Redeker, A. G.; Purcell, R. H.; Miyamura, T.; Dienstag, J. L.; Alter, M. J.; Stevens, C. E.; et al., An assay for circulating antibodies to a major etiologic virus of human non-A, non-B hepatitis. *Science* **1989,** 244, (4902), 362-4.

118. Dodd, R. Y., Current safety of the blood supply in the United States. *International journal of hematology* **2004,** 80, (4), 301-5.

119. Takamizawa, A.; Mori, C.; Fuke, I.; Manabe, S.; Murakami, S.; Fujita, J.; Onishi, E.; Andoh, T.; Yoshida, I.; Okayama, H., Structure and organization of the hepatitis C virus genome isolated from human carriers. *Journal of virology* **1991,** 65, (3), 1105-13.

120. Choo, Q. L.; Richman, K. H.; Han, J. H.; Berger, K.; Lee, C.; Dong, C.; Gallegos, C.; Coit, D.; Medina-Selby, R.; Barr, P. J.; et al., Genetic organization and diversity of the hepatitis C virus. *Proceedings of the National Academy of Sciences of the United States of America* **1991,** 88, (6), 2451-5.

121. Suzuki, R.; Suzuki, T.; Ishii, K.; Matsuura, Y.; Miyamura, T., Processing and functions of Hepatitis C virus proteins. *Intervirology* **1999,** 42, (2-3), 145-52.

122. De Francesco, R., Molecular virology of the hepatitis C virus. *Journal of hepatology* **1999,** 31 Suppl 1, 47-53.

123. Forns, X.; Bukh, J., The molecular biology of hepatitis C virus. Genotypes and quasispecies. *Clinics in liver disease* **1999,** 3, (4), 693-716, vii.

124. Lohmann, V.; Korner, F.; Koch, J.; Herian, U.; Theilmann, L.; Bartenschlager, R., Replication of subgenomic hepatitis C virus RNAs in a hepatoma cell line. *Science* **1999,** 285, (5424), 110-3.

125. Nakabayashi, H.; Taketa, K.; Miyano, K.; Yamane, T.; Sato, J., Growth of human hepatoma cells lines with differentiated functions in chemically defined medium. *Cancer research* **1982,** 42, (9), 3858-63.

126. Lohmann, V.; Bartenschlager, R., On the History of Hepatitis C Virus Cell Culture Systems. *Journal of medicinal chemistry* **2014,** 57, (5), 1627-1642.

127. Blight, K. J.; Kolykhalov, A. A.; Rice, C. M., Efficient Initiation of HCV RNA Replication in Cell Culture. **2000,** 290, (5498), 1972-1974.

128. Lohmann, V.; Körner, F.; Dobierzewska, A.; Bartenschlager, R., Mutations in hepatitis C virus RNAs conferring cell culture adaptation. *Journal of virology* **2001,** 75, (3), 1437-1449.

129. Vrolijk, J. M.; Kaul, A.; Hansen, B. E.; Lohmann, V.; Haagmans, B. L.; Schalm, S. W.; Bartenschlager, R., A replicon-based bioassay for the measurement of interferons in patients with chronic hepatitis C. *Journal of Virological Methods* **2003,** 110, (2), 201-209.

130. Frese, M.; Barth, K.; Kaul, A.; Lohmann, V.; Schwarzle, V.; Bartenschlager, R., Hepatitis C virus RNA replication is resistant to tumour necrosis factor-alpha. *The Journal of general virology* **2003,** 84, (Pt 5), 1253-9.

131. Kato, T.; Date, T.; Miyamoto, M.; Furusaka, A.; Tokushige, K.; Mizokami, M.; Wakita, T., Efficient replication of the genotype 2a hepatitis C virus subgenomic replicon. *Gastroenterology* **2003,** 125, (6), 1808-17.

132. Wakita, T.; Pietschmann, T.; Kato, T.; Date, T.; Miyamoto, M.; Zhao, Z.; Murthy, K.; Habermann, A.; Krausslich, H. G.; Mizokami, M.; Bartenschlager, R.; Liang, T. J., Production of infectious hepatitis C virus in tissue culture from a cloned viral genome. *Nature medicine* **2005,** 11, (7), 791-6.

133. Zhong, J.; Gastaminza, P.; Cheng, G.; Kapadia, S.; Kato, T.; Burton, D. R.; Wieland, S. F.; Uprichard, S. L.; Wakita, T.; Chisari, F. V., Robust hepatitis C virus infection in vitro. *Proceedings of the National Academy of Sciences of the United States of America* **2005,** 102, (26), 9294-9.

134. Wakita, T., Cell Culture Systems of HCV Using JFH-1 and Other Strains. *Cold Spring Harbor perspectives in medicine* **2019,** 9, (11).

135. Steinmann, E.; Pietschmann, T., Cell culture systems for hepatitis C virus. *Current topics in microbiology and immunology* **2013,** 369, 17-48.

136. Jo, J.; Aichele, U.; Kersting, N.; Klein, R.; Aichele, P.; Bisse, E.; Sewell, A. K.; Blum, H. E.; Bartenschlager, R.; Lohmann, V.; Thimme, R., Analysis of CD8+ T-cell-mediated inhibition of hepatitis C virus replication using a novel immunological model. *Gastroenterology* **2009,** 136, (4), 1391-401.

137. Friebe, P.; Boudet, J.; Simorre, J.-P.; Bartenschlager, R., Kissing-Loop Interaction in the 3' End of the Hepatitis C Virus Genome Essential for RNA Replication. *Journal of virology* **2005,** 79, (1), 380-392.

138. Blight, K. J.; McKeating, J. A.; Rice, C. M., Highly Permissive Cell Lines for Subgenomic and Genomic Hepatitis C Virus RNA Replication. *Journal of virology* **2002,** 76, (24), 13001-13014.

139. Lindenbach, B. D.; Thiel, H.-J.; Rice, C. M.; Thiel, H.; Rice, C.; Chanock, R., Flaviviridae: the viruses and their replication. **2007**.

140. Zeisel, M. B.; Felmlee, D. J.; Baumert, T. F., Hepatitis C virus entry. *Current topics in microbiology and immunology* **2013,** 369, 87-112.

141. André, P.; Komurian-Pradel, F.; Deforges, S.; Perret, M.; Berland, J. L.; Sodoyer, M.; Pol, S.; Bréchot, C.; Paranhos-Baccalà, G.; Lotteau, V., Characterization of low- and very-low-density hepatitis C virus RNA-containing particles. *Journal of virology* **2002,** 76, (14), 6919-28.

142. Merz, A.; Long, G.; Hiet, M. S.; Brügger, B.; Chlanda, P.; Andre, P.; Wieland, F.; Krijnse-Locker, J.; Bartenschlager, R., Biochemical and morphological properties of hepatitis C virus particles and determination of their lipidome. *The Journal of biological chemistry* **2011,** 286, (4), 3018-32.

143. Miao, Z.; Xie, Z.; Miao, J.; Ran, J.; Feng, Y.; Xia, X., Regulated Entry of Hepatitis C Virus into Hepatocytes. *Viruses* **2017,** 9, (5), 100.

144. Scarselli, E.; Ansuini, H.; Cerino, R.; Roccasecca, R. M.; Acali, S.; Filocamo, G.; Traboni, C.; Nicosia, A.; Cortese, R.; Vitelli, A., The human scavenger receptor class B type I is a novel candidate receptor for the hepatitis C virus. *The EMBO journal* **2002,** 21, (19), 5017-25.

145. Pileri, P.; Uematsu, Y.; Campagnoli, S.; Galli, G.; Falugi, F.; Petracca, R.; Weiner, A. J.; Houghton, M.; Rosa, D.; Grandi, G.; Abrignani, S., Binding of hepatitis C virus to CD81. *Science* **1998,** 282, (5390), 938-41.

146. Evans, M. J.; von Hahn, T.; Tscherne, D. M.; Syder, A. J.; Panis, M.; Wölk, B.; Hatziioannou, T.; McKeating, J. A.; Bieniasz, P. D.; Rice, C. M., Claudin-1 is a hepatitis C virus co-receptor required for a late step in entry. *Nature* **2007,** 446, (7137), 801-5.

147. Ploss, A.; Evans, M. J.; Gaysinskaya, V. A.; Panis, M.; You, H.; de Jong, Y. P.; Rice, C. M., Human occludin is a hepatitis C virus entry factor required for infection of mouse cells. *Nature* **2009,** 457, (7231), 882-6.

148. Brazzoli, M.; Bianchi, A.; Filippini, S.; Weiner, A.; Zhu, Q.; Pizza, M.; Crotta, S., CD81 is a central regulator of cellular events required for hepatitis C virus infection of human hepatocytes. *Journal of virology* **2008,** 82, (17), 8316-29.

149. Farquhar, M. J.; Hu, K.; Harris, H. J.; Davis, C.; Brimacombe, C. L.; Fletcher, S. J.; Baumert, T. F.; Rappoport, J. Z.; Balfe, P.; McKeating, J. A., Hepatitis C virus induces CD81 and claudin-1 endocytosis. *Journal of virology* **2012,** 86, (8), 4305-16.

150. Douam, F.; Lavillette, D.; Cosset, F. L., The mechanism of HCV entry into host cells. *Progress in molecular biology and translational science* **2015,** 129, 63-107.

151. Sharma, N. R.; Mateu, G.; Dreux, M.; Grakoui, A.; Cosset, F. L.; Melikyan, G. B., Hepatitis C virus is primed by CD81 protein for low pH-dependent fusion. *Journal of Biological Chemistry* **2011,** 286, (35), 30361-30376.

152. Romero-Brey, I.; Merz, A.; Chiramel, A.; Lee, J. Y.; Chlanda, P.; Haselman, U.; Santarella-Mellwig, R.; Habermann, A.; Hoppe, S.; Kallis, S.; Walther, P.; Antony, C.; Krijnse-Locker, J.; Bartenschlager, R., Three-dimensional architecture and biogenesis of membrane structures associated with hepatitis C virus replication. *PLoS pathogens* **2012,** 8, (12), e1003056.

153. Gosert, R.; Egger, D.; Lohmann, V.; Bartenschlager, R.; Blum, H. E.; Bienz, K.; Moradpour, D., Identification of the hepatitis C virus RNA replication complex in Huh-7 cells harboring subgenomic replicons. *Journal of virology* **2003,** 77, (9), 5487-92.

154. Piver, E.; Boyer, A.; Gaillard, J.; Bull, A.; Beaumont, E.; Roingeard, P.; Meunier, J.-C., Ultrastructural organisation of HCV from the bloodstream of infected patients revealed by electron microscopy after specific immunocapture. **2017,** 66, (8), 1487-1495.

155. Paul, D.; Hoppe, S.; Saher, G.; Krijnse-Locker, J.; Bartenschlager, R., Morphological and biochemical characterization of the membranous hepatitis C virus replication compartment. *Journal of virology* **2013,** 87, (19), 10612-27.

156. Welsch, S.; Miller, S.; Romero-Brey, I.; Merz, A.; Bleck, C. K.; Walther, P.; Fuller, S. D.; Antony, C.; Krijnse-Locker, J.; Bartenschlager, R., Composition and three-dimensional architecture of the dengue virus replication and assembly sites. *Cell Host Microbe* **2009,** 5, (4), 365-75.

157. Guévin, C.; Manna, D.; Bélanger, C.; Konan, K. V.; Mak, P.; Labonté, P., Autophagy protein ATG5 interacts transiently with the hepatitis C virus RNA polymerase (NS5B) early during infection. *Virology* **2010,** 405, (1), 1-7.

158. Kong, L.; Aoyagi, H.; Yang, Z.; Ouyang, T.; Matsuda, M.; Fujimoto, A.; Watashi, K.; Suzuki, R.; Arita, M.; Yamagoe, S.; Dohmae, N.; Suzuki, T.; Suzuki, T.; Muramatsu, M.; Wakita, T.; Aizaki, H., Surfeit 4 Contributes to the Replication of Hepatitis C Virus Using Double-Membrane Vesicles. **2020,** 94, (2), e00858-19.

159. Lee, J. Y.; Cortese, M.; Haselmann, U.; Tabata, K.; Romero-Brey, I.; Funaya, C.; Schieber, N. L.; Qiang, Y.; Bartenschlager, M.; Kallis, S.; Ritter, C.; Rohr, K.; Schwab, Y.; Ruggieri, A.; Bartenschlager, R., Spatiotemporal Coupling of the Hepatitis C Virus Replication Cycle by Creating a Lipid Droplet- Proximal Membranous Replication Compartment. *Cell reports* **2019,** 27, (12), 3602-3617.e5.

160. Boulant, S.; Montserret, R.; Hope, R. G.; Ratinier, M.; Targett-Adams, P.; Lavergne, J. P.; Penin, F.; McLauchlan, J., Structural determinants that target the hepatitis C virus core protein to lipid droplets. *Journal of Biological Chemistry* **2006,** 281, (31), 22236-22247.

161. Camus, G.; Herker, E.; Modi, A. A.; Haas, J. T.; Ramage, H. R.; Farese, R. V.; Ott, M., Diacylglycerol Acyltransferase-1 Localizes Hepatitis C Virus NS5A Protein to Lipid Droplets and Enhances NS5A Interaction with the Viral Capsid Core. **2013,** 288, (14), 9915-9923.

162. Ma, Y.; Anantpadma, M.; Timpe, J. M.; Shanmugam, S.; Singh, S. M.; Lemon, S. M.; Yi, M. J. J. o. v., Hepatitis C virus NS2 protein serves as a scaffold for virus assembly by interacting with both structural and nonstructural proteins. **2011,** 85, (1), 86-97.

163. Yi, M.; Ma, Y.; Yates, J.; Lemon, S. M., trans-Complementation of an NS2 Defect in a Late Step in Hepatitis C Virus (HCV) Particle Assembly and Maturation. *PLoS pathogens* **2009,** 5, (5), e1000403.

164. Lee, J.-Y.; Cortese, M.; Haselmann, U.; Tabata, K.; Romero-Brey, I.; Funaya, C.; Schieber, N. L.; Qiang, Y.; Bartenschlager, M.; Kallis, S.; Ritter, C.; Rohr, K.; Schwab, Y.; Ruggieri, A.; Bartenschlager, R., Spatiotemporal Coupling of the Hepatitis C Virus Replication Cycle by Creating a Lipid Droplet- Proximal Membranous Replication Compartment. *Cell reports* **2019,** 27, (12), 3602-3617.e5.

165. Huang, H.; Sun, F.; Owen, D. M.; Li, W.; Chen, Y.; Gale, M.; Ye, J., Hepatitis C virus production by human hepatocytes dependent on assembly and secretion of very low-density lipoproteins. **2007,** 104, (14), 5848-5853.

166. Chang, K.-S.; Jiang, J.; Cai, Z.; Luo, G., Human Apolipoprotein E Is Required for Infectivity and Production of Hepatitis C Virus in Cell Culture. **2007,** 81, (24), 13783-13793.

167. Dubuisson, J.; Cosset, F.-L., Virology and cell biology of the hepatitis C virus life cycle – An update. *Journal of hepatology* **2014,** 61, (1, Supplement), S3-S13.

168. Grassi, G.; Di Caprio, G.; Fimia, G. M.; Ippolito, G.; Tripodi, M.; Alonzi, T., Hepatitis C virus relies on lipoproteins for its life cycle. *World journal of gastroenterology* **2016,** 22, (6), 1953-1965.

169. Stoeck, I. K.; Lee, J.-Y.; Tabata, K.; Romero-Brey, I.; Paul, D.; Schult, P.; Lohmann, V.; Kaderali, L.; Bartenschlager, R., Hepatitis C Virus Replication Depends on Endosomal Cholesterol Homeostasis. *Journal of virology* **2018,** 92, (1), e01196-17.

170. Wang, H.; Perry, J. W.; Lauring, A. S.; Neddermann, P.; De Francesco, R.; Tai, A. W., Oxysterol-binding protein is a phosphatidylinositol 4-kinase effector required for HCV replication membrane integrity and cholesterol trafficking. *Gastroenterology* **2014,** 146, (5), 1373-1385.e11.

171. Yang, F.; Robotham, J. M.; Nelson, H. B.; Irsigler, A.; Kenworthy, R.; Tang, H., Cyclophilin A Is an Essential Cofactor for Hepatitis C Virus Infection and the Principal Mediator of Cyclosporine Resistance In Vitro. *Journal of virology* **2008,** 82, (11), 5269-5278.

172. Liu, Z.; Yang, F.; Robotham, J. M.; Tang, H., Critical role of cyclophilin A and its prolyl-peptidyl isomerase activity in the structure and function of the hepatitis C virus replication complex. *Journal of virology* **2009,** 83, (13), 6554-65.

173. Madan, V.; Paul, D.; Lohmann, V.; Bartenschlager, R., Inhibition of HCV Replication by Cyclophilin Antagonists Is Linked to Replication Fitness and Occurs by Inhibition of Membranous Web Formation. *Gastroenterology* **2014,** 146, (5), 1361-1372.e9.

174. Dujardin, M.; Madan, V.; Gandhi, N. S.; Cantrelle, F.-X.; Launay, H.; Huvent, I.; Bartenschlager, R.; Lippens, G.; Hanoulle, X., Cyclophilin A allows the allosteric regulation of a structural motif in the disordered domain 2 of NS5A and thereby fine-tunes HCV RNA replication. **2019,** 294, (35), 13171-13185.

175. Herker, E.; Harris, C.; Hernandez, C.; Carpentier, A.; Kaehlcke, K.; Rosenberg, A. R.; Farese, R. V.; Ott, M., Efficient hepatitis C virus particle formation requires diacylglycerol acyltransferase-1. *Nature medicine* **2010,** 16, (11), 1295-1298.

176. Hoofnagle, J. H., Course and outcome of hepatitis C. *Hepatology* **2002,** 36, (5 Suppl 1), S21-9.

177. WHO What is hepatitis? https://www.who.int/features/qa/76/en/ (08.04.2020),

178. Robert-Koch-Institut Epidemiologisches Bulletin 03/2020. https://www.rki.de/DE/Content/Infekt/EpidBull/Archiv/2020/Ausgaben/03_20.pdf?__blob=publicationFile (08.04.2020),

179. Hoofnagle, J. H.; Mullen, K. D.; Jones, D. B.; Rustgi, V.; di Bisceglie, A.; Peters, M.; Waggoner, J. G.; Park, Y.; Jones, E. A., Treatment of Chronic Non-A, Non-B Hepatitis with Recombinant Human Alpha Interferon. *New England Journal of Medicine* **1986,** 315, (25), 1575-1578.

180. Patterson, J. L.; Fernandez-Larsson, R., Molecular mechanisms of action of ribavirin. *Reviews of infectious diseases* **1990,** 12, (6), 1139-46.

181. Lindsay, K. L.; Trepo, C.; Heintges, T.; Shiffman, M. L.; Gordon, S. C.; Hoefs, J. C.; Schiff, E. R.; Goodman, Z. D.; Laughlin, M.; Yao, R.; Albrecht, J. K., A randomized, double-blind trial comparing pegylated interferon alfa-2b to interferon alfa-2b as initial treatment for chronic hepatitis C. *Hepatology* **2001,** 34, (2), 395-403.

182. Bacon, B. R.; Gordon, S. C.; Lawitz, E.; Marcellin, P.; Vierling, J. M.; Zeuzem, S.; Poordad, F.; Goodman, Z. D.; Sings, H. L.; Boparai, N.; Burroughs, M.; Brass, C. A.; Albrecht, J. K.; Esteban, R., Boceprevir for previously treated chronic HCV genotype 1 infection. *The New England journal of medicine* **2011,** 364, (13), 1207-17.

183. Poordad, F.; McCone, J., Jr.; Bacon, B. R.; Bruno, S.; Manns, M. P.; Sulkowski, M. S.; Jacobson, I. M.; Reddy, K. R.; Goodman, Z. D.; Boparai, N.; DiNubile, M. J.; Sniukiene, V.; Brass, C. A.; Albrecht, J. K.; Bronowicki, J. P., Boceprevir for untreated chronic HCV genotype 1 infection. *The New England journal of medicine* **2011,** 364, (13), 1195-206.

184. Jacobson, I. M.; McHutchison, J. G.; Dusheiko, G.; Di Bisceglie, A. M.; Reddy, K. R.; Bzowej, N. H.; Marcellin, P.; Muir, A. J.; Ferenci, P.; Flisiak, R.; George, J.; Rizzetto, M.; Shouval, D.; Sola, R.; Terg, R. A.; Yoshida, E. M.; Adda, N.; Bengtsson, L.; Sankoh, A. J.; Kieffer, T. L.; George, S.; Kauffman, R. S.; Zeuzem, S., Telaprevir for previously untreated chronic hepatitis C virus infection. *The New England journal of medicine* **2011,** 364, (25), 2405-16.

185. Zeuzem, S.; Andreone, P.; Pol, S.; Lawitz, E.; Diago, M.; Roberts, S.; Focaccia, R.; Younossi, Z.; Foster, G. R.; Horban, A.; Ferenci, P.; Nevens, F.; Müllhaupt, B.; Pockros, P.; Terg, R.; Shouval, D.; van Hoek, B.; Weiland, O.; Van Heeswijk, R.; De Meyer, S.; Luo, D.; Boogaerts, G.; Polo, R.; Picchio, G.; Beumont, M., Telaprevir for retreatment of HCV infection. *The New England journal of medicine* **2011,** 364, (25), 2417-28.

186. Scheel, T. K. H.; Rice, C. M., Understanding the hepatitis C virus life cycle paves the way for highly effective therapies. *Nature medicine* **2013,** 19, (7), 837-849.

187. de Leuw, P.; Stephan, C., Protease inhibitor therapy for hepatitis C virus-infection. *Expert Opinion on Pharmacotherapy* **2018,** 19, (6), 577-587.

188. Sofia, M. J.; Bao, D.; Chang, W.; Du, J.; Nagarathnam, D.; Rachakonda, S.; Reddy, P. G.; Ross, B. S.; Wang, P.; Zhang, H. R.; Bansal, S.; Espiritu, C.; Keilman, M.; Lam, A. M.; Steuer, H. M.; Niu, C.; Otto, M. J.; Furman, P. A., Discovery of a β-d-2'-deoxy-2'-α-fluoro-2'-β-C-methyluridine nucleotide prodrug (PSI-7977) for the treatment of hepatitis C virus. *Journal of medicinal chemistry* **2010,** 53, (19), 7202-18.

189. McQuaid, T.; Savini, C.; Seyedkazemi, S., Sofosbuvir, a Significant Paradigm Change in HCV Treatment. *J Clin Transl Hepatol* **2015,** 3, (1), 27-35.

190. Gane, E. J.; Stedman, C. A.; Hyland, R. H.; Ding, X.; Svarovskaia, E.; Symonds, W. T.; Hindes, R. G.; Berrey, M. M., Nucleotide polymerase inhibitor sofosbuvir plus ribavirin for hepatitis C. *The New England journal of medicine* **2013,** 368, (1), 34-44.

191. Jacobson, I. M.; Gordon, S. C.; Kowdley, K. V.; Yoshida, E. M.; Rodriguez-Torres, M.; Sulkowski, M. S.; Shiffman, M. L.; Lawitz, E.; Everson, G.; Bennett, M.; Schiff, E.; Al-Assi, M. T.; Subramanian, G. M.; An, D.; Lin, M.; McNally, J.; Brainard, D.; Symonds, W. T.; McHutchison, J. G.; Patel, K.; Feld, J.; Pianko, S.; Nelson, D. R., Sofosbuvir for Hepatitis C Genotype 2 or 3 in Patients without Treatment Options. **2013,** 368, (20), 1867-1877.

192. Lawitz, E.; Mangia, A.; Wyles, D.; Rodriguez-Torres, M.; Hassanein, T.; Gordon, S. C.; Schultz, M.; Davis, M. N.; Kayali, Z.; Reddy, K. R.; Jacobson, I. M.; Kowdley, K. V.; Nyberg, L.; Subramanian, G. M.; Hyland, R. H.; Arterburn, S.; Jiang, D.; McNally, J.; Brainard, D.; Symonds, W. T.; McHutchison, J. G.; Sheikh, A. M.; Younossi, Z.; Gane, E. J., Sofosbuvir for previously untreated chronic hepatitis C infection. *The New England journal of medicine* **2013,** 368, (20), 1878-87.

193. Afdhal, N.; Zeuzem, S.; Kwo, P.; Chojkier, M.; Gitlin, N.; Puoti, M.; Romero-Gomez, M.; Zarski, J. P.; Agarwal, K.; Buggisch, P.; Foster, G. R.; Bräu, N.; Buti, M.; Jacobson, I. M.; Subramanian, G. M.; Ding, X.; Mo, H.; Yang, J. C.; Pang, P. S.; Symonds, W. T.; McHutchison, J. G.; Muir, A. J.; Mangia, A.; Marcellin, P., Ledipasvir and sofosbuvir for untreated HCV genotype 1 infection. *The New England journal of medicine* **2014,** 370, (20), 1889-98.

194. Kowdley, K. V.; Gordon, S. C.; Reddy, K. R.; Rossaro, L.; Bernstein, D. E.; Lawitz, E.; Shiffman, M. L.; Schiff, E.; Ghalib, R.; Ryan, M.; Rustgi, V.; Chojkier, M.; Herring, R.; Di Bisceglie, A. M.; Pockros, P. J.; Subramanian, G. M.; An, D.; Svarovskaia, E.; Hyland, R. H.; Pang, P. S.; Symonds, W. T.; McHutchison, J. G.; Muir, A. J.; Pound, D.; Fried, M. W., Ledipasvir and sofosbuvir for 8 or 12 weeks for chronic HCV without cirrhosis. *The New England journal of medicine* **2014,** 370, (20), 1879-88.

195. Lawitz, E.; Sulkowski, M. S.; Ghalib, R.; Rodriguez-Torres, M.; Younossi, Z. M.; Corregidor, A.; DeJesus, E.; Pearlman, B.; Rabinovitz, M.; Gitlin, N.; Lim, J. K.; Pockros, P. J.; Scott, J. D.; Fevery, B.; Lambrecht, T.; Ouwerkerk-Mahadevan, S.; Callewaert, K.; Symonds, W. T.; Picchio, G.; Lindsay, K. L.; Beumont, M.; Jacobson, I. M., Simeprevir plus sofosbuvir, with or without ribavirin, to treat chronic infection with hepatitis C virus genotype 1 in non-responders to pegylated interferon and ribavirin and treatment-naive patients: the COSMOS randomised study. *Lancet* **2014,** 384, (9956), 1756-65.

196. Sulkowski, M. S.; Gardiner, D. F.; Rodriguez-Torres, M.; Reddy, K. R.; Hassanein, T.; Jacobson, I.; Lawitz, E.; Lok, A. S.; Hinestrosa, F.; Thuluvath, P. J.; Schwartz, H.; Nelson, D. R.; Everson, G. T.; Eley, T.; Wind-Rotolo, M.; Huang, S. P.; Gao, M.; Hernandez, D.; McPhee, F.; Sherman, D.; Hindes, R.; Symonds, W.; Pasquinelli, C.; Grasela, D. M., Daclatasvir plus sofosbuvir for previously treated or untreated chronic HCV infection. *The New England journal of medicine* **2014,** 370, (3), 211-21.

197. Ghany, M. G.; Morgan, T. R.; Panel, A.-I. H. C. G., Hepatitis C Guidance 2019 Update: American Association for the Study of Liver Diseases–Infectious Diseases Society of America Recommendations for Testing, Managing, and Treating Hepatitis C Virus Infection. **2020,** 71, (2), 686-721.

198. Carrion, A. F.; Martin, P., Glecaprevir + pibrentasvir for treatment of hepatitis C. *Expert Opinion on Pharmacotherapy* **2018,** 19, (4), 413-419.

199. Hézode, C., Treatment of hepatitis C: Results in real life. **2018,** 38, (S1), 21-27.

200. Feld, J. J.; Jacobson, I. M.; Hézode, C.; Asselah, T.; Ruane, P. J.; Gruener, N.; Abergel, A.; Mangia, A.; Lai, C. L.; Chan, H. L.; Mazzotta, F.; Moreno, C.; Yoshida, E.; Shafran, S. D.; Towner, W. J.; Tran, T. T.; McNally, J.; Osinusi, A.; Svarovskaia, E.; Zhu, Y.; Brainard, D. M.; McHutchison, J. G.; Agarwal, K.; Zeuzem, S., Sofosbuvir and Velpatasvir for HCV Genotype 1, 2, 4, 5, and 6 Infection. *The New England journal of medicine* **2015,** 373, (27), 2599-607.

201. Li, D. K.; Chung, R. T., Overview of Direct-Acting Antiviral Drugs and Drug Resistance of Hepatitis C Virus. In *Hepatitis C Virus Protocols*, Law, M., Ed. Springer New York: New York, NY, 2019; pp 3-32.

202. Iyengar, S.; Tay-Teo, K.; Vogler, S.; Beyer, P.; Wiktor, S.; de Joncheere, K.; Hill, S., Prices, Costs, and Affordability of New Medicines for Hepatitis C in 30 Countries: An Economic Analysis. *PLOS Medicine* **2016,** 13, (5), e1002032.

203. Stetson, D. B.; Medzhitov, R., Type I Interferons in Host Defense. *Immunity* **2006,** 25, (3), 373-381.

204. Heim, M. H.; Thimme, R., Innate and adaptive immune responses in HCV infections. *Journal of hepatology* **2014,** 61, (1 Suppl), S14-25.

205. Kwon, Y. C.; Ray, R., Complement Regulation and Immune Evasion by Hepatitis C Virus. *Methods in molecular biology (Clifton, N.J.)* **2019,** 1911, 337-347.

206. Akira, S.; Uematsu, S.; Takeuchi, O., Pathogen Recognition and Innate Immunity. *Cell* **2006,** 124, (4), 783-801.

207. Barbalat, R.; Ewald, S. E.; Mouchess, M. L.; Barton, G. M., Nucleic Acid Recognition by the Innate Immune System. **2011,** 29, (1), 185-214.

208. Burdette, D. L.; Vance, R. E., STING and the innate immune response to nucleic acids in the cytosol. *Nature Immunology* **2013,** 14, (1), 19-26.

209. Kawasaki, T.; Kawai, T.; Akira, S., Recognition of nucleic acids by pattern-recognition receptors and its relevance in autoimmunity. **2011,** 243, (1), 61-73.

210. Alexopoulou, L.; Holt, A. C.; Medzhitov, R.; Flavell, R. A., Recognition of double-stranded RNA and activation of NF-κB by Toll-like receptor 3. *Nature* **2001,** 413, (6857), 732-738.

211. Yoneyama, M.; Kikuchi, M.; Natsukawa, T.; Shinobu, N.; Imaizumi, T.; Miyagishi, M.; Taira, K.; Akira, S.; Fujita, T., The RNA helicase RIG-I has an essential function in double-stranded RNA-induced innate antiviral responses. *Nature Immunology* **2004,** 5, (7), 730-737.

212. Kang, D. C.; Gopalkrishnan, R. V.; Wu, Q.; Jankowsky, E.; Pyle, A. M.; Fisher, P. B., mda-5: An interferon-inducible putative RNA helicase with double-stranded RNA-dependent ATPase activity and melanoma growth-suppressive properties. *Proceedings of the National Academy of Sciences of the United States of America* **2002,** 99, (2), 637-642.

213. Rodriguez, K. R.; Bruns, A. M.; Horvath, C. M., MDA5 and LGP2: accomplices and antagonists of antiviral signal transduction. *Journal of virology* **2014,** 88, (15), 8194-8200.

214. Li, K.; Li, N. L.; Wei, D.; Pfeffer, S. R.; Fan, M.; Pfeffer, L. M., Activation of chemokine and inflammatory cytokine response in hepatitis C virus–infected hepatocytes depends on toll-like receptor 3 sensing of hepatitis C virus double-stranded RNA intermediates. **2012,** 55, (3), 666-675.

215. Hiet, M.-S.; Bauhofer, O.; Zayas, M.; Roth, H.; Tanaka, Y.; Schirmacher, P.; Willemsen, J.; Grünvogel, O.; Bender, S.; Binder, M.; Lohmann, V.; Lotteau, V.; Ruggieri, A.; Bartenschlager, R., Control of temporal activation of hepatitis C virus-induced interferon response by domain 2 of nonstructural protein 5A. *Journal of hepatology* **2015,** 63, (4), 829-837.

216. Sumpter, R., Jr.; Loo, Y. M.; Foy, E.; Li, K.; Yoneyama, M.; Fujita, T.; Lemon, S. M.; Gale, M., Jr., Regulating intracellular antiviral defense and permissiveness to hepatitis C virus RNA replication through a cellular RNA helicase, RIG-I. *Journal of virology* **2005,** 79, (5), 2689-99.

217. Saito, T.; Owen, D. M.; Jiang, F.; Marcotrigiano, J.; Gale Jr, M., Innate immunity induced by composition-dependent RIG-I recognition of hepatitis C virus RNA. *Nature* **2008,** 454, (7203), 523-527.

218. Saito, T.; Hirai, R.; Loo, Y.-M.; Owen, D.; Johnson, C. L.; Sinha, S. C.; Akira, S.; Fujita, T.; Gale, M., Jr., Regulation of innate antiviral defenses through a shared repressor domain in RIG-I and LGP2. *Proceedings of the National Academy of Sciences of the United States of America* **2007,** 104, (2), 582-587.

219. Ferreira, A. R.; Ramos, B.; Nunes, A.; Ribeiro, D., Hepatitis C Virus: Evading the Intracellular Innate Immunity. *Journal of clinical medicine* **2020,** 9, (3).

220. Negash, A. A.; Ramos, H. J.; Crochet, N.; Lau, D. T. Y.; Doehle, B.; Papic, N.; Delker, D. A.; Jo, J.; Bertoletti, A.; Hagedorn, C. H.; Gale, M., Jr., IL-1β Production through the NLRP3 Inflammasome by Hepatic Macrophages Links Hepatitis C Virus Infection with Liver Inflammation and Disease. *PLoS pathogens* **2013,** 9, (4), e1003330.

221. Takahashi, K.; Asabe, S.; Wieland, S.; Garaigorta, U.; Gastaminza, P.; Isogawa, M.; Chisari, F. V., Plasmacytoid dendritic cells sense hepatitis C virus–infected cells, produce interferon, and inhibit infection. **2010,** 107, (16), 7431-7436.

222. Heil, F.; Hemmi, H.; Hochrein, H.; Ampenberger, F.; Kirschning, C.; Akira, S.; Lipford, G.; Wagner, H.; Bauer, S., Species-Specific Recognition of Single-Stranded RNA via Toll-like Receptor 7 and 8. **2004,** 303, (5663), 1526-1529.

223. Kawai, T.; Akira, S., Innate immune recognition of viral infection. *Nature Immunology* **2006,** 7, (2), 131-137.

224. Fitzgerald, K. A.; McWhirter, S. M.; Faia, K. L.; Rowe, D. C.; Latz, E.; Golenbock, D. T.; Coyle, A. J.; Liao, S. M.; Maniatis, T., IKKepsilon and TBK1 are essential components of the IRF3 signaling pathway. *Nat Immunol* **2003,** 4, (5), 491-6.

225. Sharma, S.; tenOever, B. R.; Grandvaux, N.; Zhou, G. P.; Lin, R.; Hiscott, J., Triggering the interferon antiviral response through an IKK-related pathway. *Science* **2003,** 300, (5622), 1148-51.

226. Schoggins, J. W.; Rice, C. M., Innate immune responses to hepatitis C virus. *Current topics in microbiology and immunology* **2013,** 369, 219-42.

227. Bruening, J.; Weigel, B.; Gerold, G., The Role of Type III Interferons in Hepatitis C Virus Infection and Therapy. *Journal of immunology research* **2017,** 2017, 7232361.

228. Lee, H.-C.; Narayanan, S.; Park, S.-J.; Seong, S.-Y.; Hahn, Y. S., Transcriptional regulation of IFN-λ genes in hepatitis C virus-infected hepatocytes via IRF-3·IRF-7·NF-κB complex. *The Journal of biological chemistry* **2014,** 289, (8), 5310-5319.

229. Heim, M. H., Innate immunity and HCV. *Journal of hepatology* **2013,** 58, (3), 564-574.

230. Thimme, R.; Binder, M.; Bartenschlager, R., Failure of innate and adaptive immune responses in controlling hepatitis C virus infection. *FEMS microbiology reviews* **2012,** 36, (3), 663-83.

231. Kotenko, S. V.; Gallagher, G.; Baurin, V. V.; Lewis-Antes, A.; Shen, M.; Shah, N. K.; Langer, J. A.; Sheikh, F.; Dickensheets, H.; Donnelly, R. P., IFN-λs mediate antiviral protection through a distinct class II cytokine receptor complex. *Nature Immunology* **2003,** 4, (1), 69-77.

232. Prokunina-Olsson, L.; Muchmore, B.; Tang, W.; Pfeiffer, R. M.; Park, H.; Dickensheets, H.; Hergott, D.; Porter-Gill, P.; Mumy, A.; Kohaar, I.; Chen, S.; Brand, N.; Tarway, M.; Liu, L.; Sheikh, F.; Astemborski, J.; Bonkovsky, H. L.; Edlin, B. R.; Howell, C. D.; Morgan, T. R.; Thomas, D. L.; Rehermann, B.; Donnelly, R. P.; O'Brien, T. R., A variant upstream of IFNL3 (IL28B) creating a new interferon gene IFNL4 is associated with impaired clearance of hepatitis C virus. *Nature genetics* **2013,** 45, (2), 164-71.

233. Sung, P. S.; Hong, S. H.; Chung, J. H.; Kim, S.; Park, S. H.; Kim, H. M.; Yoon, S. K.; Shin, E. C., IFN-λ4 potently blocks IFN-α signalling by ISG15 and USP18 in hepatitis C virus infection. *Scientific reports* **2017,** 7, (1), 3821.

234. Onabajo, O. O.; Muchmore, B.; Prokunina-Olsson, L., The IFN-λ4 Conundrum: When a Good Interferon Goes Bad. *Journal of interferon & cytokine research : the official journal of the International Society for Interferon and Cytokine Research* **2019,** 39, (10), 636-641.

235. Loeb, K. R.; Haas, A. L., The interferon-inducible 15-kDa ubiquitin homolog conjugates to intracellular proteins. **1992,** 267, (11), 7806-13.

236. Villarroya-Beltri, C.; Guerra, S.; Sánchez-Madrid, F., ISGylation – a key to lock the cell gates for preventing the spread of threats. **2017,** 130, (18), 2961-2969.

237. Shi, H.-X.; Yang, K.; Liu, X.; Liu, X.-Y.; Wei, B.; Shan, Y.-F.; Zhu, L.-H.; Wang, C., Positive Regulation of Interferon Regulatory Factor 3 Activation by Herc5 via ISG15 Modification. **2010,** 30, (10), 2424-2436.

238. Chen, L.; Sun, J.; Meng, L.; Heathcote, J.; Edwards, A. M.; McGilvray, I. D., ISG15, a ubiquitin-like interferon-stimulated gene, promotes hepatitis C virus production in vitro: implications for chronic infection and response to treatment. **2010,** 91, (2), 382-388.

239. Malakhov, M. P.; Malakhova, O. A.; Kim, K. I.; Ritchie, K. J.; Zhang, D.-E., UBP43 (USP18) Specifically Removes ISG15 from Conjugated Proteins. **2002,** 277, (12), 9976-9981.

240. Malakhova, O. A.; Yan, M.; Malakhov, M. P.; Yuan, Y.; Ritchie, K. J.; Kim, K. I.; Peterson, L. F.; Shuai, K.; Zhang, D. E., Protein ISGylation modulates the JAK-STAT signaling pathway. *Genes & development* **2003,** 17, (4), 455-60.

241. Malakhova, O. A.; Kim, K. I.; Luo, J. K.; Zou, W.; Kumar, K. G.; Fuchs, S. Y.; Shuai, K.; Zhang, D. E., UBP43 is a novel regulator of interferon signaling independent of its ISG15 isopeptidase activity. *The EMBO journal* **2006,** 25, (11), 2358-67.

242. Schoggins, J. W.; Wilson, S. J.; Panis, M.; Murphy, M. Y.; Jones, C. T.; Bieniasz, P.; Rice, C. M., A diverse range of gene products are effectors of the type I interferon antiviral response. *Nature* **2011,** 472, (7344), 481-5.

243. Zhao, H.; Lin, W.; Kumthip, K.; Cheng, D.; Fusco, D. N.; Hofmann, O.; Jilg, N.; Tai, A. W.; Goto, K.; Zhang, L.; Hide, W.; Jang, J. Y.; Peng, L. F.; Chung, R. T., A functional genomic screen reveals novel host genes that mediate interferon-alpha's effects against hepatitis C virus. *Journal of hepatology* **2012,** 56, (2), 326-333.

244. Metz, P.; Dazert, E.; Ruggieri, A.; Mazur, J.; Kaderali, L.; Kaul, A.; Zeuge, U.; Windisch, M. P.; Trippler, M.; Lohmann, V.; Binder, M.; Frese, M.; Bartenschlager, R., Identification of type I and type II interferon-induced effectors controlling hepatitis C virus replication. *Hepatology* **2012,** 56, (6), 2082-93.

245. Itsui, Y.; Sakamoto, N.; Kurosaki, M.; Kanazawa, N.; Tanabe, Y.; Koyama, T.; Takeda, Y.; Nakagawa, M.; Kakinuma, S.; Sekine, Y.; Maekawa, S.; Enomoto, N.; Watanabe, M., Expressional screening of interferon-stimulated genes for antiviral activity against hepatitis C virus replication. *Journal of viral hepatitis* **2006,** 13, (10), 690-700.

246. Jiang, D.; Guo, H.; Xu, C.; Chang, J.; Gu, B.; Wang, L.; Block, T. M.; Guo, J.-T., Identification of Three Interferon-Inducible Cellular Enzymes That Inhibit the Replication of Hepatitis C Virus. **2008,** 82, (4), 1665-1678.

247. Metz, P.; Reuter, A.; Bender, S.; Bartenschlager, R., Interferon-stimulated genes and their role in controlling hepatitis C virus. *Journal of hepatology* **2013,** 59, (6), 1331-1341.

248. Pichlmair, A.; Lassnig, C.; Eberle, C. A.; Górna, M. W.; Baumann, C. L.; Burkard, T. R.; Bürckstümmer, T.; Stefanovic, A.; Krieger, S.; Bennett, K. L.; Rülicke, T.; Weber, F.; Colinge, J.; Müller, M.; Superti-Furga, G., IFIT1 is an antiviral protein that recognizes 5'-triphosphate RNA. *Nat Immunol* **2011,** 12, (7), 624-30.

249. Fensterl, V.; Sen, G. C., Interferon-Induced Ifit Proteins: Their Role in Viral Pathogenesis. **2015,** 89, (5), 2462-2468.

250. Wang, C.; Pflugheber, J.; Sumpter, R., Jr.; Sodora, D. L.; Hui, D.; Sen, G. C.; Gale, M., Jr., Alpha interferon induces distinct translational control programs to suppress hepatitis C virus RNA replication. *Journal of virology* **2003,** 77, (7), 3898-912.

251. Diamond, M. S.; Farzan, M., The broad-spectrum antiviral functions of IFIT and IFITM proteins. *Nat Rev Immunol* **2013,** 13, (1), 46-57.

252. Han, J. Q.; Barton, D. J., Activation and evasion of the antiviral 2'-5' oligoadenylate synthetase/ribonuclease L pathway by hepatitis C virus mRNA. *Rna* **2002,** 8, (4), 512-525.

253. Sarasin-Filipowicz, M.; Oakeley, E. J.; Duong, F. H. T.; Christen, V.; Terracciano, L.; Filipowicz, W.; Heim, M. H., Interferon signaling and treatment outcome in chronic hepatitis C. **2008,** 105, (19), 7034-7039.

254. Li, X. D.; Sun, L.; Seth, R. B.; Pineda, G.; Chen, Z. J., Hepatitis C virus protease NS3/4A cleaves mitochondrial antiviral signaling protein off the mitochondria to evade innate immunity. *Proceedings of the National Academy of Sciences of the United States of America* **2005,** 102, (49), 17717-22.

255. Foy, E.; Li, K.; Wang, C.; Sumpter, R., Jr.; Ikeda, M.; Lemon, S. M.; Gale, M., Jr., Regulation of interferon regulatory factor-3 by the hepatitis C virus serine protease. *Science* **2003,** 300, (5622), 1145-8.

256. Bellecave, P.; Sarasin-Filipowicz, M.; Donzé, O.; Kennel, A.; Gouttenoire, J.; Meylan, E.; Terracciano, L.; Tschopp, J.; Sarrazin, C.; Berg, T.; Moradpour, D.; Heim, M. H., Cleavage of mitochondrial antiviral signaling protein in the liver of patients with chronic hepatitis C correlates with a reduced activation of the endogenous interferon system. **2010,** 51, (4), 1127-1136.

257. Dansako, H.; Ikeda, M.; Kato, N., Limited suppression of the interferon-β production by hepatitis C virus serine protease in cultured human hepatocytes. **2007,** 274, (16), 4161-4176.

258. Horner, S. M.; Gale, M., Jr., Regulation of hepatic innate immunity by hepatitis C virus. *Nature medicine* **2013,** 19, (7), 879-888.

259. Chan, S. T.; Ou, J. J., Hepatitis C Virus-Induced Autophagy and Host Innate Immune Response. *Viruses* **2017,** 9, (8).

260. Ke, P. Y.; Chen, S. S., Activation of the unfolded protein response and autophagy after hepatitis C virus infection suppresses innate antiviral immunity in vitro. *The Journal of clinical investigation* **2011,** 121, (1), 37-56.

261. Shrivastava, S.; Raychoudhuri, A.; Steele, R.; Ray, R.; Ray, R. B., Knockdown of autophagy enhances the innate immune response in hepatitis C virus-infected hepatocytes. *Hepatology* **2011,** 53, (2), 406-14.

262. Kumthip, K.; Chusri, P.; Jilg, N.; Zhao, L.; Fusco, D. N.; Zhao, H.; Goto, K.; Cheng, D.; Schaefer, E. A.; Zhang, L.; Pantip, C.; Thongsawat, S.; O'Brien, A.; Peng, L. F.; Maneekarn, N.; Chung, R. T.; Lin, W., Hepatitis C virus NS5A disrupts STAT1 phosphorylation and suppresses type I interferon signaling. *Journal of virology* **2012,** 86, (16), 8581-91.

263. Lin, W.; Kim, S. S.; Yeung, E.; Kamegaya, Y.; Blackard, J. T.; Kim, K. A.; Holtzman, M. J.; Chung, R. T., Hepatitis C virus core protein blocks interferon signaling by interaction with the STAT1 SH2 domain. *Journal of virology* **2006,** 80, (18), 9226-35.

264. Lin, W.; Choe, W. H.; Hiasa, Y.; Kamegaya, Y.; Blackard, J. T.; Schmidt, E. V.; Chung, R. T., Hepatitis C virus expression suppresses interferon signaling by degrading STAT1. *Gastroenterology* **2005,** 128, (4), 1034-41.

265. Convery, O.; Gargan, S.; Kickham, M.; Schroder, M.; O'Farrelly, C.; Stevenson, N. J., The hepatitis C virus (HCV) protein, p7, suppresses inflammatory responses to tumor necrosis factor (TNF)-α via signal transducer and activator of transcription (STAT)3 and extracellular signal-regulated kinase (ERK)–mediated induction of suppressor of cytokine signaling (SOCS)3. **2019,** 33, (8), 8732-8744.

266. Ho, D. D.; Neumann, A. U.; Perelson, A. S.; Chen, W.; Leonard, J. M.; Markowitz, M., Rapid turnover of plasma virions and CD4 lymphocytes in HIV-1 infection. *Nature* **1995,** 373, (6510), 123-6.

267. Perelson, A. S.; Neumann, A. U.; Markowitz, M.; Leonard, J. M.; Ho, D. D., HIV-1 Dynamics in Vivo: Virion Clearance Rate, Infected Cell Life-Span, and Viral Generation Time. **1996,** 271, (5255), 1582-1586.

268. Wei, X.; Ghosh, S. K.; Taylor, M. E.; Johnson, V. A.; Emini, E. A.; Deutsch, P.; Lifson, J. D.; Bonhoeffer, S.; Nowak, M. A.; Hahn, B. H.; et al., Viral dynamics in human immunodeficiency virus type 1 infection. *Nature* **1995,** 373, (6510), 117-22.

269. Neumann, A. U.; Lam, N. P.; Dahari, H.; Gretch, D. R.; Wiley, T. E.; Layden, T. J.; Perelson, A. S., Hepatitis C Viral Dynamics in Vivo and the Antiviral Efficacy of Interferon-α Therapy. **1998,** 282, (5386), 103-107.

270. Lam, N. P.; Neumann, A. U.; Gretch, D. R.; Wiley, T. E.; Perelson, A. S.; Layden, T. J., Dose-dependent acute clearance of hepatitis C genotype 1 virus with interferon alfa. *Hepatology* **1997,** 26, (1), 226-31.

271. Dahari, H.; Major, M.; Zhang, X.; Mihalik, K.; Rice, C. M.; Perelson, A. S.; Feinstone, S. M.; Neumann, A. U., Mathematical modeling of primary hepatitis C infection: Noncytolytic clearance and early blockage of virion production. *Gastroenterology* **2005,** 128, (4), 1056-1066.

272. Dahari, H.; Feliu, A.; Garcia-Retortillo, M.; Forns, X.; Neumann, A. U., Second hepatitis C replication compartment indicated by viral dynamics during liver transplantation. *Journal of hepatology* **2005,** 42, (4), 491-8.

273. Powers, K. A.; Ribeiro, R. M.; Patel, K.; Pianko, S.; Nyberg, L.; Pockros, P.; Conrad, A. J.; McHutchison, J.; Perelson, A. S., Kinetics of hepatitis C virus reinfection after liver transplantation. *Liver transplantation : official publication of the American Association for the Study of Liver Diseases and the International Liver Transplantation Society* **2006,** 12, (2), 207-16.

274. Dahari, H.; Ribeiro, R. M.; Rice, C. M.; Perelson, A. S., Mathematical modeling of subgenomic hepatitis C virus replication in Huh-7 cells. *Journal of virology* **2007,** 81, (2), 750-60.

275. Eigen, M.; Biebricher, C. K.; Gebinoga, M.; Gardiner, W. C., The hypercycle. Coupling of RNA and protein biosynthesis in the infection cycle of an RNA bacteriophage. *Biochemistry* **1991,** 30, (46), 11005-11018.

276. Reigadas, S.; Ventura, M.; Sarih-Cottin, L.; Castroviejo, M.; Litvak, S.; Astier-Gin, T., HCV RNA-dependent RNA polymerase replicates in vitro the 3' terminal region of the minus-strand viral RNA more efficiently than the 3' terminal region of the plus RNA. *European journal of biochemistry* **2001,** 268, (22), 5857-67.

277. Binder, M.; Sulaimanov, N.; Clausznitzer, D.; Schulze, M.; Huber, C. M.; Lenz, S. M.; Schloder, J. P.; Trippler, M.; Bartenschlager, R.; Lohmann, V.; Kaderali, L., Replication vesicles are load- and choke-points in the hepatitis C virus lifecycle. *PLoS pathogens* **2013,** 9, (8), e1003561.

278. Dächert, C.; Gladilin, E.; Binder, M., Gene Expression Profiling of Different Huh7 Variants Reveals Novel Hepatitis C Virus Host Factors. *Viruses* **2019,** 12, (1), E36.

279. Koutsoudakis, G.; Herrmann, E.; Kallis, S.; Bartenschlager, R.; Pietschmann, T., The level of CD81 cell surface expression is a key determinant for productive entry of hepatitis C virus into host cells. *Journal of virology* **2007,** 81, (2), 588-98.

280. Lohmann, V.; Hoffmann, S.; Herian, U.; Penin, F.; Bartenschlager, R., Viral and cellular determinants of hepatitis C virus RNA replication in cell culture. *Journal of virology* **2003,** 77, (5), 3007-3019.

281. Windisch, M. P.; Frese, M.; Kaul, A.; Trippler, M.; Lohmann, V.; Bartenschlager, R., Dissecting the interferon-induced inhibition of hepatitis C virus replication by using a novel host cell line. *Journal of virology* **2005,** 79, (21), 13778-13793.

282. Friebe, P.; Lohmann, V.; Krieger, N.; Bartenschlager, R., Sequences in the 5' nontranslated region of hepatitis C virus required for RNA replication. *Journal of virology* **2001,** 75, (24), 12047-57.

283. Pietschmann, T.; Kaul, A.; Koutsoudakis, G.; Shavinskaya, A.; Kallis, S.; Steinmann, E.; Abid, K.; Negro, F.; Dreux, M.; Cosset, F. L.; Bartenschlager, R., Construction and characterization of infectious intragenotypic and intergenotypic hepatitis C virus chimeras. *Proceedings of the National Academy of Sciences of the United States of America* **2006,** 103, (19), 7408-13.

284. Fischl, W.; Bartenschlager, R., High-Throughput Screening Using Dengue Virus Reporter Genomes. In *Antiviral Methods and Protocols*, Gong, E. Y., Ed. Humana Press: Totowa, NJ, 2013; pp 205-219.

285. Kuri, T.; Habjan, M.; Penski, N.; Weber, F., Species-independent bioassay for sensitive quantification of antiviral type I interferons. *Virol J* **2010,** 7, 50-50.

286. Schindelin, J.; Arganda-Carreras, I.; Frise, E.; Kaynig, V.; Longair, M.; Pietzsch, T.; Preibisch, S.; Rueden, C.; Saalfeld, S.; Schmid, B.; Tinevez, J.-Y.; White, D. J.; Hartenstein, V.; Eliceiri, K.; Tomancak, P.; Cardona, A., Fiji: an open-source platform for biological-image analysis. *Nature Methods* **2012,** 9, (7), 676-682.

287. Reece-Hoyes, J. S.; Walhout, A. J. M., Gateway Recombinational Cloning. *Cold Spring Harb Protoc* **2018,** 2018, (1), pdb.top094912-pdb.top094912.

288. Graham, F. L.; Smiley, J.; Russell, W. C.; Nairn, R., Characteristics of a Human Cell Line Transformed by DNA from Human Adenovirus Type 5. *Journal of General Virology* **1977,** 36, (1), 59-72.

289. Willemsen, J.; Wicht, O.; Wolanski, J. C.; Baur, N.; Bastian, S.; Haas, D. A.; Matula, P.; Knapp, B.; Meyniel-Schicklin, L.; Wang, C.; Bartenschlager, R.; Lohmann, V.; Rohr, K.; Erfle, H.; Kaderali, L.; Marcotrigiano, J.; Pichlmair, A.; Binder, M., Phosphorylation-Dependent Feedback Inhibition of RIG-I by DAPK1 Identified by Kinome-wide siRNA Screening. *Molecular cell* **2017,** 65, (3), 403-415.e8.

290. Jones, C. T.; Catanese, M. T.; Law, L. M. J.; Khetani, S. R.; Syder, A. J.; Ploss, A.; Oh, T. S.; Schoggins, J. W.; MacDonald, M. R.; Bhatia, S. N.; Rice, C. M., Real-time imaging of hepatitis C virus infection using a fluorescent cell-based reporter system. *Nat Biotechnol* **2010,** 28, (2), 167-171.

291. van den Hoff, M. J.; Moorman, A. F.; Lamers, W. H., Electroporation in 'intracellular' buffer increases cell survival. *Nucleic acids research* **1992,** 20, (11), 2902.

292. Potter, H., Transfection by electroporation. *Current protocols in molecular biology* **2003,** Chapter 9, Unit 9.3.

293. https://www.klinikum.uni-heidelberg.de/Downloads.126386.0.html.

294. Chomczynski, P.; Sacchi, N., Single-step method of RNA isolation by acid guanidinium thiocyanate-phenol-chloroform extraction. *Analytical biochemistry* **1987,** 162, (1), 156-9.

295. Grünvogel, O.; Colasanti, O.; Lee, J.-Y.; Klöss, V.; Belouzard, S.; Reustle, A.; Esser-Nobis, K.; Hesebeck-Brinckmann, J.; Mutz, P.; Hoffmann, K.; Mehrabi, A.; Koschny, R.; Vondran, F. W. R.; Gotthardt, D.; Schnitzler, P.; Neumann-Haefelin, C.; Thimme, R.; Binder, M.; Bartenschlager, R.; Dubuisson, J.; Dalpke, A. H.; Lohmann, V., Secretion of Hepatitis C Virus Replication Intermediates Reduces Activation of Toll-Like Receptor 3 in Hepatocytes. *Gastroenterology* **2018,** 154, (8), 2237-2251.e16.

296. Zayas, M.; Long, G.; Madan, V.; Bartenschlager, R., Coordination of Hepatitis C Virus Assembly by Distinct Regulatory Regions in Nonstructural Protein 5A. *PLoS pathogens* **2016,** 12, (1), e1005376.

297. R Core Team *A Language and Environment for Statistical*, R Foundation for Statistical Computing.

298. ORFeome, T.; Wiemann, S.; Pennacchio, C.; Hu, Y.; Hunter, P.; Harbers, M.; Amiet, A.; Bethel, G.; Busse, M.; Carninci, P.; Dunham, I.; Hao, T.; Harper, J. W.; Hayashizaki, Y.; Heil, O.; Hennig, S.; Hotz-Wagenblatt, A.; Jang, W.; Jöcker, A.; Kawai, J.; Koenig, C.; Korn, B.; Lambert, C.; LeBeau, A.; Lu, S.; Maurer, J.; Moore, T.; Ohara, O.; Park, J.; Rolfs, A.; Salehi-Ashtiani, K.; Seiler, C.; Simmons, B.; van Brabant Smith, A.; Steel, J.; Wagner, L.; Weaver, T.; Wellenreuther, R.; Yang, S.; Vidal, M.; Gerhard, D. S.; LaBaer, J.; Temple, G.; Hill, D. E., The ORFeome Collaboration: a genome-scale human ORF-clone resource. *Nature Methods* **2016,** 13, 191.

299. Clones, t. O. C. O. c. http://www.orfeomecollaboration.org/

300. Zoratti, M. J.; Siddiqua, A.; Morassut, R. E.; Zeraatkar, D.; Chou, R.; van Holten, J.; Xie, F.; Druyts, E., Pangenotypic direct acting antivirals for the treatment of chronic hepatitis C virus infection: A systematic literature review and meta-analysis. *EClinicalMedicine* **2020,** 18, 100237-100237.

301. Nakamoto, S.; Kanda, T.; Wu, S.; Shirasawa, H.; Yokosuka, O., Hepatitis C virus NS5A inhibitors and drug resistance mutations. *World journal of gastroenterology* **2014,** 20, (11), 2902-2912.

302. Shanmugam, S.; Nichols, A. K.; Saravanabalaji, D.; Welsch, C.; Yi, M., HCV NS5A dimer interface residues regulate HCV replication by controlling its self-interaction, hyperphosphorylation, subcellular localization and interaction with cyclophilin A. *PLoS pathogens* **2018,** 14, (7), e1007177.

303. Berger, C.; Romero-Brey, I.; Radujkovic, D.; Terreux, R.; Zayas, M.; Paul, D.; Harak, C.; Hoppe, S.; Gao, M.; Penin, F.; Lohmann, V.; Bartenschlager, R., Daclatasvir-like inhibitors of NS5A block early biogenesis of hepatitis C virus-induced membranous replication factories, independent of RNA replication. *Gastroenterology* **2014,** 147, (5), 1094-105.e25.

304. Chatterji, U.; Bobardt, M.; Tai, A.; Wood, M.; Gallay, P. A., Cyclophilin and NS5A inhibitors, but not other anti-hepatitis C virus (HCV) agents, preclude HCV-mediated formation of double-membrane-vesicle viral factories. *Antimicrobial agents and chemotherapy* **2015,** 59, (5), 2496-507.

305. Daclatasvir; Approval https://www.drugs.com/history/daklinza.html (retrieved 20.04.2020),

306. Montgomery, M.; Ho, N.; Chung, E.; Marzella, N., Daclatasvir (Daklinza): A Treatment Option for Chronic Hepatitis C Infection. *P T* **2016,** 41, (12), 751-755.

307. Gao, M.; Nettles, R. E.; Belema, M.; Snyder, L. B.; Nguyen, V. N.; Fridell, R. A.; Serrano-Wu, M. H.; Langley, D. R.; Sun, J. H.; O'Boyle, D. R., 2nd; Lemm, J. A.; Wang, C.; Knipe, J. O.; Chien, C.; Colonno, R. J.; Grasela, D. M.; Meanwell, N. A.; Hamann, L. G., Chemical genetics strategy identifies an HCV NS5A inhibitor with a potent clinical effect. *Nature* **2010,** 465, (7294), 96-100.

308. Belema, M.; Meanwell, N. A., Discovery of Daclatasvir, a Pan-Genotypic Hepatitis C Virus NS5A Replication Complex Inhibitor with Potent Clinical Effect. *Journal of medicinal chemistry* **2014,** 57, (12), 5057-5071.

309. Thorne, N.; Inglese, J.; Auld, D. S., Illuminating insights into firefly luciferase and other bioluminescent reporters used in chemical biology. *Chem Biol* **2010,** 17, (6), 646-657.

310. Lindenbach, B. D.; Evans, M. J.; Syder, A. J.; Wolk, B.; Tellinghuisen, T. L.; Liu, C. C.; Maruyama, T.; Hynes, R. O.; Burton, D. R.; McKeating, J. A.; Rice, C. M., Complete replication of hepatitis C virus in cell culture. *Science* **2005,** 309, (5734), 623-6.

311. Seth, R. B.; Sun, L.; Ea, C. K.; Chen, Z. J., Identification and characterization of MAVS, a mitochondrial antiviral signaling protein that activates NF-kappaB and IRF 3. *Cell* **2005,** 122, (5), 669-82.

312. Foy, E.; Li, K.; Sumpter, R., Jr.; Loo, Y. M.; Johnson, C. L.; Wang, C.; Fish, P. M.; Yoneyama, M.; Fujita, T.; Lemon, S. M.; Gale, M., Jr., Control of antiviral defenses through hepatitis C virus disruption of retinoic acid-inducible gene-I signaling. *Proceedings of the National Academy of Sciences of the United States of America* **2005,** 102, (8), 2986-91.

313. Pawlotsky, J.-M., Treatment of Chronic Hepatitis C: Current and Future. In *Hepatitis C Virus: From Molecular Virology to Antiviral Therapy*, Bartenschlager, R., Ed. Springer Berlin Heidelberg: Berlin, Heidelberg, 2013; pp 321-342.

314. Fung, A.; Jin, Z.; Dyatkina, N.; Wang, G.; Beigelman, L.; Deval, J., Efficiency of incorporation and chain termination determines the inhibition potency of 2'-modified nucleotide analogs against hepatitis C virus polymerase. *Antimicrobial agents and chemotherapy* **2014,** 58, (7), 3636-3645.

REFERENCES

315. Macfarlan, T.; Kutney, S.; Altman, B.; Montross, R.; Yu, J.; Chakravarti, D., Human THAP7 is a chromatin-associated, histone tail-binding protein that represses transcription via recruitment of HDAC3 and nuclear hormone receptor corepressor. *The Journal of biological chemistry* **2005,** 280, (8), 7346-58.

316. Macfarlan, T.; Parker, J. B.; Nagata, K.; Chakravarti, D., Thanatos-associated protein 7 associates with template activating factor-Ibeta and inhibits histone acetylation to repress transcription. *Molecular endocrinology (Baltimore, Md.)* **2006,** 20, (2), 335-47.

317. Seol, W.; Choi, H. S.; Moore, D. D., An orphan nuclear hormone receptor that lacks a DNA binding domain and heterodimerizes with other receptors. *Science* **1996,** 272, (5266), 1336-9.

318. Conti, B.; Porcu, C.; Viscomi, C.; Minutolo, A.; Costantini, S.; Corazzari, M.; Iannucci, G.; Barbaro, B.; Balsano, C., Small heterodimer partner 1 directly interacts with NS5A viral protein and has a key role in HCV related liver cell transformation. *Oncotarget* **2016,** 7, (51), 84575-84586.

319. Forman, B. M.; Goode, E.; Chen, J.; Oro, A. E.; Bradley, D. J.; Perlmann, T.; Noonan, D. J.; Burka, L. T.; McMorris, T.; Lamph, W. W.; Evans, R. M.; Weinberger, C., Identification of a nuclear receptor that is activated by farnesol metabolites. *Cell* **1995,** 81, (5), 687-693.

320. Makishima, M.; Okamoto, A. Y.; Repa, J. J.; Tu, H.; Learned, R. M.; Luk, A.; Hull, M. V.; Lustig, K. D.; Mangelsdorf, D. J.; Shan, B., Identification of a Nuclear Receptor for Bile Acids. **1999,** 284, (5418), 1362-1365.

321. Parks, D. J.; Blanchard, S. G.; Bledsoe, R. K.; Chandra, G.; Consler, T. G.; Kliewer, S. A.; Stimmel, J. B.; Willson, T. M.; Zavacki, A. M.; Moore, D. D.; Lehmann, J. M., Bile acids: natural ligands for an orphan nuclear receptor. *Science* **1999,** 284, (5418), 1365-8.

322. Wang, H.; Chen, J.; Hollister, K.; Sowers, L. C.; Forman, B. M., Endogenous bile acids are ligands for the nuclear receptor FXR/BAR. *Molecular cell* **1999,** 3, (5), 543-53.

323. Hofmann, A. F., The continuing importance of bile acids in liver and intestinal disease. *Archives of internal medicine* **1999,** 159, (22), 2647-58.

324. Lu, T. T.; Makishima, M.; Repa, J. J.; Schoonjans, K.; Kerr, T. A.; Auwerx, J.; Mangelsdorf, D. J., Molecular Basis for Feedback Regulation of Bile Acid Synthesis by Nuclear Receptors. *Molecular cell* **2000,** 6, (3), 507-515.

325. **!!! INVALID CITATION !!! {}**.

326. Schwarz, M.; Lund, E. G.; Russell, D. W., Two 7 alpha-hydroxylase enzymes in bile acid biosynthesis. *Current opinion in lipidology* **1998,** 9, (2), 113-8.

327. Maloney, P. R.; Parks, D. J.; Haffner, C. D.; Fivush, A. M.; Chandra, G.; Plunket, K. D.; Creech, K. L.; Moore, L. B.; Wilson, J. G.; Lewis, M. C.; Jones, S. A.; Willson, T. M., Identification of a chemical tool for the orphan nuclear receptor FXR. *Journal of medicinal chemistry* **2000,** 43, (16), 2971-4.

328. Goodwin, B.; Jones, S. A.; Price, R. R.; Watson, M. A.; McKee, D. D.; Moore, L. B.; Galardi, C.; Wilson, J. G.; Lewis, M. C.; Roth, M. E.; Maloney, P. R.; Willson, T. M.; Kliewer, S. A., A regulatory cascade of the nuclear receptors FXR, SHP-1, and LRH-1 represses bile acid biosynthesis. *Molecular cell* **2000,** 6, (3), 517-26.

329. Urizar, N. L.; Liverman, A. B.; Dodds, D. N. T.; Silva, F. V.; Ordentlich, P.; Yan, Y.; Gonzalez, F. J.; Heyman, R. A.; Mangelsdorf, D. J.; Moore, D. D., A Natural Product That Lowers Cholesterol As an Antagonist Ligand for FXR. *Science* **2002,** 296, (5573), 1703-1706.

330. Wu, J.; Xia, C.; Meier, J.; Li, S.; Hu, X.; Lala, D. S., The Hypolipidemic Natural Product Guggulsterone Acts as an Antagonist of the Bile Acid Receptor. *Molecular Endocrinology* **2002,** 16, (7), 1590-1597.

331. Whitfield, G. B.; Brock, T. D.; Ammann, A.; Gottlieb, D.; Carter, H. E., Filipin, an Antifungal Antibiotic: Isolation and Properties. *Journal of the American Chemical Society* **1955,** 77, (18), 4799-4801.

332. Osuna-Ramos, J. F.; Reyes-Ruiz, J. M.; Del Ángel, R. M., The Role of Host Cholesterol During Flavivirus Infection. *Front Cell Infect Microbiol* **2018,** 8, 388-388.

333. Villareal, V. A.; Rodgers, M. A.; Costello, D. A.; Yang, P. L., Targeting host lipid synthesis and metabolism to inhibit dengue and hepatitis C viruses. *Antiviral research* **2015,** 124, 110-121.

334. Pinkham, C.; Ahmed, A.; Bracci, N.; Narayanan, A.; Kehn-Hall, K., Host-based processes as therapeutic targets for Rift Valley fever virus. *Antiviral research* **2018,** 160, 64-78.

335. Koutsoudakis, G.; Kaul, A.; Steinmann, E.; Kallis, S.; Lohmann, V.; Pietschmann, T.; Bartenschlager, R., Characterization of the Early Steps of Hepatitis C Virus Infection by Using Luciferase Reporter Viruses. *Journal of virology* **2006,** 80, (11), 5308-5320.

336. Sumpter, R., Jr.; Loo, Y.-M.; Foy, E.; Li, K.; Yoneyama, M.; Fujita, T.; Lemon, S. M.; Gale, M., Jr., Regulating intracellular antiviral defense and permissiveness to hepatitis C virus RNA replication through a cellular RNA helicase, RIG-I. *Journal of virology* **2005,** 79, (5), 2689-2699.

337. Binder, M.; Kochs, G.; Bartenschlager, R.; Lohmann, V., Hepatitis C virus escape from the interferon regulatory factor 3 pathway by a passive and active evasion strategy. *Hepatology* **2007,** 46, (5), 1365-1374.

338. Michel, A. M.; Choudhury, K. R.; Firth, A. E.; Ingolia, N. T.; Atkins, J. F.; Baranov, P. V., Observation of dually decoded regions of the human genome using ribosome profiling data. *Genome Res* **2012,** 22, (11), 2219-2229.

339. Oyama, M.; Kozuka-Hata, H.; Suzuki, Y.; Semba, K.; Yamamoto, T.; Sugano, S., Diversity of Translation Start Sites May Define Increased Complexity of the Human Short ORFeome. **2007,** 6, (6), 1000-1006.

340. Chen, L.; Chen, W.; Zhao, L.; Yu, H. Z.; Li, X., Immunoscreening of urinary bladder cancer cDNA library and identification of potential tumor antigen. *World journal of urology* **2009,** 27, (1), 107-12.

341. Qanbari, S.; Rubin, C. J.; Maqbool, K., Genetics of adaptation in modern chicken. **2019,** 15, (4), e1007989.

342.   Gibert, J. M.; Karch, F.; Schlotterer, C., Segregating variation in the polycomb group gene cramped alters the effect of temperature on multiple traits. *PLoS Genet* **2011,** 7, (1), e1001280.

343.   Suzuki, S.; Mori, J.; Hashizume, K., mu-crystallin, a NADPH-dependent T(3)-binding protein in cytosol. *Trends in endocrinology and metabolism: TEM* **2007,** 18, (7), 286-9.

344.   Hallen, A.; Cooper, A. J.; Jamie, J. F.; Karuso, P., Insights into Enzyme Catalysis and Thyroid Hormone Regulation of Cerebral Ketimine Reductase/μ-Crystallin Under Physiological Conditions. *Neurochemical research* **2015,** 40, (6), 1252-66.

345.   Serrano, M.; Moreno, M.; Ortega, F. J.; Xifra, G.; Ricart, W.; Moreno-Navarrete, J. M.; Fernández-Real, J. M., Adipose tissue μ-crystallin is a thyroid hormone-binding protein associated with systemic insulin sensitivity. *The Journal of clinical endocrinology and metabolism* **2014,** 99, (11), E2259-68.

346.   Oshima, A.; Suzuki, S.; Takumi, Y.; Hashizume, K.; Abe, S.; Usami, S., CRYM mutations cause deafness through thyroid hormone binding properties in the fibrocytes of the cochlea. *Journal of medical genetics* **2006,** 43, (6), e25.

347.   Cachefo, A.; Boucher, P.; Vidon, C.; Dusserre, E.; Diraison, F.; Beylot, M., Hepatic lipogenesis and cholesterol synthesis in hyperthyroid patients. *The Journal of clinical endocrinology and metabolism* **2001,** 86, (11), 5353-7.

348.   Fernández-Real, J.-M.; López-Bermejo, A.; Castro, A.; Casamitjana, R.; Ricart, W., Thyroid Function Is Intrinsically Linked to Insulin Sensitivity and Endothelium-Dependent Vasodilation in Healthy Euthyroid Subjects. *The Journal of Clinical Endocrinology & Metabolism* **2006,** 91, (9), 3337-3343.

349.   Bernsmeier, C.; Calabrese, D.; Heim, M. H.; Duong, H. T. F., Hepatitis C virus dysregulates glucose homeostasis by a dual mechanism involving induction of PGC1α and dephosphorylation of FoxO1. **2014,** 21, (1), 9-18.

350.   Arrese, M.; Riquelme, A.; Soza, A., Insulin resistance, hepatic steatosis and hepatitis C: a complex relationship with relevant clinical implications. *Annals of hepatology* **2010,** 9 Suppl, 112-8.

351.   Ohkubo, Y.; Sekido, T.; Nishio, S. I.; Sekido, K.; Kitahara, J.; Suzuki, S.; Komatsu, M., Loss of mu-crystallin causes PPARgamma activation and obesity in high-fat diet-fed mice. *Biochem Biophys Res Commun* **2019,** 508, (3), 914-920.

352.   Takeshige, K.; Sekido, T.; Kitahara, J.; Ohkubo, Y.; Hiwatashi, D.; Ishii, H.; Nishio, S.; Takeda, T.; Komatsu, M.; Suzuki, S., Cytosolic T3-binding protein modulates dynamic alteration of T3-mediated gene expression in cells. *Endocrine journal* **2014,** 61, (6), 561-70.

353.   Polyak, S. J.; Tang, N.; Wambach, M.; Barber, G. N.; Katze, M. G., The P58 cellular inhibitor complexes with the interferon-induced, double-stranded RNA-dependent protein kinase, PKR, to regulate its autophosphorylation and activity. *The Journal of biological chemistry* **1996,** 271, (3), 1702-7.

354.   Now, H.; Yoo, J. Y., A protein-kinase, IFN-inducible double-stranded RNA dependent inhibitor and repressor of p58 (PRKRIR) enhances type I IFN-mediated antiviral response through the stability control of RIG-I protein. *Biochem Biophys Res Commun* **2011,** 413, (3), 487-93.

355.   Saito, S.; Miyaji-Yamaguchi, M.; Shimoyama, T.; Nagata, K., Functional domains of template-activating factor-I as a protein phosphatase 2A inhibitor. *Biochem Biophys Res Commun* **1999,** 259, (2), 471-5.

356.   Georgopoulou, U.; Tsitoura, P.; Kalamvoki, M.; Mavromara, P., The protein phosphatase 2A represents a novel cellular target for hepatitis C virus NS5A protein. *Biochimie* **2006,** 88, (6), 651-62.

357.   Duong, F. H.; Christen, V.; Berke, J. M.; Penna, S. H.; Moradpour, D.; Heim, M. H., Upregulation of protein phosphatase 2Ac by hepatitis C virus modulates NS3 helicase activity through inhibition of protein arginine methyltransferase 1. *Journal of virology* **2005,** 79, (24), 15342-50.

358.   Zhou, Y.; Wang, Q.; Yang, Q.; Tang, J.; Xu, C.; Gai, D.; Chen, X.; Chen, J., Histone Deacetylase 3 Inhibitor Suppresses Hepatitis C Virus Replication by Regulating Apo-A1 and LEAP-1 Expression. *Virologica Sinica* **2018,** 33, (5), 418-428.

359.   Mancone, C.; Steindler, C.; Santangelo, L.; Simonte, G.; Vlassi, C.; Longo, M. A.; D'Offizi, G.; Di Giacomo, C.; Pucillo, L. P.; Amicone, L.; Tripodi, M.; Alonzi, T., Hepatitis C virus production requires apolipoprotein A-I and affects its association with nascent low-density lipoproteins. *Gut* **2011,** 60, (3), 378-86.

360.   Chanda, D.; Park, J. H.; Choi, H. S., Molecular basis of endocrine regulation by orphan nuclear receptor Small Heterodimer Partner. *Endocrine journal* **2008,** 55, (2), 253-68.

361.   Goodwin, B.; Jones, S. A.; Price, R. R.; Watson, M. A.; McKee, D. D.; Moore, L. B.; Galardi, C.; Wilson, J. G.; Lewis, M. C.; Roth, M. E.; Maloney, P. R.; Willson, T. M.; Kliewer, S. A., A Regulatory Cascade of the Nuclear Receptors FXR, SHP-1, and LRH-1 Represses Bile Acid Biosynthesis. *Molecular cell* **2000,** 6, (3), 517-526.

362.   Chang, K. O.; George, D. W., Bile acids promote the expression of hepatitis C virus in replicon-harboring cells. *Journal of virology* **2007,** 81, (18), 9633-40.

363.   Scholtes, C.; Diaz, O.; Icard, V.; Kaul, A.; Bartenschlager, R.; Lotteau, V.; Andre, P., Enhancement of genotype 1 hepatitis C virus replication by bile acids through FXR. *Journal of hepatology* **2008,** 48, (2), 192-9.

364.   Chhatwal, P.; Bankwitz, D.; Gentzsch, J.; Frentzen, A.; Schult, P.; Lohmann, V.; Pietschmann, T., Bile acids specifically increase hepatitis C virus RNA-replication. *PLoS one* **2012,** 7, (4), e36029-e36029.

365.   Patton, J. B.; George, D.; Chang, K. O., Bile acids promote HCV replication through the EGFR/ERK pathway in replicon-harboring cells. *Intervirology* **2011,** 54, (6), 339-48.

REFERENCES

366. Chen, J.; Zhou, Y.; Zhuang, Y.; Qin, T.; Guo, M.; Jiang, J.; Niu, J.; Li, J. Z.; Chen, X.; Wang, Q., The metabolic regulator small heterodimer partner contributes to the glucose and lipid homeostasis abnormalities induced by hepatitis C virus infection. *Metabolism* **2019**, 153954.

367. Jung, G.-S.; Jeon, J.-H.; Choi, Y.-K.; Jang, S. Y.; Park, S. Y.; Kim, M.-K.; Shin, E.-C.; Jeong, W.-I.; Lee, I.-K.; Kang, Y. N.; Park, K.-G., Small heterodimer partner attenuates profibrogenic features of hepatitis C virus-infected cells. *Liver International* **2015,** 35, (10), 2233-2245.

368. Zou, A.; Magee, N.; Deng, F.; Lehn, S.; Zhong, C.; Zhang, Y., Hepatocyte nuclear receptor SHP suppresses inflammation and fibrosis in a mouse model of nonalcoholic steatohepatitis. *The Journal of biological chemistry* **2018,** 293, (22), 8656-8671.

369. Song, Y.; Lu, S.; Zhao, J.; Wang, L., Nuclear Receptor SHP: A Critical Regulator of miRNA and lncRNA Expression and Function. *Nuclear receptor research* **2017,** 4.

370. Harak, C.; Meyrath, M.; Romero-Brey, I.; Schenk, C.; Gondeau, C.; Schult, P.; Esser-Nobis, K.; Saeed, M.; Neddermann, P.; Schnitzler, P.; Gotthardt, D.; Perez-Del-Pulgar, S.; Neumann-Haefelin, C.; Thimme, R.; Meuleman, P.; Vondran, F. W.; De Francesco, R.; Rice, C. M.; Bartenschlager, R.; Lohmann, V., Tuning a cellular lipid kinase activity adapts hepatitis C virus to replication in cell culture. *Nature microbiology* **2016,** 2, 16247.

371. Yang, D.-R.; Zhu, H.-Z., Hepatitis C virus and antiviral innate immunity: who wins at tug-of-war? *World journal of gastroenterology* **2015,** 21, (13), 3786-3800.

372. Li, K.; Lemon, S. M., Innate immune responses in hepatitis C virus infection. *Semin Immunopathol* **2013,** 35, (1), 53-72.

373. Silverman, R. H., Viral encounters with 2',5'-oligoadenylate synthetase and RNase L during the interferon antiviral response. *Journal of virology* **2007,** 81, (23), 12720-9.

374. Kato, J.; Kato, N.; Moriyama, M.; Goto, T.; Taniguchi, H.; Shiratori, Y.; Omata, M., Interferons specifically suppress the translation from the internal ribosome entry site of hepatitis C virus through a double-stranded RNA-activated protein kinase-independent pathway. *The Journal of infectious diseases* **2002,** 186, (2), 155-63.

375. Shimazaki, T.; Honda, M.; Kaneko, S.; Kobayashi, K., Inhibition of internal ribosomal entry site-directed translation of HCV by recombinant IFN-alpha correlates with a reduced La protein. *Hepatology* **2002,** 35, (1), 199-208.

376. Pedersen, I. M.; Cheng, G.; Wieland, S.; Volinia, S.; Croce, C. M.; Chisari, F. V.; David, M., Interferon modulation of cellular microRNAs as an antiviral mechanism. *Nature* **2007,** 449, (7164), 919-922.

377. Fusco, D. N.; Brisac, C.; John, S. P.; Huang, Y.-W.; Chin, C. R.; Xie, T.; Zhao, H.; Jilg, N.; Zhang, L.; Chevaliez, S.; Wambua, D.; Lin, W.; Peng, L.; Chung, R. T.; Brass, A. L., A genetic screen identifies interferon-α effector genes required to suppress hepatitis C virus replication. *Gastroenterology* **2013,** 144, (7), 1438-1449.e14499.

378. Amador-Cañizares, Y.; Bernier, A.; Wilson, J. A.; Sagan, S. M., miR-122 does not impact recognition of the HCV genome by innate sensors of RNA but rather protects the 5' end from the cellular pyrophosphatases, DOM3Z and DUSP11. *Nucleic acids research* **2018,** 46, (10), 5139-5158.

379. Machlin, E. S.; Sarnow, P.; Sagan, S. M., Masking the 5' terminal nucleotides of the hepatitis C virus genome by an unconventional microRNA-target RNA complex. *Proceedings of the National Academy of Sciences of the United States of America* **2011,** 108, (8), 3193-8.

380. Li, Y.; Yamane, D.; Lemon, S. M., Dissecting the roles of the 5' exoribonucleases Xrn1 and Xrn2 in restricting hepatitis C virus replication. *Journal of virology* **2015,** 89, (9), 4857-65.

381. Ross-Thriepland, D.; Harris, M., Hepatitis C virus NS5A: enigmatic but still promiscuous 10 years on! **2015,** 96, (4), 727-738.

382. Tellinghuisen, T. L.; Marcotrigiano, J.; Gorbalenya, A. E.; Rice, C. M., The NS5A Protein of Hepatitis C Virus Is a Zinc Metalloprotein. **2004,** 279, (47), 48576-48587.

383. Love, R. A.; Brodsky, O.; Hickey, M. J.; Wells, P. A.; Cronin, C. N., Crystal structure of a novel dimeric form of NS5A domain I protein from hepatitis C virus. *Journal of virology* **2009,** 83, (9), 4395-403.

384. Lambert, S. M.; Langley, D. R.; Garnett, J. A.; Angell, R.; Hedgethorne, K.; Meanwell, N. A.; Matthews, S. J., The crystal structure of NS5A domain 1 from genotype 1a reveals new clues to the mechanism of action for dimeric HCV inhibitors. *Protein science : a publication of the Protein Society* **2014,** 23, (6), 723-34.

385. Hwang, J.; Huang, L.; Cordek, D. G.; Vaughan, R.; Reynolds, S. L.; Kihara, G.; Raney, K. D.; Kao, C. C.; Cameron, C. E., Hepatitis C Virus Nonstructural Protein 5A: Biochemical Characterization of a Novel Structural Class of RNA-Binding Proteins. **2010,** 84, (24), 12480-12491.

386. Foster, T. L.; Belyaeva, T.; Stonehouse, N. J.; Pearson, A. R.; Harris, M., All three domains of the hepatitis C virus nonstructural NS5A protein contribute to RNA binding. *Journal of virology* **2010,** 84, (18), 9267-77.

387. Lim, P. J.; Chatterji, U.; Cordek, D.; Sharma, S. D.; Garcia-Rivera, J. A.; Cameron, C. E.; Lin, K.; Targett-Adams, P.; Gallay, P. A., Correlation between NS5A dimerization and hepatitis C virus replication. *The Journal of biological chemistry* **2012,** 287, (36), 30861-73.

388. Ascher, D. B.; Wielens, J.; Nero, T. L.; Doughty, L.; Morton, C. J.; Parker, M. W., Potent hepatitis C inhibitors bind directly to NS5A and reduce its affinity for RNA. *Scientific reports* **2014,** 4, 4765.

389. Bhattacharya, D.; Ansari, I. H.; Hamatake, R.; Walker, J.; Kazmierski, W. M.; Striker, R., Pharmacological disruption of hepatitis C NS5A protein intra- and intermolecular conformations. **2014,** 95, (2), 363-372.

390. Machner, M. P.; Frese, S.; Schubert, W. D.; Orian-Rousseau, V.; Gherardi, E.; Wehland, J.; Niemann, H. H.; Heinz, D. W., Aromatic amino acids at the surface of InlB are essential for host cell invasion by Listeria monocytogenes. *Molecular microbiology* **2003,** 48, (6), 1525-36.

391. Daito, T.; Watashi, K.; Sluder, A.; Ohashi, H.; Nakajima, S.; Borroto-Esoda, K.; Fujita, T.; Wakita, T., Cyclophilin inhibitors reduce phosphorylation of RNA-dependent protein kinase to restore expression of IFN-stimulated genes in HCV-infected cells. *Gastroenterology* **2014,** 147, (2), 463-72.

392. McGivern, D. R.; Masaki, T.; Williford, S.; Ingravallo, P.; Feng, Z.; Lahser, F.; Asante-Appiah, E.; Neddermann, P.; De Francesco, R.; Howe, A. Y.; Lemon, S. M., Kinetic Analyses Reveal Potent and Early Blockade of Hepatitis C Virus Assembly by NS5A Inhibitors. *Gastroenterology* **2014,** 147, (2), 453-462.e7.

393. Lee, C.; Ma, H.; Hang, J. Q.; Leveque, V.; Sklan, E. H.; Elazar, M.; Klumpp, K.; Glenn, J. S., The hepatitis C virus NS5A inhibitor (BMS-790052) alters the subcellular localization of the NS5A non-structural viral protein. *Virology* **2011,** 414, (1), 10-8.

394. Miyanari, Y.; Atsuzawa, K.; Usuda, N.; Watashi, K.; Hishiki, T.; Zayas, M.; Bartenschlager, R.; Wakita, T.; Hijikata, M.; Shimotohno, K., The lipid droplet is an important organelle for hepatitis C virus production. *Nature cell biology* **2007,** 9, (9), 1089-97.

395. Guedj, J.; Dahari, H.; Rong, L.; Sansone, N. D.; Nettles, R. E.; Cotler, S. J.; Layden, T. J.; Uprichard, S. L.; Perelson, A. S., Modeling shows that the NS5A inhibitor daclatasvir has two modes of action and yields a shorter estimate of the hepatitis C virus half-life. *Proceedings of the National Academy of Sciences of the United States of America* **2013,** 110, (10), 3991-6.

396. Lin, C.; Kwong, A. D.; Perni, R. B., Discovery and development of VX-950, a novel, covalent, and reversible inhibitor of hepatitis C virus NS3.4A serine protease. *Infectious disorders drug targets* **2006,** 6, (1), 3-16.

397. Kohlway, A.; Pirakitikulr, N.; Ding, S. C.; Yang, F.; Luo, D.; Lindenbach, B. D.; Pyle, A. M., The linker region of NS3 plays a critical role in the replication and infectivity of hepatitis C virus. *Journal of virology* **2014,** 88, (18), 10970-10974.

398. Kohlway, A.; Pirakitikulr, N.; Barrera, F. N.; Potapova, O.; Engelman, D. M.; Pyle, A. M.; Lindenbach, B. D., Hepatitis C virus RNA replication and virus particle assembly require specific dimerization of the NS4A protein transmembrane domain. *Journal of virology* **2014,** 88, (1), 628-642.

399. Roder, A. E.; Vazquez, C.; Horner, S. M., The acidic domain of the hepatitis C virus NS4A protein is required for viral assembly and envelopment through interactions with the viral E1 glycoprotein. *PLoS pathogens* **2019,** 15, (2), e1007163-e1007163.

400. Yan, Y.; He, Y.; Boson, B.; Wang, X.; Cosset, F. L.; Zhong, J., A Point Mutation in the N-Terminal Amphipathic Helix α(0) in NS3 Promotes Hepatitis C Virus Assembly by Altering Core Localization to the Endoplasmic Reticulum and Facilitating Virus Budding. *Journal of virology* **2017,** 91, (6).

401. McGivern, D. R.; Masaki, T.; Lovell, W.; Hamlett, C.; Saalau-Bethell, S.; Graham, B., Protease Inhibitors Block Multiple Functions of the NS3/4A Protease-Helicase during the Hepatitis C Virus Life Cycle. **2015,** 89, (10), 5362-5370.

402. Kazakov, T.; Yang, F.; Ramanathan, H. N.; Kohlway, A.; Diamond, M. S.; Lindenbach, B. D., Hepatitis C virus RNA replication depends on specific cis- and trans-acting activities of viral nonstructural proteins. *PLoS pathogens* **2015,** 11, (4), e1004817-e1004817.

403. Frick, D. N.; Rypma, R. S.; Lam, A. M.; Gu, B., The nonstructural protein 3 protease/helicase requires an intact protease domain to unwind duplex RNA efficiently. *The Journal of biological chemistry* **2004,** 279, (2), 1269-80.

404. Ndjomou, J.; Kolli, R.; Mukherjee, S.; Shadrick, W. R.; Hanson, A. M.; Sweeney, N. L.; Bartczak, D.; Li, K.; Frankowski, K. J.; Schoenen, F. J.; Frick, D. N., Fluorescent primuline derivatives inhibit hepatitis C virus NS3-catalyzed RNA unwinding, peptide hydrolysis and viral replicase formation. *Antiviral research* **2012,** 96, (2), 245-255.

405. Shimakami, T.; Welsch, C.; Yamane, D.; McGivern, D. R.; Yi, M.; Zeuzem, S.; Lemon, S. M., Protease inhibitor-resistant hepatitis C virus mutants with reduced fitness from impaired production of infectious virus. *Gastroenterology* **2011,** 140, (2), 667-75.

406. Yan, Y.; He, Y.; Boson, B.; Wang, X.; Cosset, F.-L.; Zhong, J., A Point Mutation in the N-Terminal Amphipathic Helix α(0) in NS3 Promotes Hepatitis C Virus Assembly by Altering Core Localization to the Endoplasmic Reticulum and Facilitating Virus Budding. *Journal of virology* **2017,** 91, (6), e02399-16.

407. Urbanelli, L.; Buratta, S.; Tancini, B.; Sagini, K.; Delo, F.; Porcellati, S.; Emiliani, C., The Role of Extracellular Vesicles in Viral Infection and Transmission. *Vaccines (Basel)* **2019,** 7, (3), 102.

408. Pietschmann, T.; Lohmann, V.; Kaul, A.; Krieger, N.; Rinck, G.; Rutter, G.; Strand, D.; Bartenschlager, R., Persistent and transient replication of full-length hepatitis C virus genomes in cell culture. *Journal of virology* **2002,** 76, (8), 4008-4021.

409. Dreux, M.; Garaigorta, U.; Boyd, B.; Décembre, E.; Chung, J.; Whitten-Bauer, C.; Wieland, S.; Chisari, Francis V., Short-Range Exosomal Transfer of Viral RNA from Infected Cells to Plasmacytoid Dendritic Cells Triggers Innate Immunity. *Cell Host & Microbe* **2012,** 12, (4), 558-570.

410. Bukong, T. N.; Momen-Heravi, F.; Kodys, K.; Bala, S.; Szabo, G., Exosomes from Hepatitis C Infected Patients Transmit HCV Infection and Contain Replication Competent Viral RNA in Complex with Ago2-miR122-HSP90. *PLoS pathogens* **2014,** 10, (10), e1004424.

REFERENCES

411.   Longatti, A.; Boyd, B.; Chisari, F. V., Virion-independent transfer of replication-competent hepatitis C virus RNA between permissive cells. *Journal of virology* **2015,** 89, (5), 2956-2961.

412.   Andreu, Z.; Yáñez-Mó, M., Tetraspanins in extracellular vesicle formation and function. *Frontiers in immunology* **2014,** 5, 442-442.

7. APPENDIX
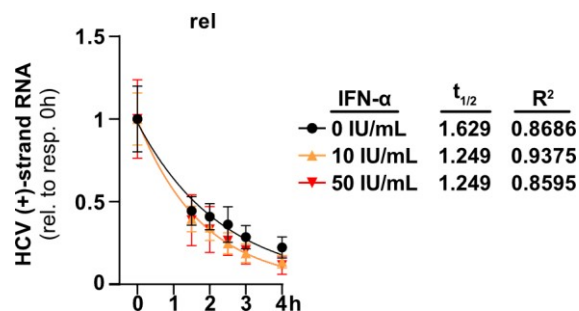
Click ↑ to get back to the according text passage.

Figure A1 ↑ The antiviral response triggered by IFN-α reduces HCV RNA half-life. Non-linear regression of HCV RNA levels over time after electroporation of the replication-deficient subgenomic firefly luciferase-encoding HCV RNA sgJFH$^{\Delta GDD}$ into untreated or IFN-α pre- and co-treated Huh7-Lunet cells quantified from strand-specific Northern blot, relative to 0 hours (n=3).
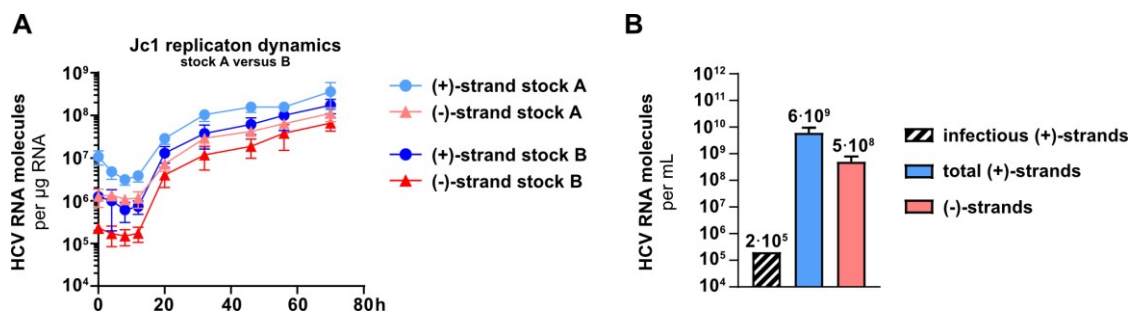

Figure A2 ↑ ↑ Comparison of HCV$_{cc}$ (Jc1) replication dynamics of two different stock preparations (stock A 01/16, stock B 06/19) in Lunet-CGM cells (A) and quantification of HCV RNAs in stock A (B). (A) (+)- and (-)-strand RNA quantification after infection of Lunet-CGM cells at an MOI of 1 (stock A) or 2.42 (stock B) using a strand-specific RT-qPCR (stock A n=3, stock B n=5). **(B)** (+)- and (-)-strand RNA quantification by strand-specific RT-qPCR from virus stock A (n=2). Virus stock titer suggested $2 \cdot 10^5$ infectious (+)-strands per mL as determined by end-point dilution assay (TCID$_{50}$).
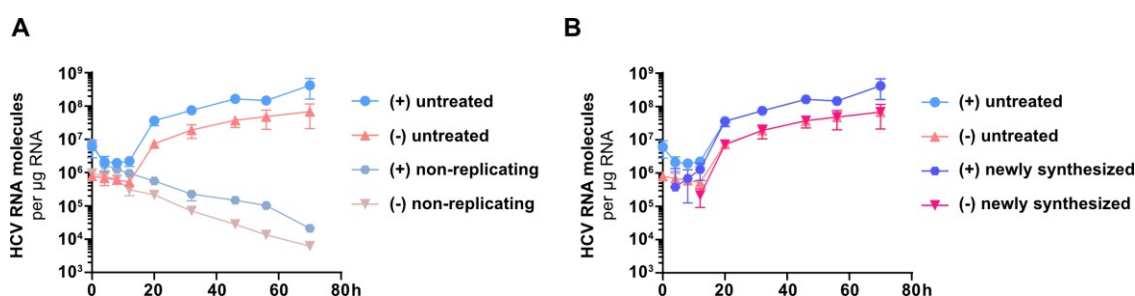
Figure A3 ↑ ↑ Jc1 infection dynamics in Lunet-CGM cells with or without complete inhibition of replication (A) and the same infection dynamics cleared from non-replicating RNA (newly synthesized) (B). (A) (+)- and (-)-strand RNA quantification after infection of Lunet-CGM cells with Jc1 stock A at an MOI of 1 using a strand-specific RT-qPCR (n=2 for untreated, n=1 for non-replicating). Complete inhibition was assured by treatment with 1 μM Telaprevir and Sofosbuvir each. **(B)** Same data as in (A) but non-replicating RNA molecules were subtracted from untreated ones. The remaining RNA molecules are presented as "newly synthesized".
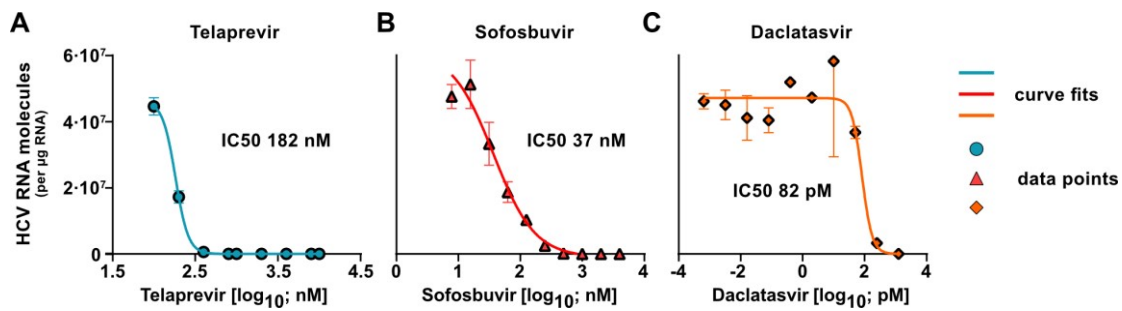
Figure A4 ↑ Titration of three different inhibitors (DAAs) against HCV and calculation of their respective IC$_{50}$s. Lunet-CGM cells were infected with HCV$_{cc}$ (Jc1) with an MOI of 2.42 and either left untreated or treated with varying concentrations of Telaprevir **(A)**, Sofosbuvir **(B)**, or Daclatasvir **(C)** for 72 hours (n=1 each). HCV RNA levels were assessed by strand-unspecific qRT-PCR (Taqman). Curve fits are non-linear regressions (four parameters, variable slope; 4PL) generated with GraphPad Prism 8 software. For Sofosbuvir, the top value was constrained to a non-treated control (6.15·10^7 HCV RNA molecules per µg RNA).
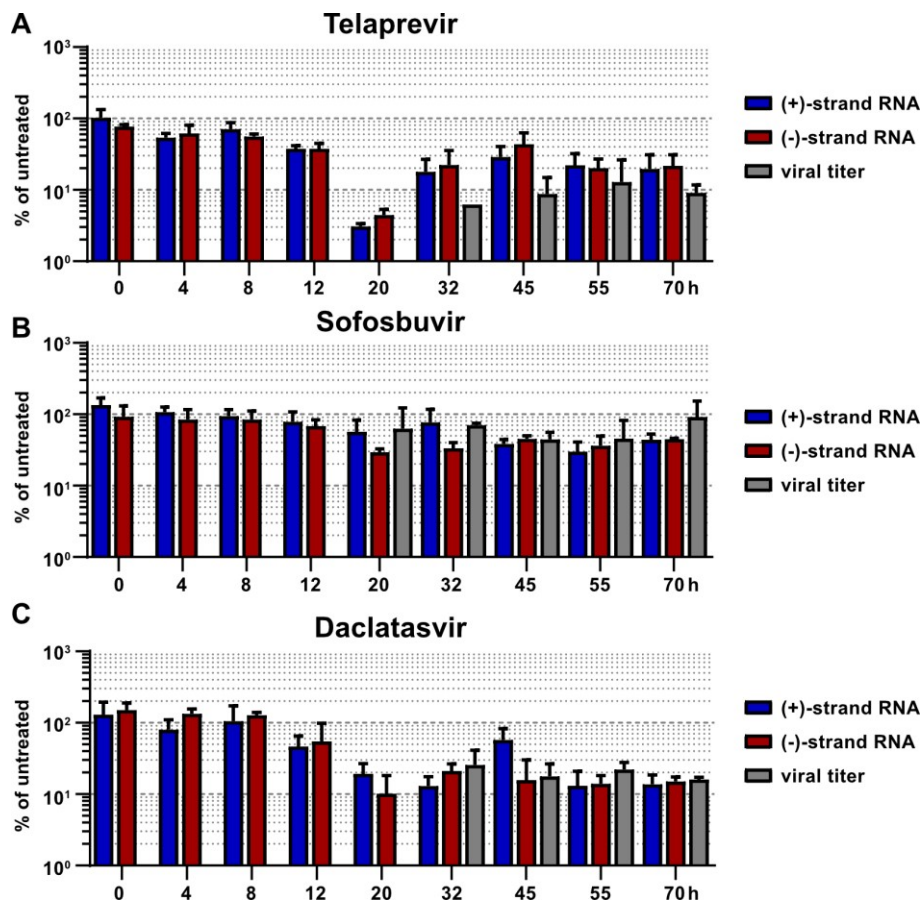
Figure A5 ↑ ↑ ↑ Ratios of viral determinants during Jc1 infection of Lunet-CGM cells under treatment. (+)- and (-)-strand RNA quantification using a strand-specific RT-qPCR and viral titer determination (endpoint dilution assay, TCID$_{50}$) after infection of Lunet-CGM cells with Jc1 stock B (MOI 2.42) and treatment with IC$_{50}$s of TEL **(A)**, SOF **(B)**, or DCV **(C)** (n=4-5 for untreated, n=2 for treatments). Data is shown in means +/- SD from the indicated number of independent experiments.
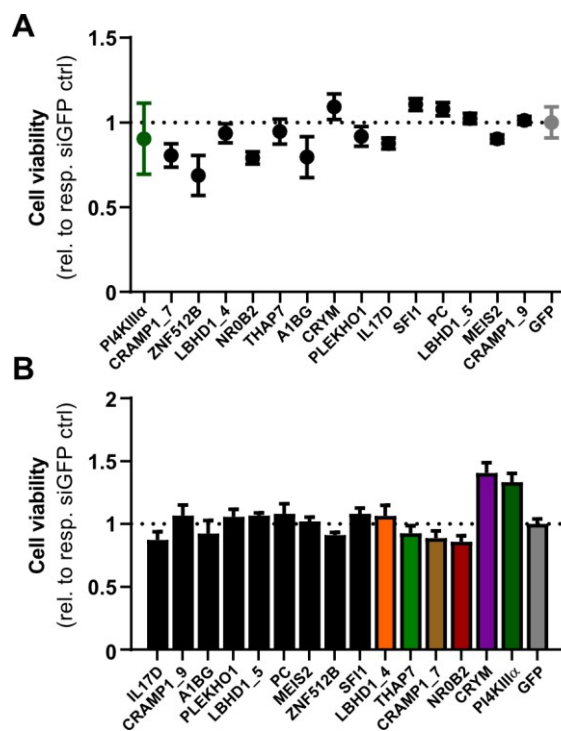
Figure A6 ↑ ↑ Cell viability after siRNA reverse-transfection in Huh7-Lunet (A) and Huh7-LucUbiNeo cells (B).
(A) Huh7-Lunet cells were reverse-transfected in white 96-well plates with indicated siRNAs 24 hours prior to mock infection. 72 hours later, cell viability was measured using the CellTiterGlo® substrate. **(B)** Huh7-LucUbiNeo cells were reverse-transfected with indicated siRNAs and cell viability was measured 96 hours later using the CellTiterGlo® substrate. Data shows means +/- standard deviation from two independent biological experiments. Adapted from [278].

Figure A7 ↑ Impact of siRNA knockdown of HF candidate genes on JcR2a replication (A) and cell viability (B). (A) Huh7-Lunet cells were reverse-transfected with three different siRNAs per candidate gene 24 hours prior to JcR2a infection (MOI ~0.1). Luciferase activity was measured 72 hours later and is given relative to the eGFP control. **(B)** Huh7-Lunet cells were reverse-transfected with three different siRNAs per candidate gene 24 hours prior to mock infection. Luciferase activity was measured 72 hours later and is given relative to the eGFP control. Data shows means +/- standard deviation from three (A) and two (B) independent biological experiments, respectively. Adapted from [278].

Table A1 ↑ Results of JcR2a replication (n=3) and cell viability assay (n=2) after siRNA-mediated knockdown of HF candidate genes. In grey color highlighted and bold are candidate genes that we studied further. Adapted from [278].

| #	siRNA	HCV replication mean	HCV replication SD	cell viability mean	cell viability SD	#	siRNA	HCV replication mean	HCV replication SD	cell viability mean	cell viability SD
1	MEIS2_6	0,04	0,01	0,50	0,09	73	NAT8L_1	0,90	0,40	0,62	0,13
2	PI4KIIIα	0,05	0,01	0,90	0,21	74	THBS4_7	0,95	0,21	1,04	0,04
3	HAS2_4	0,08	0,03	0,33	0,15	75	MYOM1_9	0,97	0,31	0,77	0,09
4	NR0B2_4	0,09	0,03	0,78	0,09	76	SULT1E1_8	1,01	0,26	1,13	0,09
5	**CRAMP1_7**	0,12	0,04	0,81	0,07	77	UCP2_11	1,00	0,19	0,78	0,13
6	TMED3_6	0,13	0,07	0,46	0,15	78	LBHD1_6	1,02	0,31	0,79	0,05
7	LOC400655_6	0,15	0,04	0,74	0,09	79	MYOM1_7	1,04	0,17	0,93	0,06
8	IL17D_5	0,15	0,09	0,60	0,05	80	NAV3_10	1,05	0,25	0,81	0,04
9	CRYM_11	0,16	0,06	0,71	0,07	81	HAS2_6	1,06	0,28	0,90	0,05
10	**ZNF512B_3**	0,17	0,04	0,69	0,12	82	SORCS2_1	1,08	0,29	1,05	0,04
11	MICAL3_11	0,17	0,05	0,71	0,09	83	PPP1R15A_7	1,07	0,12	0,79	0,07
12	**LBHD1_4**	0,18	0,06	0,94	0,06	84	ZNF512B_4	1,14	0,20	0,98	0,09
13	**NR0B2_7**	0,19	0,03	0,79	0,04	85	TMED3_5	1,17	0,21	1,03	0,06
14	**THAP7_5**	0,19	0,04	0,95	0,07	86	THAP7_1	1,18	0,42	1,15	0,10
15	**A1BG_2**	0,21	0,08	0,80	0,12	87	PPP1R15A_6	1,18	0,33	0,83	0,07
16	ZNF512B_6	0,22	0,08	0,72	0,07	88	C8orf4_6	1,25	0,36	1,11	0,05
17	CRYM_9	0,25	0,08	1,09	0,08	89	C8orf4_8	1,24	0,39	1,18	0,10
18	THAP7_6	0,25	0,14	0,67	0,08	90	SNUPN_2	1,29	0,43	0,93	0,13
19	SFI1_8	0,27	0,07	0,66	0,06	91	IL17D_2	1,32	0,36	0,94	0,04
20	A1BG_9	0,29	0,12	0,64	0,08	92	ALPK2_6	1,44	0,64	1,20	0,17
21	**PLEKHO1_5**	0,28	0,12	0,92	0,06	93	CRAMP1_8	1,41	0,42	0,82	0,03
22	UCP2_10	0,31	0,08	0,71	0,07	94	TUBB2B_3	1,43	0,51	1,26	0,08
23	NAV3_9	0,32	0,11	0,77	0,07	95	SFI1_9	1,48	0,58	0,73	0,05
24	NR0B2_6	0,32	0,10	0,82	0,09	96	PDE8A_9	1,55	0,37	1,01	0,04
25	**IL17D_6**	0,34	0,07	0,88	0,03	97	NAV3_11	1,55	0,45	1,07	0,07
26	CKLF_13	0,34	0,09	0,96	0,02	98	FOXF2_2	1,55	0,28	0,97	0,10
27	CKLF_5	0,35	0,10	1,24	0,18	99	SNUPN_8	1,69	0,51	1,03	0,14
28	**SFI1_10**	0,35	0,06	1,11	0,04	100	CRYM_10	1,66	0,58	1,07	0,04
29	TUBB2B_2	0,35	0,06	0,79	0,04	101	SORCS2_5	1,78	0,72	0,82	0,04
30	**PC_11**	0,35	0,06	1,08	0,04	102	SNUPN_1	2,14	0,44	1,02	0,23
31	**LBHD1_5**	0,35	0,07	1,02	0,03	103	CYP2B6_9	2,18	0,96	1,14	0,13
32	MAP2_6	0,35	0,14	0,84	0,08						
33	**MEIS2_7**	0,36	0,06	0,90	0,02						
34	MAP2_3	0,38	0,17	0,68	0,08						
35	BCR_7	0,38	0,11	0,86	0,05						
36	A1BG_4	0,40	0,24	0,51	0,05						
37	THBS4_5	0,42	0,10	1,04	0,07						
38	**CRAMP1_9**	0,42	0,06	1,01	0,02						
39	ALPK2_7	0,42	0,09	0,94	0,03						
40	PDE8A_10	0,44	0,07	1,06	0,05						
41	PC_10	0,45	0,10	0,83	0,04						
42	NAT8L_2	0,47	0,16	0,74	0,05						
43	UCP2_7	0,47	0,06	0,79	0,09						
44	CYP2B6_6	0,47	0,14	0,55	0,06						
45	LOC400655_7	0,47	0,11	0,96	0,05						
46	SORCS2_3	0,50	0,19	1,03	0,13						
47	MAP2_5	0,57	0,14	1,07	0,10						
48	BCR_8	0,57	0,08	0,82	0,05						
49	PDE8A_5	0,58	0,17	1,10	0,02						
50	MICAL3_14	0,61	0,12	0,98	0,03						
51	CYP2B6_5	0,60	0,24	0,66	0,07						
52	TMED3_3	0,63	0,21	0,99	0,09						
53	SULT1E1_5	0,62	0,22	0,82	0,02						
54	MEIS2_8	0,65	0,11	1,02	0,04						
55	PC_7	0,65	0,18	1,06	0,05						
56	PLEKHO1_4	0,67	0,44	1,00	0,08						
57	NAT8L_3	0,68	0,20	0,92	0,08						
58	THBS4_6	0,70	0,15	0,96	0,08						
59	ALPK2_11	0,71	0,15	0,97	0,05						
60	PLEKHO1_3	0,72	0,19	1,06	0,04						
61	SULT1E1_7	0,73	0,21	1,09	0,04						
62	CKLF_11	0,79	0,09	0,97	0,06						
63	MYOM1_10	0,79	0,22	0,79	0,08						
64	MICAL3_17	0,80	0,13	0,84	0,13						
65	HAS2_5	0,81	0,17	0,97	0,08						
66	TUBB2B_1	0,85	0,14	0,93	0,08						
67	FOXF2_5	0,89	0,32	0,85	0,09						
68	PPP1R15A_5	0,88	0,13	1,11	0,04						
69	C8orf4_7	0,88	0,17	1,00	0,05						
70	BCR_5	0,92	0,38	0,95	0,06						
71	FOXF2_4	0,86	0,33	0,91	0,03						
72	LOC400655_8	0,92	0,20	1,14	0,04						
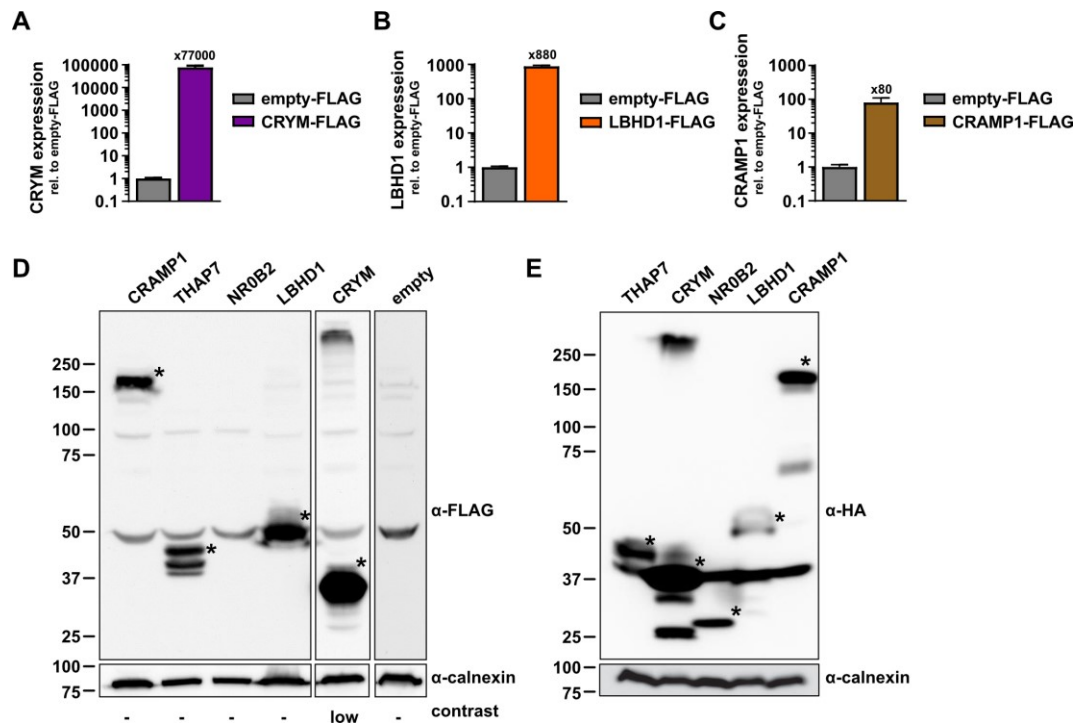
Figure A8 ↑ Expression controls of HF candidate genes stably expressed in Huh7-LP cells. (A) mRNA level of CRYM in Huh7-LP-CRYM-FLAG relative to -empty-FLAG cells as assessed via qPCR. **(B)** mRNA level of LBHD1 in Huh7-LP-LBHD1-FLAG relative to -empty-FLAG cells as assessed via qPCR. **(C)** mRNA level of CRAMP1 in Huh7-LP-CRAMP1-FLAG relative to -empty-FLAG cells as assessed via qPCR. **(D), (E)** Immunoblots for expression control of HF candidate genes expressed as C-terminally FLAG- (D) or N-terminally HA-tagged constructs (E). Asterisks indicate correct molecular weights of indicated constructs. Adapted from [278].
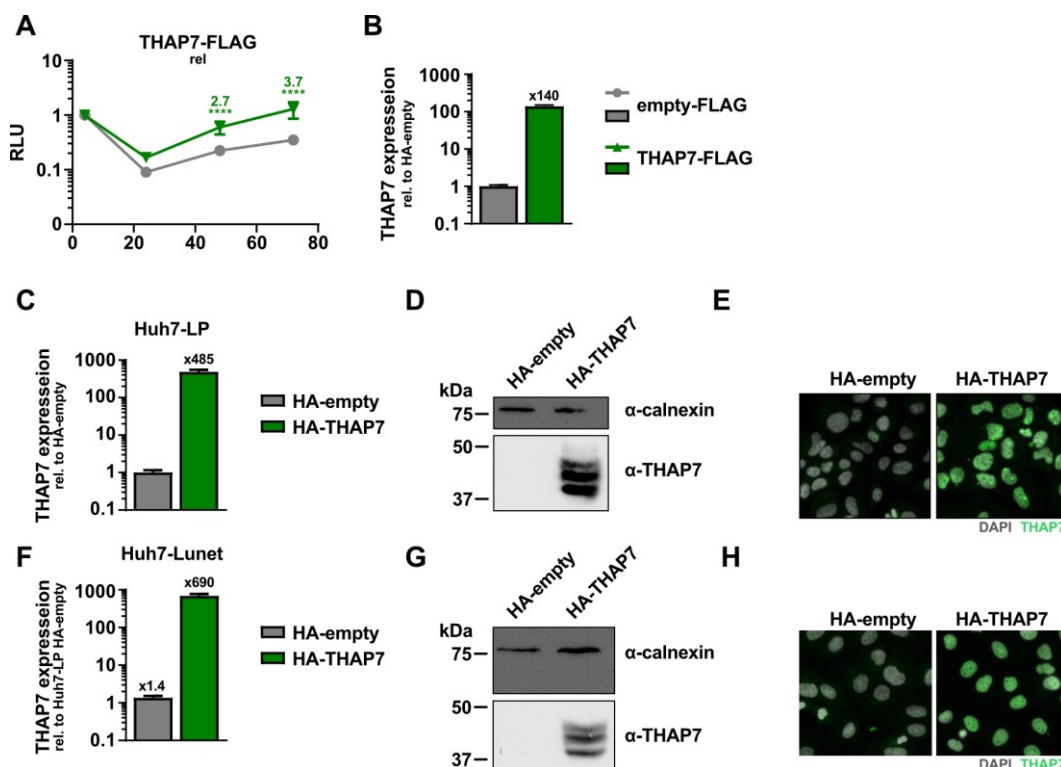
Figure A9 ↑ ↑ ↑ HCV replication upon overexpression of THAP7-FLAG and expression controls. (A) Huh7-LP cells stably overexpressing THAP7-FLAG or an empty-FLAG control were electroporated with a subgenomic gt1b luciferase reporter replicon (sgCon1-ET) and luciferase activity was measured after 4, 24, 48, and 72 hours. **(B)** qPCR of Huh7-LP overexpressing THAP7-FLAG or empty-FLAG. Expression in (Huh7-LP-)THAP7-FLAG is normalized to GAPDH and relative to the control cell line (Huh7-LP-)empty-FLAG. **(C–E)** Overexpression control of Huh7-LP-HA-THAP7 cells via qPCR (C), immunoblot (D), or immunofluorescence (E) using a THAP7-specific antibody. **(F–H)** Overexpression control of Huh7-Lunet-HA-THAP7 cells via qPCR (F), immunoblot (G), or immunofluorescence (H) using a THAP7-specific antibody. **** $p \leq 0.0001$. Adapted from [278].
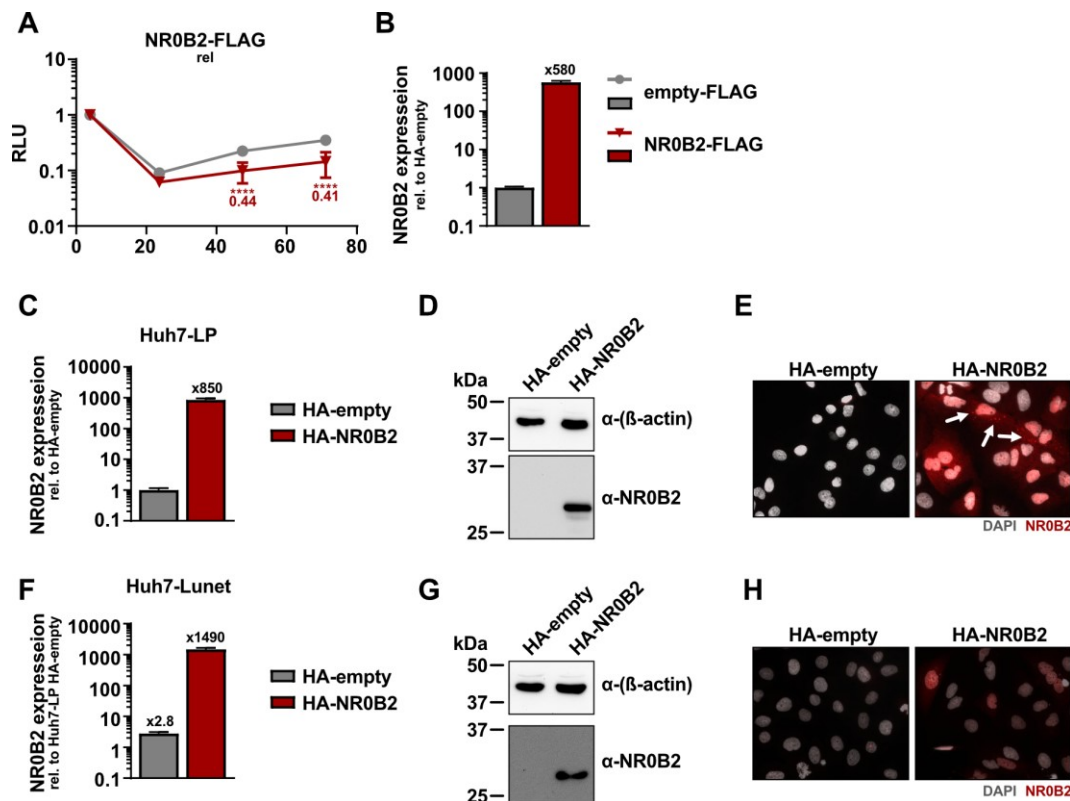
Figure A10 ↑ ↑ ↑ HCV replication upon overexpression of NR0B2-FLAG and expression controls. (A) Huh7-LP cells stably overexpressing NR0B2-FLAG or an empty-FLAG control were electroporated with a subgenomic gt1b luciferase reporter replicon (sgCon1-ET) and luciferase activity was measured after 4, 24, 48, and 72 hours. **(B)** qPCR of Huh7-LP overexpressing NR0B2-FLAG or empty-FLAG. Expression in (Huh7-LP-)NR0B2-FLAG is normalized to GAPDH and relative to the control cell line (Huh7-LP-)empty-FLAG. **(C–E)** Overexpression control of Huh7-LP-HA-NR0B2 cells via qPCR (C), immunoblot (D), or immunofluorescence (E) using a NR0B2-specific antibody. **(F–H)** Overexpression control of Huh7-Lunet-HA-NR0B2 cells via qPCR (F), immunoblot (G), or immunofluorescence (H) using an NR0B2-specific antibody. White arrows in (E) indicate cytoplasmic, punctate NR0B2 localization. **** $p \leq 0.0001$. Adapted from [278].
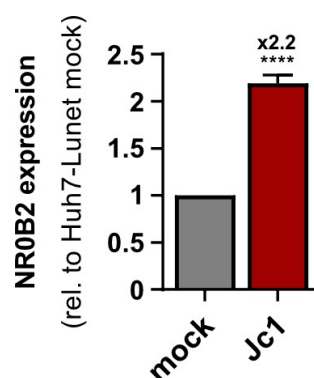

Figure A11 ↑ Jc1 infection increases NR0B2 expression in Huh7-Lunet cells. Huh7-Lunet cells were infected with cell culture produced Jc1 (MOI 1) for 72 hours. RNA was extracted and mRNA levels were quantified by qPCR. Data shows mean +/- standard deviation from three independent biological experiments. **** $p \leq 0.0001$. Adapted from [278].
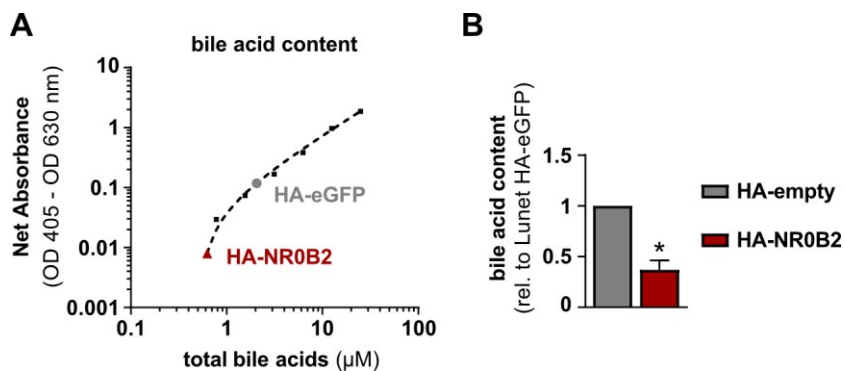
Figure A12 ↑ HA-NR0B2 overexpression reduces bile acid content in Huh7-Lunet cells. (A) Total bile acid content of Huh7-Lunet-HA-NR0B2 or -HA-eGFP cells was assessed using the Total Bile Acid Assay Kit (Cell Biolabs). Squares represent standard samples and the blocked dotted line is a linear regression. (B) Quantification of total bile acids in Huh7-Lunet-HA-NR0B2 or -HA-eGFP cells. Data shows mean +/- standard deviation from two independent experiments. * p ≤ 0.05. Adapted from [278].